



National Library of Canada  
Collections Development Branch

Canadian Theses on  
Microfiche Service

Bibliothèque nationale du Canada  
Direction du développement des collections

Service des thèses canadiennes  
sur microfiche

## NOTICE

The quality of this microfiche is heavily dependent upon the quality of the original thesis submitted for microfilming. Every effort has been made to ensure the highest quality of reproduction possible.

If pages are missing, contact the university which granted the degree.

Some pages may have indistinct print especially if the original pages were typed with a poor typewriter ribbon or if the university sent us a poor photocopy.

Previously copyrighted materials (journal articles, published tests, etc.) are not filmed.

Reproduction in full or in part of this film is governed by the Canadian Copyright Act, R.S.C. 1970, c. C-30. Please read the authorization forms which accompany this thesis.

THIS DISSERTATION  
HAS BEEN MICROFILMED  
EXACTLY AS RECEIVED

## AVIS

La qualité de cette microfiche dépend grandement de la qualité de la thèse soumise au microfilmage. Nous avons tout fait pour assurer une qualité supérieure de reproduction.

S'il manque des pages, veuillez communiquer avec l'université qui a conféré le grade:

La qualité d'impression de certaines pages peut laisser à désirer, surtout si les pages originales ont été dactylographiées à l'aide d'un ruban usé ou si l'université nous a fait parvenir une photocopie de mauvaise qualité.

Les documents qui font déjà l'objet d'un droit d'auteur (articles de revue, examens publiés, etc.) ne sont pas microfilmés.

La reproduction, même partielle, de ce microfilm est soumise à la Loi canadienne sur le droit d'auteur, SRC 1970, c. C-30. Veuillez prendre connaissance des formules d'autorisation qui accompagnent cette thèse.

LA THÈSE A ÉTÉ  
MICROFILMÉE TELLE QUE  
NOUS L'AVONS REÇUE

REINFORCED CONCRETE CORNER JOINTS  
SUBJECTED TO REVERSED LOADING

by

Hee Chaung FU

A thesis

submitted to the School of Graduate Studies

in partial fulfillment of

the requirements for the degree of

Master of Applied Science

© Hee Chaung Fu, Ottawa, Canada, 1981

TO MY PARENTS

3

## ABSTRACT

Earthquakes impose severe time varying lateral loads and displacements on structures. For framed structures, lateral loads cause large bending moments and shear forces in the beam-column connections. Earthquake motion causes reversals of bending moments and shear forces and the beam-column connections must survive several cycles of high intensity loading without significant stiffness degradation.

This thesis studies the behavior of reinforced concrete beam-column corner joints. A systematic experimental study of the behavior of reinforced concrete beam-column corner connections was carried out by constructing and loading nine specimens to failure. Four specimens were tested under monotonic loading while the remaining five were tested under increasing magnitude cyclic loading to simulate the effect of severe earthquake loading. The principal variables of the study were the flexural reinforcement ratio and the reinforcement detail of the joint. Tests were conducted on corner joints with different reinforcement details and the flexural reinforcement ratios varied from 0.7 % to 1.27 %. All specimens had nominal beam and column cross section dimensions of 6X6.25 in. (152X158 mm), reinforcing steel with

nominal yield strength of 413.7 MPa and a nominal concrete compressive strength of 34.47 MPa.

Analysis of the results shows that no difficulties were encountered with reinforced concrete corner joints subjected to a closing moment. When beam-column corner joints were subjected to an opening moment, the diagonal tension failure at the corner limited the capacity of the corner. The behavior of the joint is sensitive to the load history applied with load reversals causing incremental bond failure and shear cracks. Joint performance, strength, ductility and stiffness all improved with decreasing flexural steel ratio. The addition of diagonal reinforcement at the corner, of the same size as the flexural reinforcement, is necessary for a corner joint under opening moment. One specimen, No. 9, which modelled an edge corner joint, with beams perpendicular to the plane of the joint, showed much improved performance compared with the specimen without lateral beams.

## ACKNOWLEDGEMENTS

The writer wishes to express his sincere appreciation to Dr. N.J. Gardner for his suggestions, valuable comments and assistance during the course of the study.

The help received from the technical personnel of the Civil Engineering Department, especially Mr. William Watson, Mr. Claude Lavigne, Mr. Greg Duchesne and Mr. Mike Burns, made the experimental work possible and is gratefully acknowledged.

The writer is most indebted to his brother, Mr. Hee Ning Fu and the writer's fiancée, Miss Chi Wah Wong, for their warmest and ever-lasting encouragement and support.

## TABLE OF CONTENTS

ABSTRACT . . . . .		ii
ACKNOWLEDGEMENTS . . . . .		iv
Chapter		page
I. INTRODUCTION . . . . .		1
1.1 General . . . . .		1
1.1.1 Ductility . . . . .		8
1.2 Study Goals . . . . .		11 <sup>e</sup>
II. ANALYSIS OF REINFORCED CONCRETE CORNERS . . . . .		13
2.1 General Remarks . . . . .		13
2.2 Theoretical Analysis . . . . .		14
1.2.1 Corners Subjected to Closing Moment. . . . .		14
1.2.2 Corners Subjected to Opening Moment. . . . .		17
2.3 Modes of Failure . . . . .		21
2.4 Ductility and Stiffness of Structures . . . . .		28
1.4.1 Ductility. . . . .		28
1.4.2 Stiffness. . . . .		29
III. REVIEW OF LITERATURE . . . . .		31
3.1 Introductory Remarks . . . . .		31
3.2 Previous Research. . . . .		32
3.3 Review of Building Design Codes. . . . .		42
3.4 Aim of The Investigation . . . . .		46
IV. EXPERIMENTAL WORK AND INSTRUMENTATION. . . . .		47
4.1 General Consideration. . . . .		47
4.2 Uni-Directional Loading. . . . .		49
4.2.1 Test Set-Up and Load Simulation. . . . .		50
4.2.2 Test Procedure . . . . .		50
4.3 Cyclic Loading . . . . .		52
4.3.1 Test Set-Up and Load Simulation. . . . .		52
4.3.2 Test Procedure . . . . .		58
4.4 Formwork . . . . .		60
4.5 Test Specimens . . . . .		63
4.6 Material Properties . . . . .		64
4.6.1 Concrete . . . . .		64
4.6.2 Steel Reinforcement. . . . .		66

4.7 Instrumentation . . . . .	69
4.7.1 Concrete Strain . . . . .	70
4.7.2 Corner Relations . . . . .	71
V. PRESENTATION AND DISCUSSION OF RESULTS . . . . .	73
5.1 Introduction . . . . .	73
5.1.1 Load-Deflection Curves . . . . .	73
5.1.2 Moment-Rotation Curves . . . . .	74
5.1.3 Steel Strain-Load Curves . . . . .	74
5.1.4 Concrete Strain-Moment Curves . . . . .	75
5.2 Presentation of Results . . . . .	77
5.2.1 Monotonic Loading . . . . .	77
5.2.1.1 Specimen # 1 . . . . .	77
5.2.1.2 Specimen # 2 . . . . .	78
5.2.1.3 Specimen # 3 . . . . .	79
5.2.1.4 Specimen # 8 . . . . .	80
5.2.2 Cyclic Loading . . . . .	81
5.2.2.1 Specimen # 4 . . . . .	81
5.2.2.2 Specimen # 5 . . . . .	83
5.2.2.3 Specimen # 6 . . . . .	85
5.2.2.4 Specimen # 7 . . . . .	88
5.2.2.5 Specimen # 9 . . . . .	91
5.3 Discussion of Results . . . . .	92
5.3.1 Monotonic Loading . . . . .	94
5.3.1.1 Specimens # 1, 8 . . . . .	94
5.3.1.2 Specimens # 2, 3 . . . . .	95
5.3.2 Cyclic Loading . . . . .	96
5.3.2.1 Specimens # 4, 5 . . . . .	96
5.3.2.2 Specimens # 6, 7 . . . . .	98
5.3.2.3 Specimen # 9 . . . . .	100
5.4 Comparison of Results . . . . .	100
VI. CONCLUSION AND RECOMMENDATION . . . . .	103
6.1 Conclusion . . . . .	103
6.2 Recommendation . . . . .	105
BIBLIOGRAPHY . . . . .	109
Appendix . . . . .	page
A. LAYOUT OF SPECIMENS . . . . .	112
B. TABLES . . . . .	121
C. RESULTS . . . . .	122

LIST OF TABLES

Table	page
1. Test Schedule . . . . .	48
2. Specimens Properties and Test Results . . . . .	121

## LIST OF FIGURES

Figure	page
1. El Centro Earthquake (1940) . . . . .	2
2. Response of a Structure to El Centro E.Q. . . . .	3
3. S.D.O.F. System Subjected to Base Translation . . . . .	5
4. Ductility and Brittle Behavior . . . . .	7
5. Definition of Ductility Factor . . . . .	7
6. Frame Subjected to Lateral Forces . . . . .	14
7. Stress Distribution, Theory of Elasticity . . . . .	16
8. Closing Corner at Ultimate Load . . . . .	16
9. Finite Element Method . . . . .	18
10. Stress Distribution, F.E.M. . . . .	19
11. Opening Corner at Ultimate Load . . . . .	20
12. Ductile Failure . . . . .	22
13. Diagonal Tension Crack Failure . . . . .	24
14. Stress Distribution, F.E.M. . . . .	25
15. Opening Corner at Diagonal Crack . . . . .	25
16. Stress-Strain Relation of a R.C. Section . . . . .	27
17. Corner Tests by Wastlund (1934) . . . . .	32
18. Corner Detail By Posey and Kofoid, 1943 . . . . .	34
19. Corner Tests by Sandbye, 1967 . . . . .	36
20. Corner Tests by Kordina and Fuchs, 1970 . . . . .	38
21. Corner Test by Mayfield et al, 1972 . . . . .	38
22. Corner Detail Proposed by Nilsson, 1973 . . . . .	41

23.	Corner Details by a British Committee, 1970 . . . . .	43
24.	Corner Detail by ACI 318-74 . . . . .	43
25.	Standard Corner Layout Recommended in German Building Code . . . . .	45
26.	Standard Corner Layout Recommended in Russian Building Code . . . . .	45
27.	Test Rig for One-Way Loading . . . . .	51
28.	Test Rig for Two-Way Loading . . . . .	54
29.	Base of Test Rig . . . . .	55
30.	Point Load System At Beam Section . . . . .	56
31.	Simulated Moments . . . . .	57
32.	Typical Loading History . . . . .	59
33.	Plane Form Work . . . . .	61
34.	Three-Dimensional Form Work . . . . .	62
35.	Member Cross Sections . . . . .	64
36.	Dimensions of Specimens . . . . .	65
45.	Concrete Strength Curves . . . . .	67
46.	Stress-Strain Curves, Reinforcement . . . . .	68
47.	Rotation Measurement . . . . .	71
57.	Concrete Strains Measurements . . . . .	76
58.	Comparison of Results . . . . .	101
37.	Reinforcement Layout : Specimens # 1 , 8 . . . . .	113
38.	Reinforcement Layout : Specimen # 2 . . . . .	114
39.	Reinforcement Layout : Specimen # 3 . . . . .	115
40.	Reinforcement Layout : Specimens # 4 , 5 . . . . .	116
41.	Reinforcement Layout : Specimen # 6 . . . . .	117
42.	Reinforcement Layout : Specimen # 7 . . . . .	118
43.	Reinforcement Layout : Specimen # 9 . . . . .	119

44.	Member Stirrups . . . . .	120
48.	Test Results : Specimen # 1 . . . . .	123
49.	Test Results : Specimen # 2 . . . . .	124
50.	Test Results : Specimen # 3 . . . . .	128
51.	Test Results : Specimen # 4 . . . . .	131
52.	Test Results : Specimen # 5 . . . . .	136
53.	Test Results : Specimen # 6 . . . . .	141
54.	Test Results : Specimen # 7 . . . . .	150
55.	Test Results : Specimen # 8 . . . . .	161
56.	Test Results : Specimen # 9 . . . . .	165

## NOMENCLATURE

$A_s$	area of tensile reinforcement
b or t	width of rectangular section
C	compressive force in the concrete
d	efficient depth of flexural member
d'	distance from extreme compressive fibre to the centroid of the compressive reinforcement
$d_a$	distance between the centre lines of compressive and tensile reinforcement
$E_c$	Young's modulus of elasticity of concrete
$E_s$	Young's modulus of elasticity of steel
F	inclined force applied to the corner joint
$F_x$	components of the inclined force applied to the corner
$F_s$	tensile force in reinforcement at first diagonal crack
$f'_c (\sigma_c)$	concrete compressive strength
$f_t$	tensile strength of concrete
$f_y$	design strength required in a member (known member strength) or yield strength of reinforcement in tension
$f_{max}$	maximum elastic member force
$f_{su}$	stress in tensile reinforcement at ultimate
$f_{cu}$	average flexural compressive stress of confined concrete at ultimate
h	total depth of member

J	$1-K/3$ , ratio of distance between centroids of compressive and tensile stresses to effective depth
K	ratio of distance between extreme compressive fibre and neutral axis to effective depth
$K_u$	value of K at ultimate
L	the distance between the point of inclined load to the centre of the column section
$L_1$	distance <u>between</u> the two dial gauges for rotation measurements
$l_{dc}$	length of diagonal crack
M	bending moment
$M_y$	yielding moment, moment at yielding of tensile steel
n	$E_s/E_c$ , modulus ratio
r	radius of reinforcement loop
T	tensile force in reinforcement or period of vibration
$U_H$	maximum displacement of an elasto-plastic system for a given T
$U_o$	maximum displacement of an elastic system for a given T
$U_y$	displacement of mass relative to ground at yield
$V_t$	total displacement
$V_g$	ground displacement
$V$	displacement (horizontal) of a system
$\mu$	ductility factor, the ratio of total deformation to yield deformation
$\delta(\Delta)$	deformation
$d_{max}$	maximum deflection

$d_y$	elastic limit deformation
$x$	displacement of ground
$\ddot{x}$	second derivative of $x$ with respect to time, ground acceleration
$\epsilon_{cu}$	concrete strain at ultimate
$\epsilon_{su}$	strain of reinforcing steel at ultimate
$\epsilon_y$	yield strain of reinforcing steel
$\phi$	curvature of a member due to an applied moment
$\phi_u$	curvature at ultimate
$\phi_y$	curvature at yield
$\rho$	$A_s/bd$ , flexural reinforcement ratio
$\rho_b$	flexural reinforcement ratio producing balanced strain conditions
$\phi$	diameter of reinforcing bar
$\sigma_s$	steel stress at failure of the concrete

Note : in this report, both Imperial and the equivalent S.I. units (in brackets) , were used for numerals and equations. Units were in S.I. if only one of the two units was employed.

Chapter I  
INTRODUCTION

1.1 GENERAL

Earthquakes are violent and unpredictable movements of the earth's crust. For the structural engineer, earthquakes bring the challenge of designing structures that will not collapse in a catastrophic manner during a major earthquake and will remain reasonably serviceable after most moderate earthquakes.

Figure 1 (a) shows the accelerogram of ground movement of the N.S. component of the El Centro 1940 earthquake. To a structure, the effect of translating the base of the structure is equivalent to applying a time varying series of lateral loads to the structure.

A simple structure, such as a single bay single storey portal frame can be mathematically represented as a single degree of freedom system. If the natural frequency and damping properties of the system are known and it can be assumed that the system is linear and elastic, the equation of motion can be numerically integrated to get the response of the system as is shown in Figure 2-a (a) For a ground motion

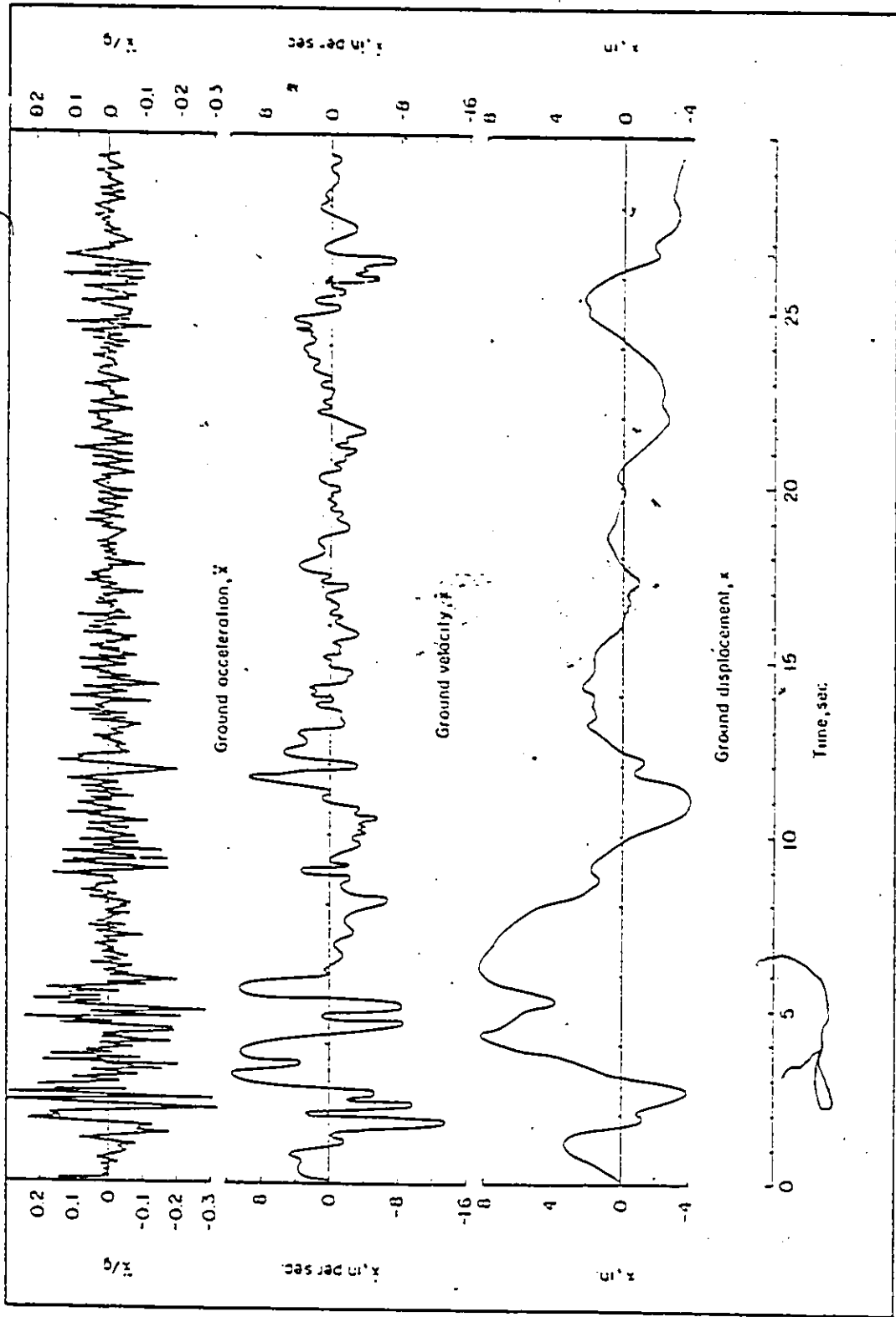
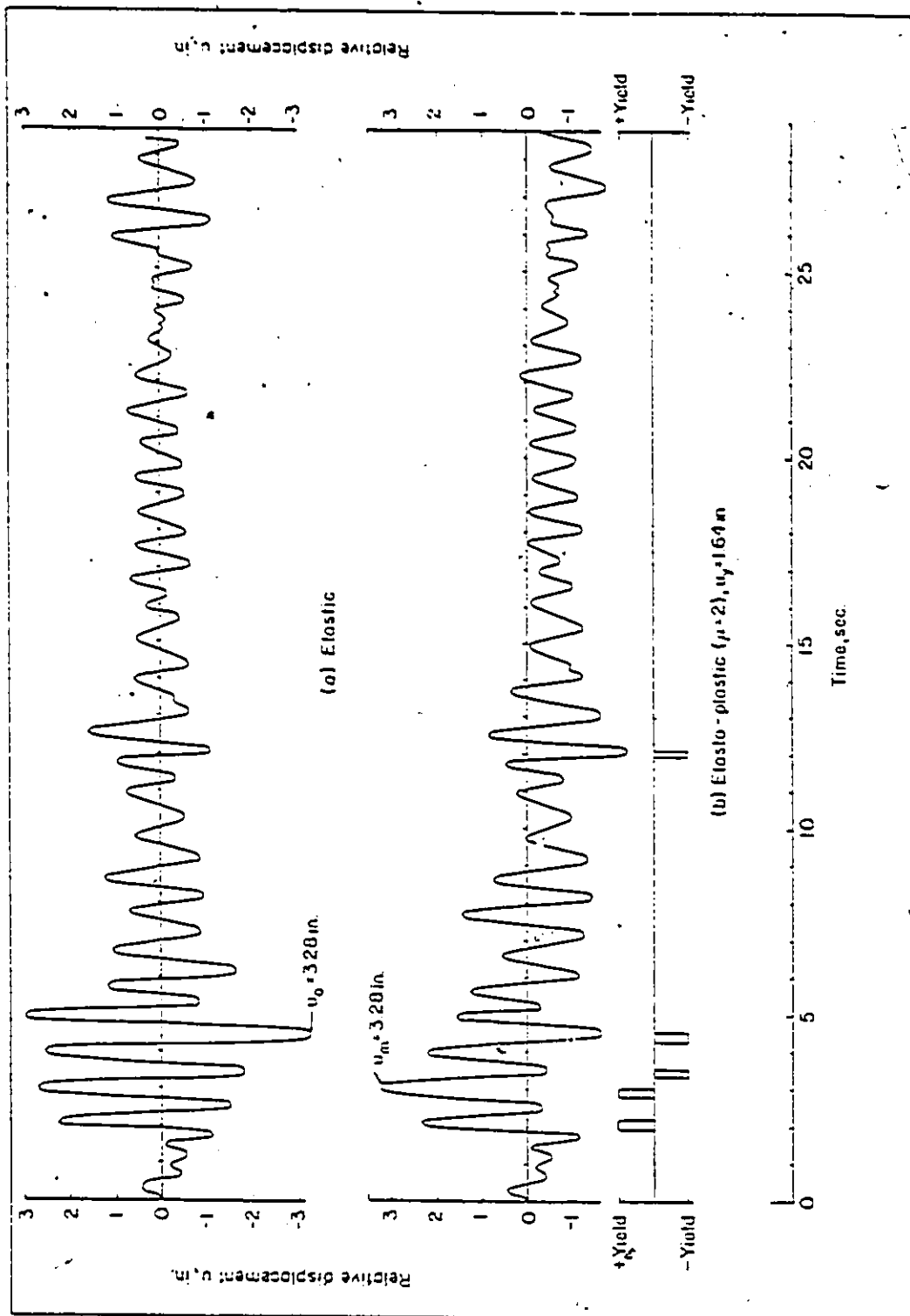


FIG. 1 EL CENTRO EARTHQUAKE (1940) (Ref. 7)

Ground acceleration, velocity, and displacement, El Centro, Calif., earthquake of May 18, 1940, N-S component.



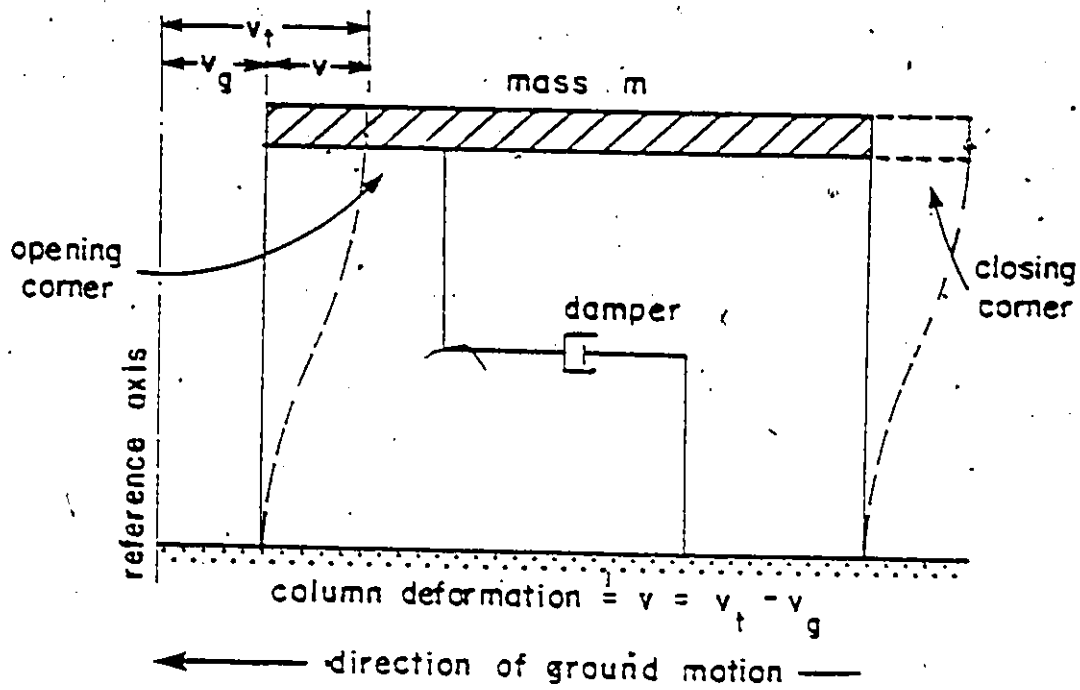
Response of a system with  $\gamma = 1.0$  second,  $\beta = 0.10$ , 19-10 El Centro, Calif., earthquake, N-S component.

FIG. 2 RESPONSE OF A STRUCTURE TO EL CENTRO EARTHQUAKE (Ref. 7)

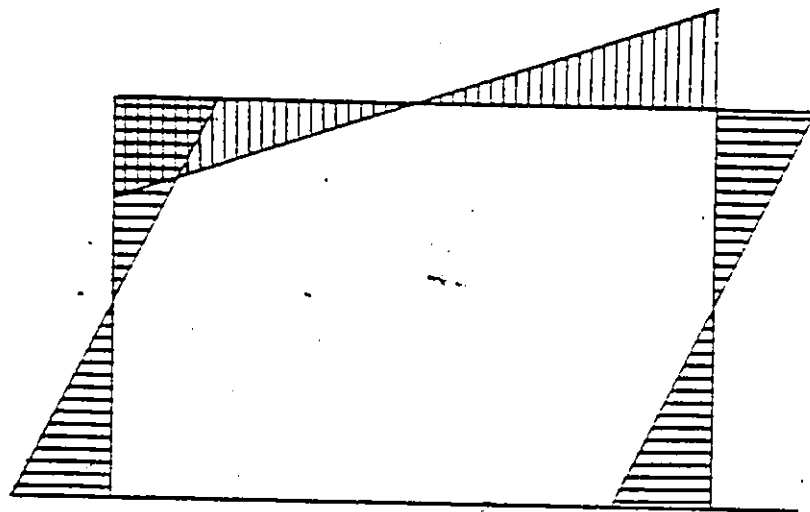
identical to the 1940 El Centro earthquake, Figure 2-a represents the response of an elastic system having a period of vibration ( $T$ ) of 1.0 second and a damping coefficient ( $\beta$ ) of 10 % of critical. This particular system under the El Centro earthquake would result in a maximum lateral displacement of 3.28 in. (83.3 mm) after 4.3 seconds.

Most structural systems do not remain elastic in response to severe earthquake action: Numerical analysis of the system of Figure assuming the structure has an elasto-plastic load-displacement response with a yield displacement of 1.64 in. (41.7 mm) has been carried out with the results illustrated in Figure 2-b. It can be noted that the maximum displacement is again 3.28 in (83.3 mm) but, at a time of 3 seconds. The nearly identical displacements, even though at different times, is the basis of the ductility design philosophy described later.

When a simple structure is subjected to earthquake ground motion, the response of the frame to base translation will be similar to that produced by a lateral load, as shown in Figure 3-a, and the resulting bending moments experienced by the frame due to base motion can be represented as in Figure 3-b. One corner is subjected to a moment which tends to open the corner and the other a moment which tends to close the corner. The sense of the moments will be reversed



(a) single-degree-of-freedom system



(b) resulting bending moments

FIG. 3 S.D.O.F. SYSTEM SUBJECTED TO BASE TRANSLATION

if the direction of the horizontal component of the ground motion reverses. This shows the necessity of designing a corner to resist the reversals of moments during earthquake excitation.

Figure 3-b shows the bending moment diagram for a single storey portal frame under lateral load; it is useful to note that the maximum bending moments occur at the beam-column connections. The connection must be as strong as the weakest connecting member, namely the weaker of either the beam or the column. It must also be noted that failure of a connection in a structure is catastrophic as it implies failure of both the beams and columns.

Two categories of structural behavior can be identified as shown in Figure 4, namely brittle or ductile. In the design of structures for seismic safety, the concept has been adopted that the response of a structure to earthquake excitation be ductile so that the structure can carry load reversals or overload by inelastic deformations of the members.

It is understood that during an earthquake, significant overstress in a structure is expected; The overstress in the columns can be substantially reduced by the yielding of the beams, during which the majority of the released energy can

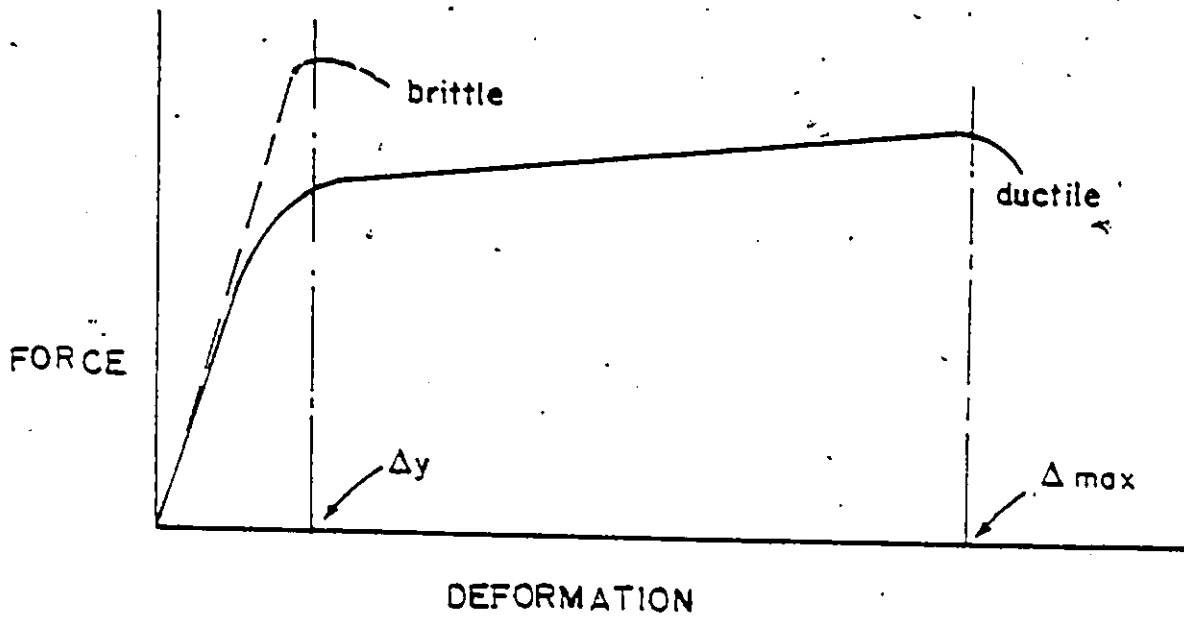


FIG. 4 DUCTILE AND BRITTLE BEHAVIOR

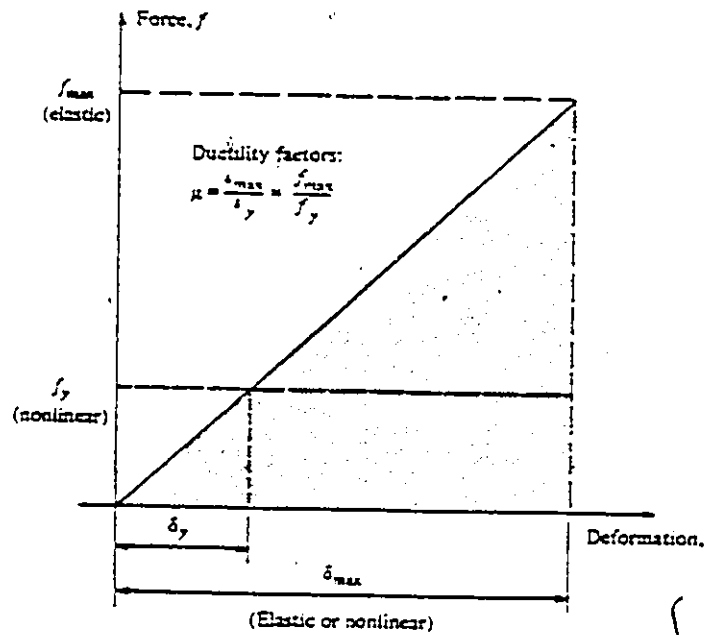


FIG. 5 DEFINITION OF DUCTILITY FACTOR (Ref. 9)

be absorbed by the beams through inelastic deformation. It is clear that although failure of a beam may not be critical, column failure is usually accompanied by the collapse of the structure. Although a balance of the strengths of the beams and columns appears to be applicable, a strong-column-weak-beam philosophy is to be recommended in the design of earthquake resistant structures. Over the years, a design philosophy has evolved to improve the behavior of earthquake resistant structures by increasing the ductility of members thus allowing the structure to absorb energy by inelastic deformations.

When the lateral force induced by earthquake ground motion is so high that yielding is expected to occur, the capacity of the structure to deform beyond yield with minimum loss of strength depends mainly on the ductility of its members. It has been commonly believed that failure of connections is usually accompanied with the failure of the structure; hence, corner connections should be designed so that both sufficient ductility and adequate strength or stiffness be achieved to ensure the survival of structures during a severe earthquake.

### 1.1.1 Ductility

The ductility  $\phi_u / \phi_y$  or  $\delta_u / \delta_y$ , defined as the ratio of the maximum deformation developed in a member to its

elastic-limit deformation, is the most commonly used measure of the ductility of a member because of its simple application; In the field of the earthquake-resistant structural design, the concept of energy absorption is preferred. This is equal to the area under the force-deformation curve as shown in Figure 5 .

From comparisons of the stress-strain relationships of the reinforcement steel and the concrete, it is easily understood that steel can develop much more ductility, and therefore, the reinforcement is usually the critical factor for a reinforced concrete section to display ductility.

Clough and Penzien (9), from the comparison of the results of the nonlinear analysis and elastic analysis of a structure, found that the maximum displacements are essentially identical in both cases with the maximum displacements of the nonlinear system only a few percent larger. By considering the nonlinear dynamic and elastic deformations being the same, Clough and Penzien defined the ductility factor,  $\mu$ , as

$$\mu = \frac{\delta_{\max}}{\delta_y}$$

where  $\delta_{\max}$  is the maximum deflection and  $\delta_y$  is the elastic limit deformation. The results of a standard build-

ing presented in "Dynamics of Structures" (\*) demonstrated that the use of approximate inelastic-response analysis procedure can be adequate. The procedure involves performing a linear earthquake-response analysis and providing the strengths of all the members with the computed elastic member forces reduced by a ductility factor. The nominal design strength can be represented by the elastic earthquake-response force and a ductility factor specified for the member; as represented in Figure 5, it was obtained that:

$$f_y = \frac{1}{\mu} f_{\max}$$

In this case, the ductility factor refers to the amount of inelastic deformations acceptable in the member and can be taken as :

$$\mu = \frac{f_{\max}}{f_y}$$

In the past, the absorption of energy by inelastic deformation of the frame was not critical because buildings were mostly constructed with nonstructural partitions and walls whose capacities for energy absorption were sufficient and significant. On the other hand, the current high-rise buildings with partition walls of negligible weight have to depend on the structural frame to provide the capacity to absorb energy.

Current earthquake-resistant design practice involves detailing the beam-column joints to carry the large lateral loads and displacements and to minimize stiffness degradation at the joints. Where lateral displacement is concerned, the maximum values frequently occur at the top story corners and this is the reason the analysis of corner joints is of equal importance to that for interior joints or other primary members, if the integrity of the joint and the structure is to be maintained under a severe earthquake.

## 1.2 STUDY GOALS

In an effort to improve the behavior of buildings and structures to fulfill the necessary requirements for reliable earthquake resistant design, extensive research into the response of structures under earthquake loads has been carried out using model tests. Most research has used two-dimensional reinforced concrete specimens. This is for several reasons, which include simplification of the loading system, the construction and the theoretical analysis of the specimens.

With a view to gradually improving the level of earthquake resistance of buildings, the purpose of this study is to review and evaluate, by means of small-scaled model tests, the response of reinforced concrete corner joints to simulated seismic action. A reinforcing detail is recom-

mended to minimize the damage to structures from future earthquakes.

From the laboratory results, the efficiency of external beam-column corners, which is defined as the ratio of the measured maximum moment capacity to the calculated flexural capacity of the beam, is found to be dependent on the flexural steel percentage and the geometry of the reinforcement of the joint. The failure modes could be used for prediction of the strength of the corners.

It has been shown in this study that the time sequence and the magnitudes of the loading program have a significant influence on the non-elastic behavior of all reinforced-concrete connections; consequently, detailed comparison of results with beam-column corner joints tests by other researchers are difficult and rarely successful. Hence, it is suggested that the results and recommendations herein summarized be treated as a guideline to the study of the behavior of corners under seismic loading conditions. Meaningful comparisons of member or joint performance from various researches can be only achieved using an internationally recognized standard test sequence.

## Chapter II

### ANALYSIS OF REINFORCED CONCRETE CORNERS

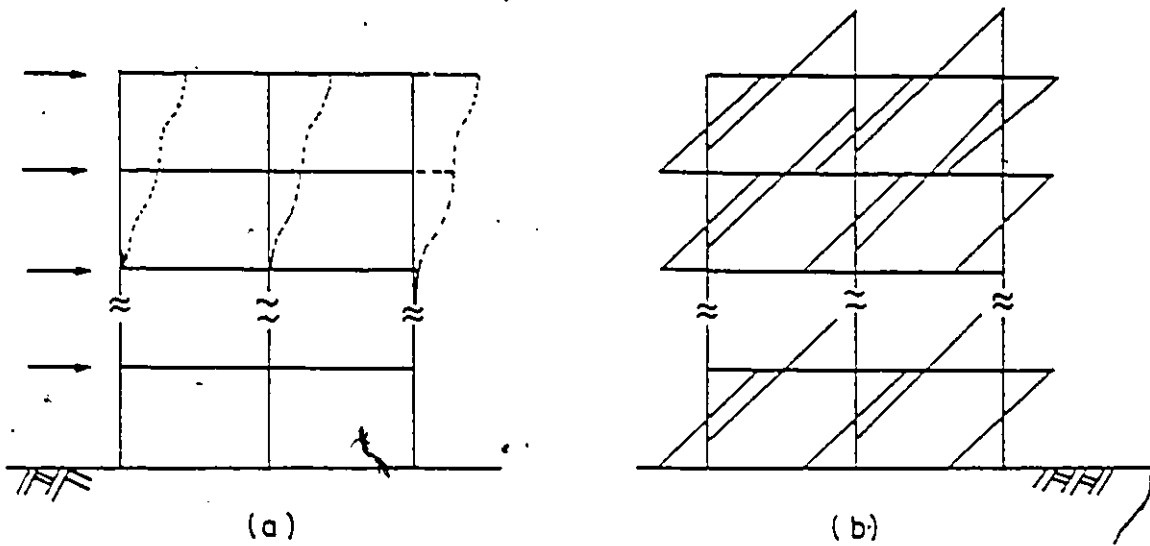
#### 2.1 GENERAL REMARKS

For the purpose of structural analysis, it is commonly assumed that the beam-column connections of reinforced concrete structures are rigid zones. However, when reinforced concrete frames are subjected to bending moments from lateral forces as shown in Figure 6, the beam-column connections are subjected to large shear forces and large moments, and thus the assumption of a rigid joint block can be inappropriate.

With reference to the response of a structure under reversed high-intensity loads, flexural yielding as well as the ductility of the components should be emphasized to ensure the amount of energy dissipated. The primary objective of this study was to investigate the behavior of beam-column corners of reinforced concrete frames subjected to lateral loads.

In the analysis of reinforced concrete corner joints of a structural frame as seen from Figure 6-b, when one corner is subjected to an induced moment which tends to open the

corner, the other corner is closed by a moment such that the relative lateral displacement is essentially zero.



(a) Deformation and

(b) Bending Moments

Due to Lateral Forces

FIG. 6 FRAME SUBJECTED TO LATERAL FORCES

## 2.2 THEORETICAL ANALYSIS

### 2.2.1 Corners Subjected to Closing Moment

Using the theory of elasticity, which is valid for concrete only before cracking occurs, and assuming the corner

as one homogeneous body, Paduart in 1940 (20) derived an expression for the stress function of a point inside the joint block. The stresses thus given satisfied the equilibrium conditions of the element but not the conditions applicable to geometrical compatibility. The calculated tensile and compressive stresses perpendicular to the corner diagonals are reproduced as in Figure 7 which are valid only within the elastic limit, i.e. for an uncracked section subjected to bending moment only.

As cracks develop, the concrete can no longer be assumed to be homogeneous, isotropic and elastic and the deformations and forces of the joint block are usually represented as shown in Figure 8 .

It can be seen from Figure 8-a that the resulting force of the steel force (T) and the concrete force (C) is a diagonal compression force along line EF. It has been realized that detailing for this type of corner does not encounter many difficulties. This is because the compressive stresses can normally be resisted by the concrete without exceeding the strength of the concrete. The relatively large tensile forces indicated at points A and B from the elastic analysis are easily provided for by the beam and column steel which continue around the outside of the joint. Possible failure modes are bearing splitting, shear cracks or bond deterioration, usually after yielding of the main reinforcement.

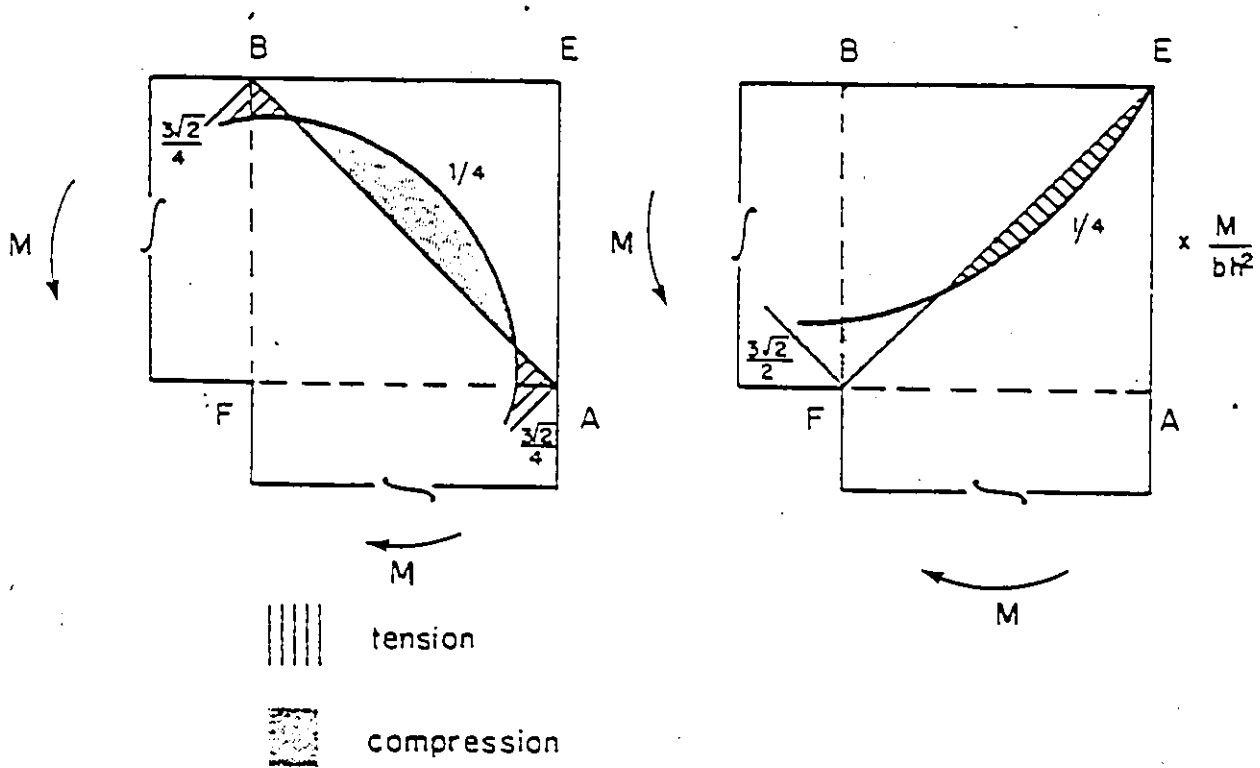
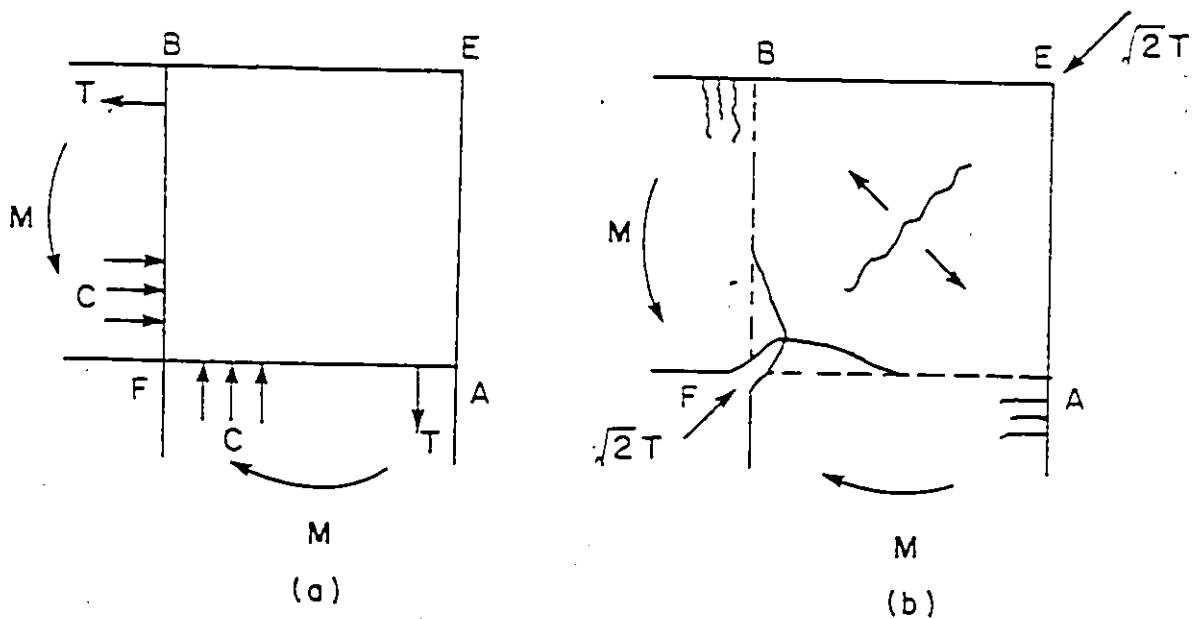


FIG. 7 STRESS DISTRIBUTION  
THEORY OF ELASTICITY



(a) forces  
(b) deformations

FIG. 8 CLOSING CORNER AT ULTIMATE LOAD

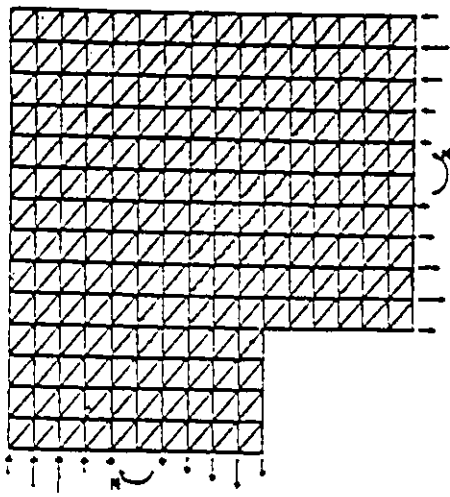
### 2.2.2 Corners Subjected to Opening Moment

Most problems exist in the detailing of beam-column joints when the bending moments tend to open the corner. With the rapid development and availability of computer facilities, a study has been made of the stresses in the region of corner joints in a plane building frame, having members of rectangular cross-section using the Finite Element Method. It divides the corner into several hundred triangular elements as shown in Figure 9. The Concrete Structures Division of Chalmers University of Technology, Sweden, have developed a computer program in Fortran for the analysis of stresses in the region of the joint before it cracks.

Assumptions were that;

1. the material is linearly elastic and
2. the applied moments on the joint are replaced in the analysis by point loads at the element boundaries.

The results of the analysis were presented in the form of stress flow with the principal stresses being indicated in magnitude and direction at the centroids of the elements. The method of analysis assumes that strains and thus stresses are constant in each element.



Division into elements

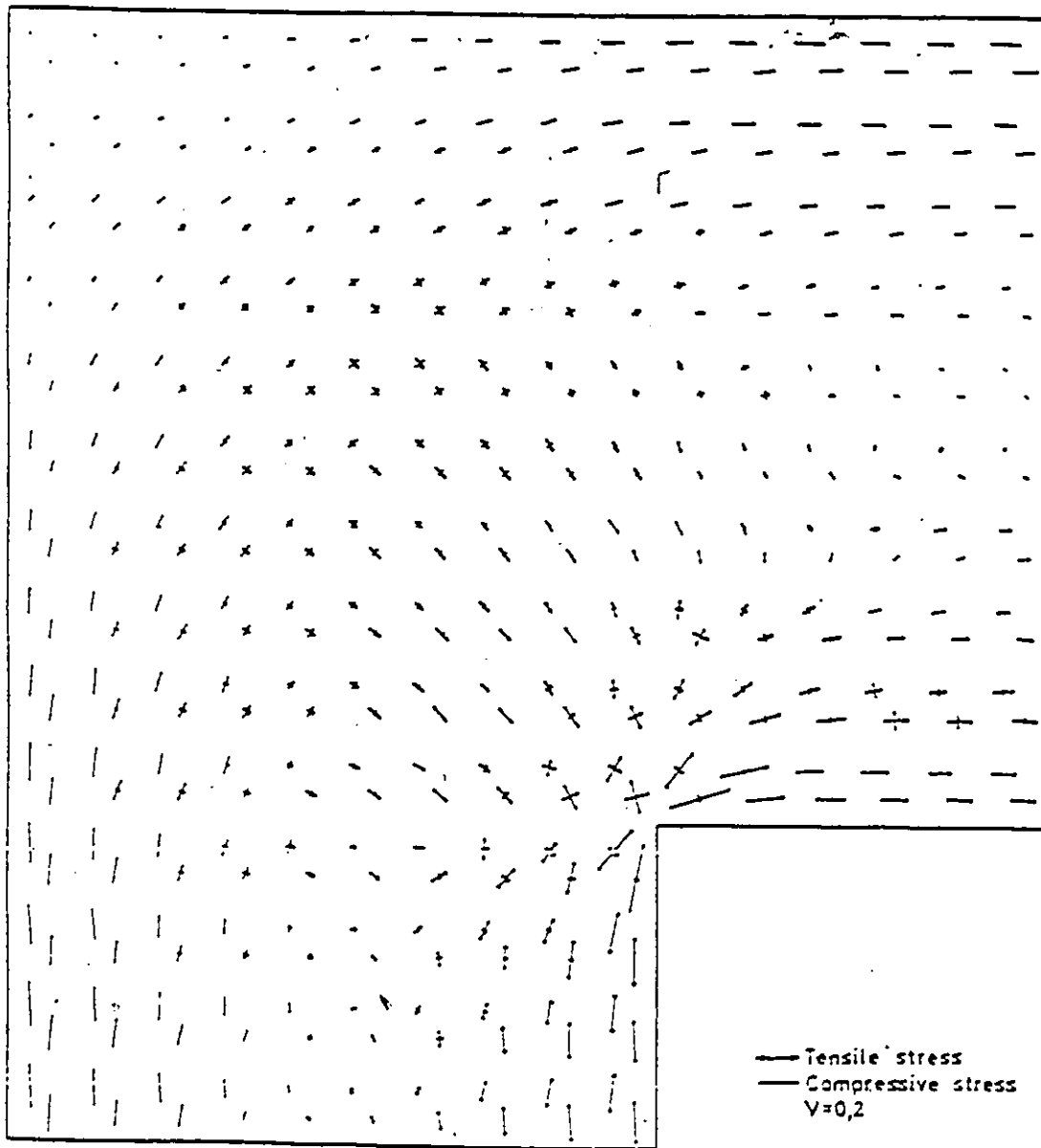


FIG. 9 FINITE ELEMENT METHOD (Ref. 18)

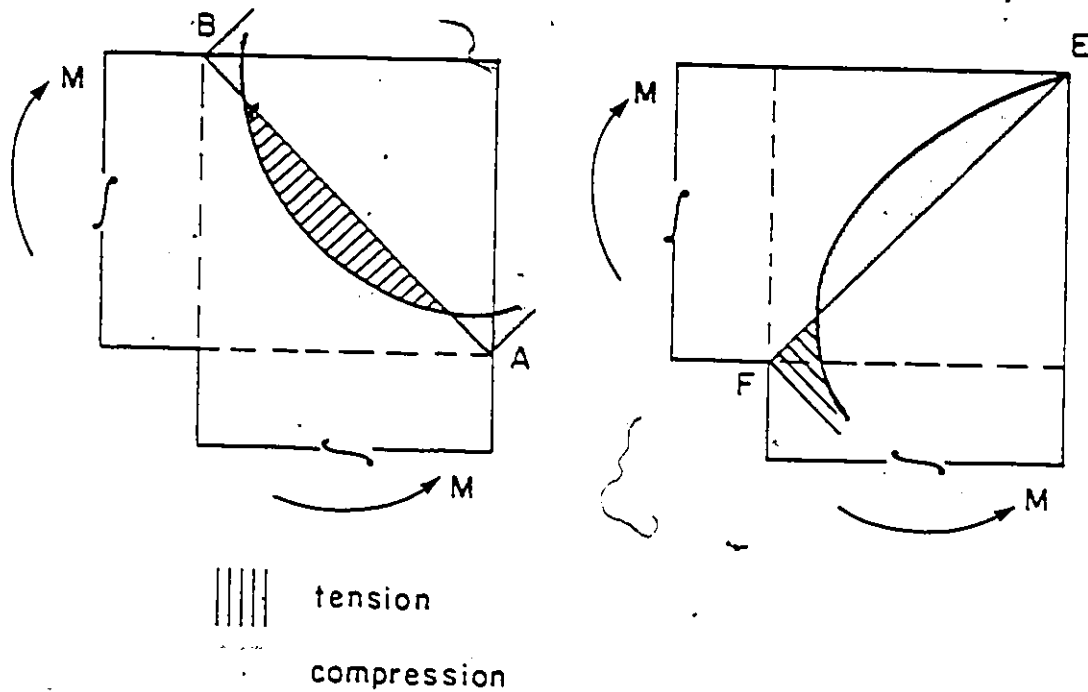
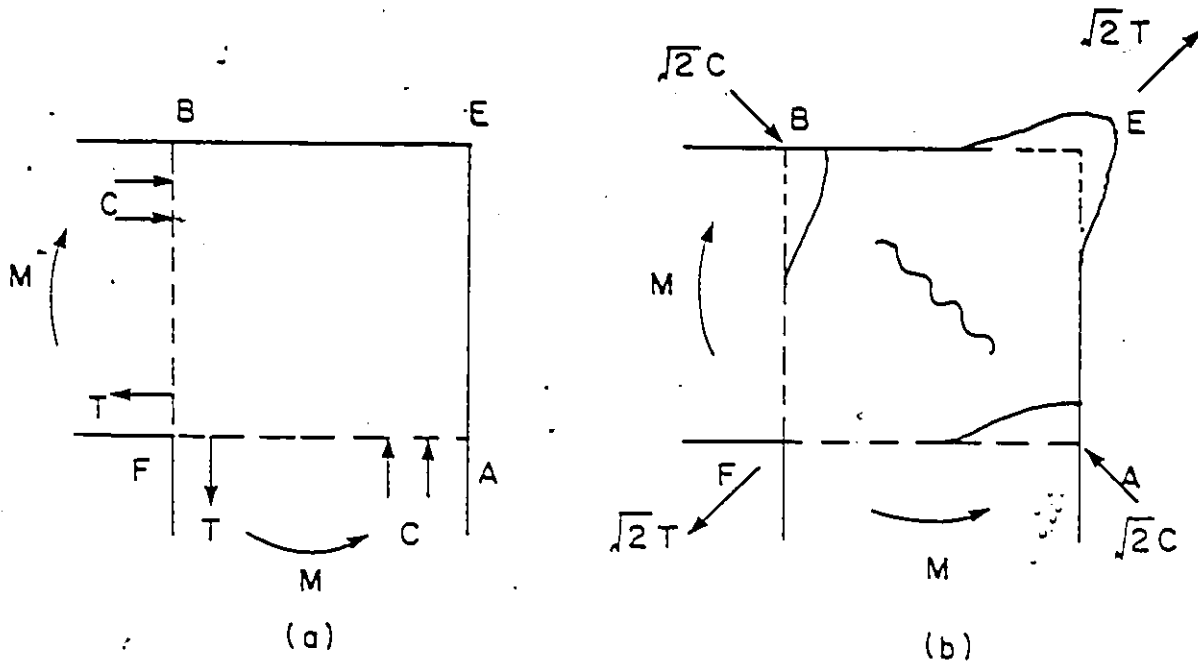


FIG. 10 STRESS DISTRIBUTION  
 FINITE ELEMENT METHOD (Ref. 18)

It was found that, when the corner concrete is assumed to be homogeneous, isotropic and elastic, the tensile stress across the corner section is very high at the inner angle, which explains the reason why cracks develop in this region at very low loads. These tensile stresses across the corner diagonal resemble a parabolic distribution which is similar to Paduart's results. The results in the form of the magnitude and directions of principal stresses are reproduced in Figure 10 .



(a) forces  
(b) deformations

FIG. 11 OPENING CORNER AT ULTIMATE LOAD

At ultimate load, Figure 11 represents the forces and deformations of the joint which is now regarded as a non-homogeneous, non-isotropic and inelastic system. In Figure 11-a, the resultant force of the steel force (T) and concrete force (C) is a tensile force along diagonal EF. This resulting tensile force tends to cause diagonal tensile cracks as shown in Figure 11-b. resulting in a sudden failure of the member. It is understood that additional reinforcement along diagonal EF is necessary to carry the diagonal tension force to maintain the integrity of the corner.

### 2.3 MODES OF FAILURE

In order to accurately predict the behavior of corner joints when subjected to either monotonically increasing load or repeated and reversed loading, it is essential that the reasons for failure of the connection be understood.

When a corner joint is subjected to flexural bending, it can fail in any of the following five modes :

1. Yielding of the Tension Reinforcement - Such a failure, caused primarily by yielding of the tension reinforcement is preferred to give a ductile response to load. In this case, large deformations ( $\Delta$ ) are involved. Possible consequences after the yielding of the tension reinforcement are illustrated in Figure 12 .

In the case of closing moment, Figure 12-a shows crushing of the concrete at the inside corner whilst flexural cracks developed on the outside surface and extended towards the inside corner. Figure 12-b shows diagonal tension cracks together with flexural cracks at the inner corner in the case of an opening moment.

2. Compression Failure - If the concrete strengths of the corner core and the adjacent connected members are the same, failure by crushing of the con-

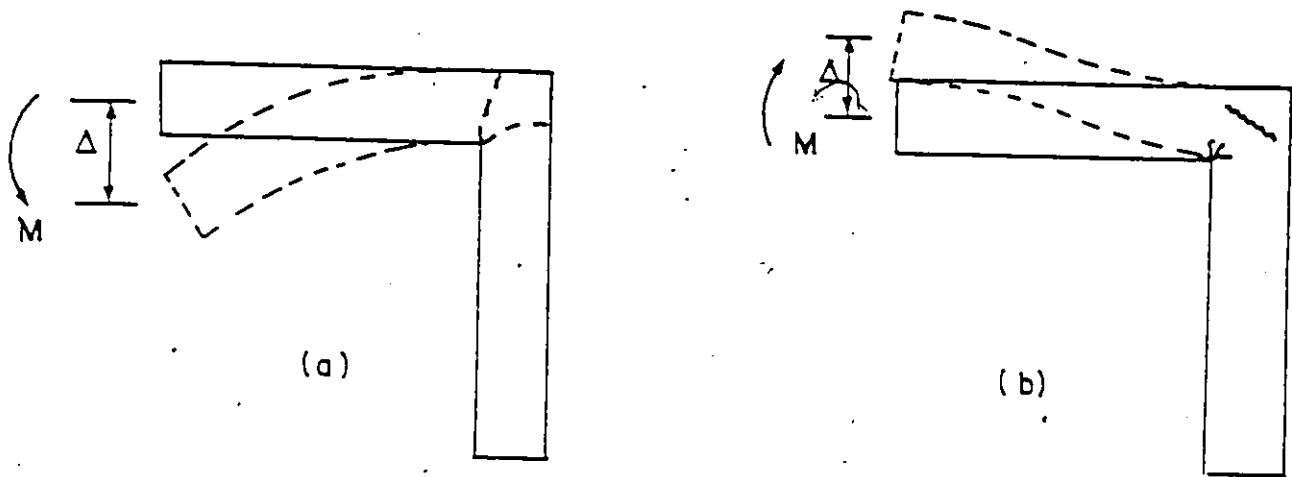


FIG. 12 DUCTILE FAILURE (a) closing corner  
(b) opening corner

crete rarely occurs because the specified design compressive strength of concrete can usually resist the compression force.

3. Anchorage Failure - Although sufficient anchorage length has been provided, this mode of failure can occur due to the gradual deterioration of bond caused by repeated and reversed loadings. Large cracks and slip of the reinforcement would be observed at failure; flexural cracks and diagonal cracks will reduce the bond capacity with pulling out of the reinforcing bar as a consequence.

4. Splitting Failure - When the corner is subjected to closing moment, tensile stresses are expected to occur perpendicular to the direction of the reinforcement at the bends. The tensile stress causes splitting of the concrete at the bends resulting in sudden failure of the joints.
5. Diagonal Tension Crack Failure - This occurs in a corner if the large tensile forces developed in the corner core along the diagonals are not resisted by tensile reinforcement. This failure happens often to a corner when it is subjected to moment which tends to open it.

In Figure 13-a, using truss analogy, the concrete compression zone is regarded as compression strut (A'E' and B'E') with the tension reinforcement as tension bars (A'F' and B'F'). The resultant force across diagonal EF is a tensile force of a magnitude  $\sqrt{2} T$  or  $\sqrt{2} C$  as shown in Figure 13-b. The theory of elasticity predicted a parabolical distribution of stress across the diagonal struts (A'B' and E'F') and is shown in Figure 14 .

If  $f_c$  is the tensile strength of the concrete,  $b$  is the width of the connection and  $l_{dc}$  is the diagonal crack length, an expression for the occurrence of the first diagonal crack can be found from the equilibrium of forces. In

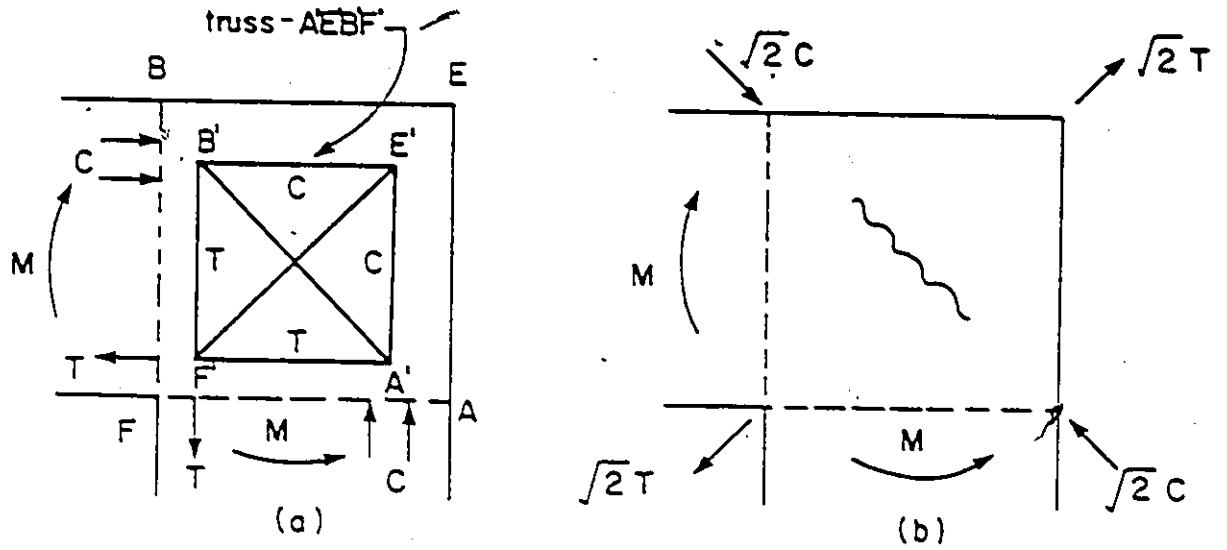


FIG. 13 DIAGONAL TENSION CRACK FAILURE

Figure 14-a, the area of tension portion along the diagonal crack length  $l_{dc}$  can be written as :

$$\text{Area} = \frac{2}{3} l_{dc} f_t$$

with the force thus produced equivalent to

$$\text{Force} = \frac{2}{3} l_{dc} f_t b$$

If  $F_s$  is the tensile reinforcement force at the first diagonal crack, the resulting diagonal force  $\sqrt{2}F_s$  can be expressed as :

$$\sqrt{2}F_s = \frac{2}{3} l_{dc} f_t b \quad (a)$$

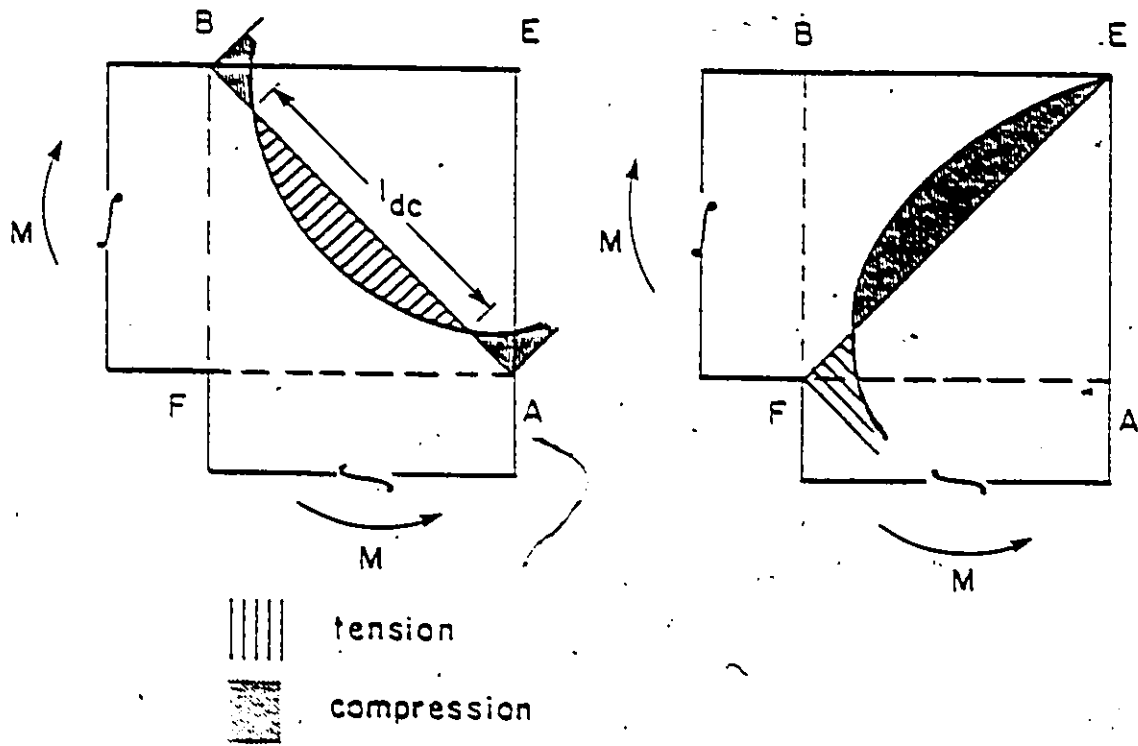


FIG. 14 STRESS DISTRIBUTION  
FINITE ELEMENT METHOD.

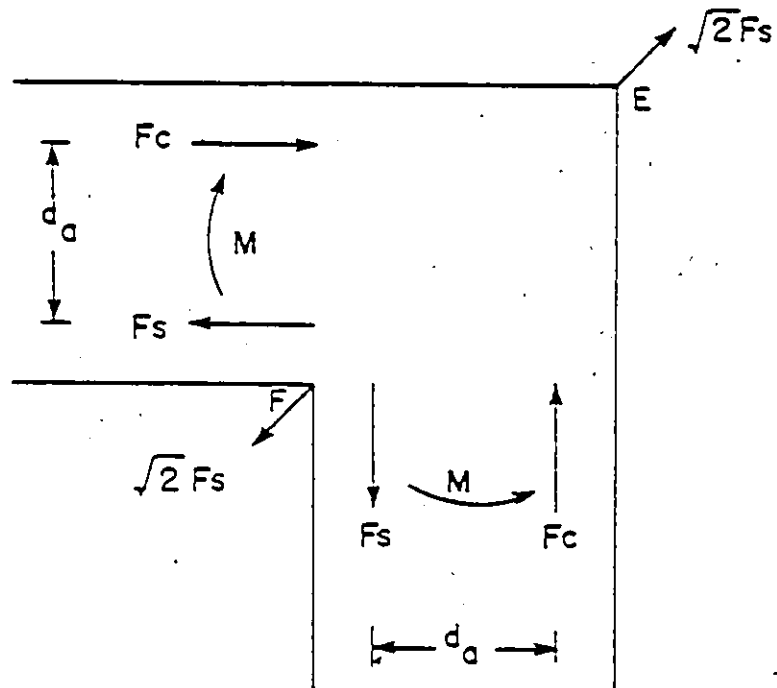


FIG. 15 OPENING CORNER AT DIAGONAL CRACKING

According to Figure 15, the corresponding moment by the tensile force  $F_s$  at the corner can be written as :

$$M = F_s d_a \quad (b)$$

thus, combining equations (a) and (b) and referring to Figure 15 gives :

$$M = (\sqrt{2}/3) l_{dc} f_t b d_a \quad (c)$$

Equation (c), which gives the moment to cause a diagonal tension crack, is dependent on the value taken for the tensile strength of concrete. ACI-318-77 suggests that a conservative estimate for the tensile strength of concrete can be taken as  $f_t = 6 \sqrt{f_c'}$  ( $0.5 \sqrt{f_c'}$ ), then equation (c) becomes :

$$M = 2\sqrt{2} l_{dc} b d_a \sqrt{f_c'}$$

or

$$(\sqrt{2}/6) l_{dc} b d_a \sqrt{f_c'} \quad (S.I. Units)$$

which can be used to predict the occurrence of the first diagonal crack at the corner.

## 2.4 DUCTILITY AND STIFFNESS OF STRUCTURES

### 2.4.1 Ductility

According to Blüme, Newmark and Corning (7) with reference to Figure 16, the yielding moment of a reinforced concrete cross section can be written as :

$$M_y = A_s f_y j d$$

and the curvature of a section as

$$\phi_y = \frac{v}{d(1-K)}$$

where  $\rho = A_s / bd =$  tensile reinforcement ratio

$$n = \frac{E_s}{E_c} = \text{modular ratio}$$

$M_y =$  yielding moment of cross section

$A_s =$  cross section area of tensile reinforcement

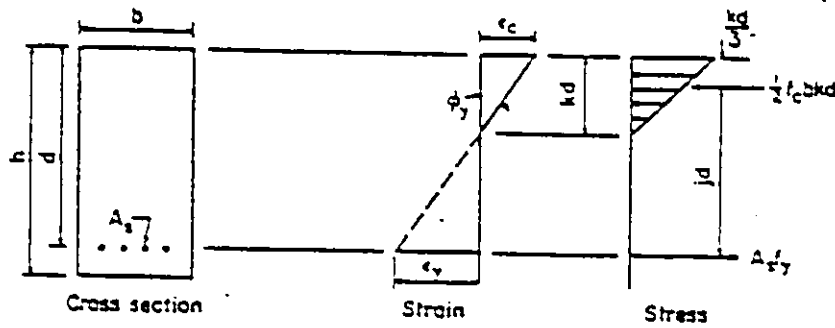
For a reinforced concrete section with only tension reinforcement, the ductility ratio of a member,  $\phi_u / \phi_y$ , defined as the ratio of deformation at ultimate to that at yield, can be expressed as :

$$\frac{\phi_u}{\phi_y} = \frac{\epsilon_{cu}(1-K)}{\epsilon_y K_u}$$

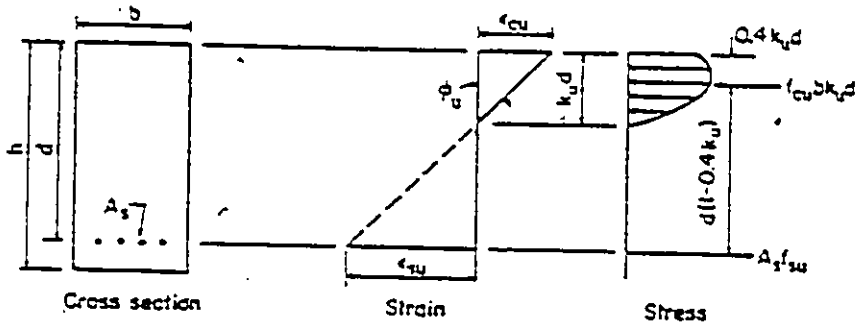
where

$$K_u = (\rho - \rho') \bar{f}_y / f_{cu}$$

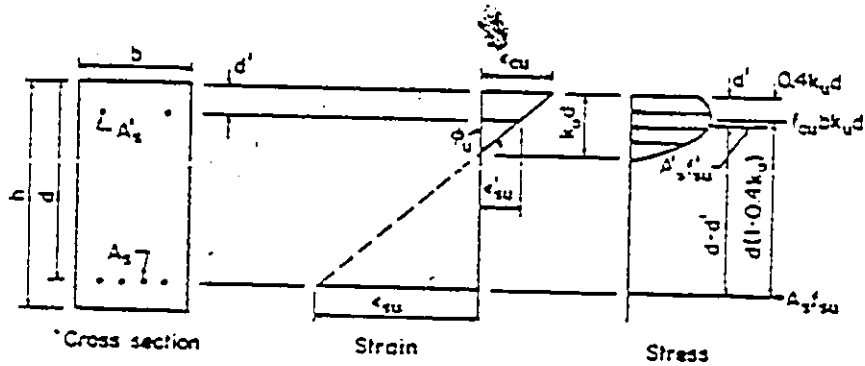
$$K = \sqrt{(\rho - \rho')^2 n^2 + 2(\rho - \rho')n} - (\rho - \rho')n$$



Distribution of strain and stress at yield capacity.



Distribution of strain and stress at ultimate capacity.



Distribution of strain and stress at ultimate capacity for a section with compression reinforcement.

FIG. 16 STRESS-STRAIN RELATION OF A R. C. SECTION ( Ref. 7)

For specimens with compression reinforcement, the ductility will be increased due to a decrease in the value of  $K_u$ ; Fintel (12) and Blume et al (7) noted that an increase of ductility can be achieved by :

1. a decrease in the tensile reinforcement ratio, which decreases the strength but increases the ductility of a section.
2. addition of compression reinforcement which does increase the ductility of a section but the influence is of small value.
3. an increase in concrete compressive strength
4. decrease of yield strength of the reinforcement

The ACI 318-77 Building Code Requirements dealing with earthquake resistant design specify a minimum concrete strength of 3,000 psi (20.68 MPa), maximum yield strength of reinforcement of 60,000 psi (413.7 MPa), and minimum and maximum flexural reinforcement ratios of  $200/f_y$  ( $1.4/f_y$ ) and  $0.5 \rho_b$  respectively.

#### 2.4.2 Stiffness

Stiffness is the moment required to develop unit lateral rotation. In the case of a beam-column joint, the magnitude of the joint rotations gives measurements of the stiffness of the corner.

Swann (28) compared the deflection due to normal flexural behavior, assuming a rigid joint block, with the measured rotation of the beam. It was found that the measured beam deflections were often greater than those expected. Thus, he concluded that the additional deflection occurred because of the presence of the joint, i.e. rotation of the joint block.

## Chapter III

### REVIEW OF LITERATURE

#### 3.1 INTRODUCTORY REMARKS

One of the problems in designing reinforced concrete structures for seismic resistance is good detailing of beam-column joints. Numerous series of tests and investigations have been carried out with most of them concentrated on the analysis of the interior or exterior beam-column joints. However, in this thesis, only those concerned with the behavior of corner joints will be reviewed.

In general, the corner joint subjected to an applied moment which tends to open its reentrant corner is weaker than a similar joint designed to resist an applied moment which tends to close the reentrant corner. The strength of an opening corner depends to a great extent upon its detailing, and many possible details are applicable.

Unless otherwise stated, all the previous research described in the following sections involved loading corner joints under monotonic loading only.

### 3.2 PREVIOUS RESEARCH

As early as 1934, Wastlund (29) conducted laboratory tests on beam-column connections with corner reinforcement consisting of loops, as shown in Figure 17. Parameters considered included concrete quality ( $\sigma_c$ ), the radius of curvature of the loop ( $r$ ), the width of the concrete specimen perpendicular to the plane of the loop ( $t$ ), model scale and, most important of all, the capacity of concrete to resist bearing stress caused by such reinforcement loops.

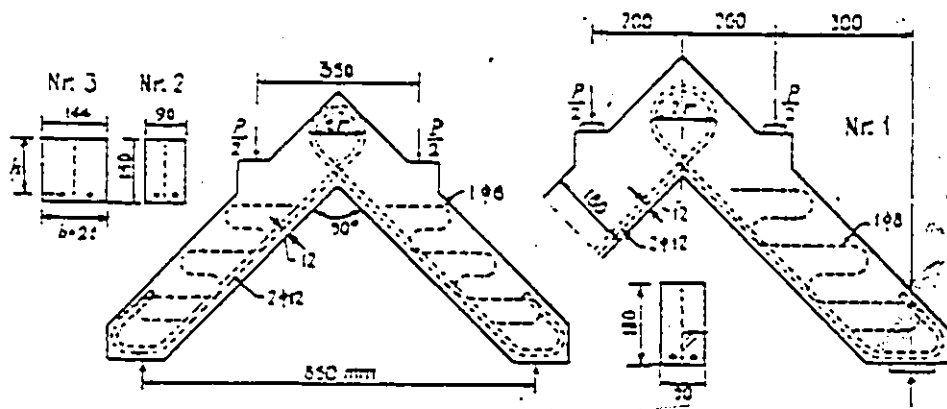


FIG. 17 CORNER TESTS BY WASTLUND (1934)

(Ref. 29)

Wastlund derived an empirical formula which expressed the steel stress ( $\sigma_s$ ) at failure of the concrete in terms

of the compressive strength of the concrete, radius of the loop as well as the diameter of the reinforcement bar. The expression is now reproduced as follows :

$$\sigma_s = 3.53 (\sigma_c)^{2/3} \left(\frac{r}{\phi}\right)^{0.8} \left(\frac{r}{\phi}\right) \left(\frac{1}{\phi}\right)^{0.3} \text{ kgf/cm}^2$$

$\sigma_c$  = compressive strength of concrete      kgf/cm<sup>2</sup>

$r$  = radius of loop      cm

$\phi$  = diameter of bar      cm

However, the formula is certainly out of date due to the differences in concrete strength, steel qualities, and bond characteristics compared to those used in current practice.

In 1943, Posay and Kofoid (22) performed tests on opening corners. The reinforcing details developed consisted of inner corner main bars, diagonal corner bars and trimming bars all welded together at the inner corner of the main bars as shown in Figure 18 .

In a study of corner joints under opening moments in 1943, Guzensky (13) proposed the use of reinforcing loops

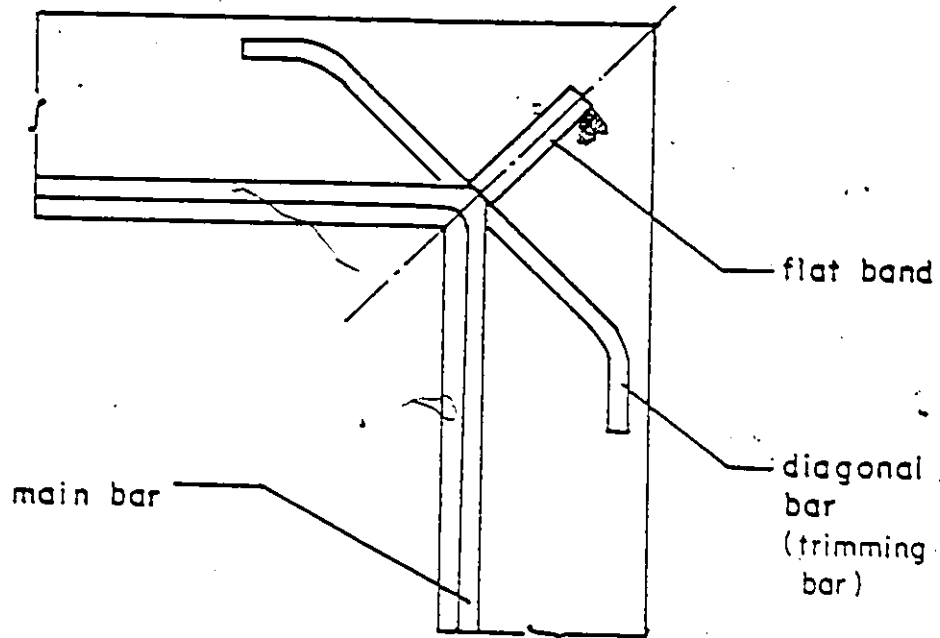


FIG. 18 CORNER DETAIL BY POSEY & KOFOID  
(1943) (Ref.22)

and a crossbar. It was noted that, when the external moment tends to open the corner, the concrete itself could never develop sufficient resistance to the tensile force induced in the joint and thus, a reinforcing strip is necessary so as to provide the concrete core with tension reinforcement.

Ostlund (19) in 1963 investigated the risk of splitting failure of the concrete at the corner with the results summarized in the Swedish Concrete Building Code, "Regulations for Concrete Structures".

Ostlund developed an expression for the tensile force in the reinforcement bend in terms of the concrete compressive strength, steel yield stress, diameter of the bend and the diameter of the reinforcement; the formula so derived can be used to predict the occurrence of the splitting failure at the bends.

Sandbye (24,25,26) published three technical articles on the behavior of corner joints between 1967 and 1970. Sandbye's tests were conducted simply by applying uni-directional moments either opening or closing the joint. It is worth noting that, for the loading arrangements of specimens as shown in Figure 17 and Figure 19, the load was applied at an angle of 45 degrees to the beam section whilst the majority of other investigations used force applied perpendicularly to the beam section.

Considerable work was carried out by Swann (28) at the Cement and Concrete Association, England, between 1969 and 1970, in which eighteen reinforced concrete specimens of beam-column corner joints were tested with thirteen of them subjected to opening moments and five to closing moments.

A beam reinforcement ratio as high as 3 % ( $0.667 \rho_b$ ) was used in Swann's tests. Nevertheless, joint efficiencies, which were defined as the ratio of the measured moment ca-

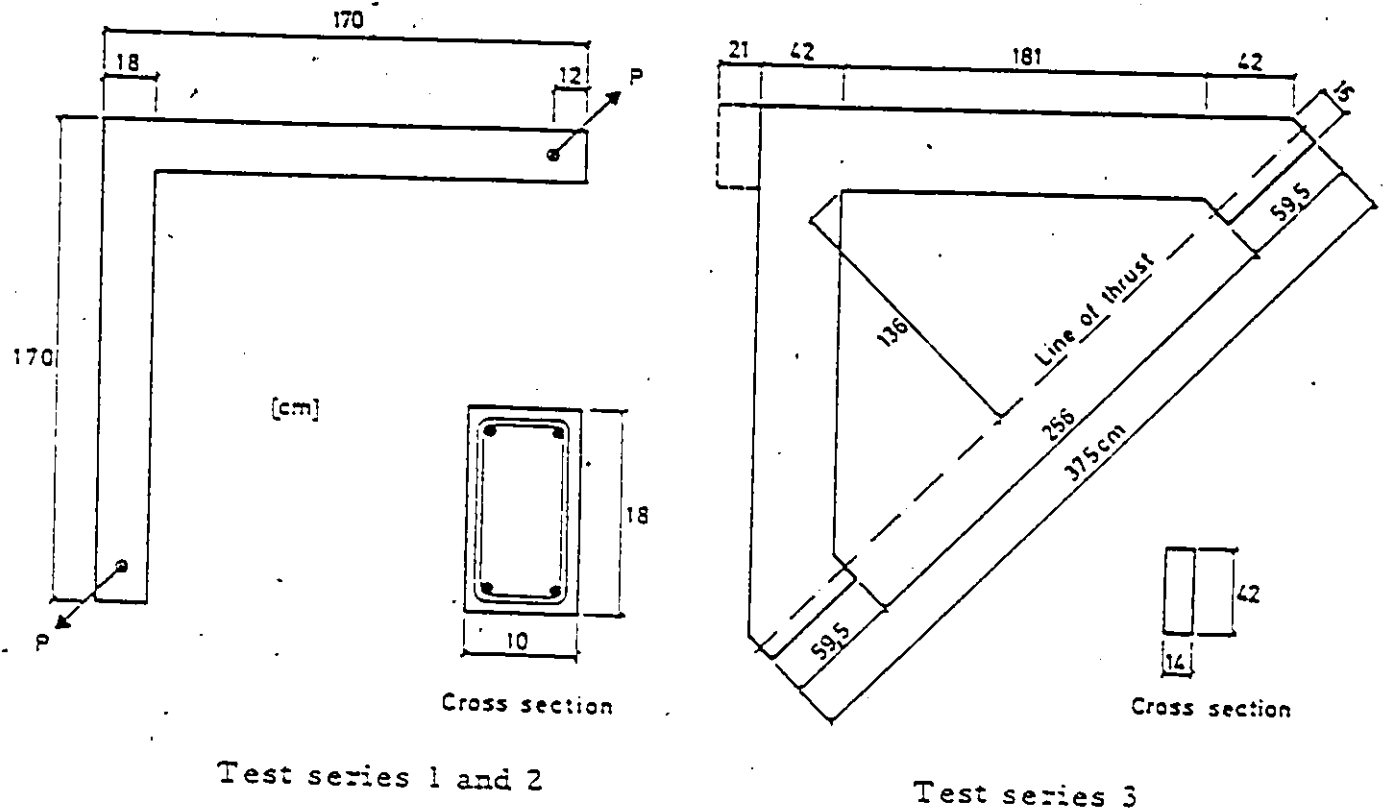


FIG. 19 CORNER TESTS BY SANDBYE (1967)  
(Ref. 24)

capacity to the theoretical moment capacity, as high as 90 % were obtained when the applied moment tended to open the corner for two reasons. Firstly, the area of the diagonal stiffeners was twice that of the main reinforcement in the corner, and as a result, the joint core was expected to be able to resist the resulting diagonal tension forces with the diagonal steel. Secondly, the nominal yield strength of

the main reinforcement was low with a value of 45,000 psi (310.3 MPa). As mentioned in Chapter II, a decrease in the reinforcement yield strength increases the ductility of the member. Due to the heavy reinforcement at the corner, failures of the corner were observed to be mainly by splitting cracks under the bends of the reinforcement.

Swann recommended the use of a steel-frame design at the joint. Three very important conclusions can be made from Swann's work, namely : -

1. a high percentage of flexural steel ratio should be avoided;
2. bearing failure limited the strength of the specimens and
3. the use of trimming bars at the inner corner does not increase the strength of the corner significantly.

Test results on six corners under opening moments conducted by Kordina and Fuchs (16) in 1970 were satisfactory with corner efficiencies as high as 99 %. The method of loading was similar to that used by Sandbye. The reinforcing details and crack patterns are reproduced in Figure 20 . The respective corner efficiencies of 88, 88, 93, 97, 99 and 96 percent accordingly could be explained by the use of a very low reinforcement ratio of 0.78 % ( $=0.28 \rho_b$ ).

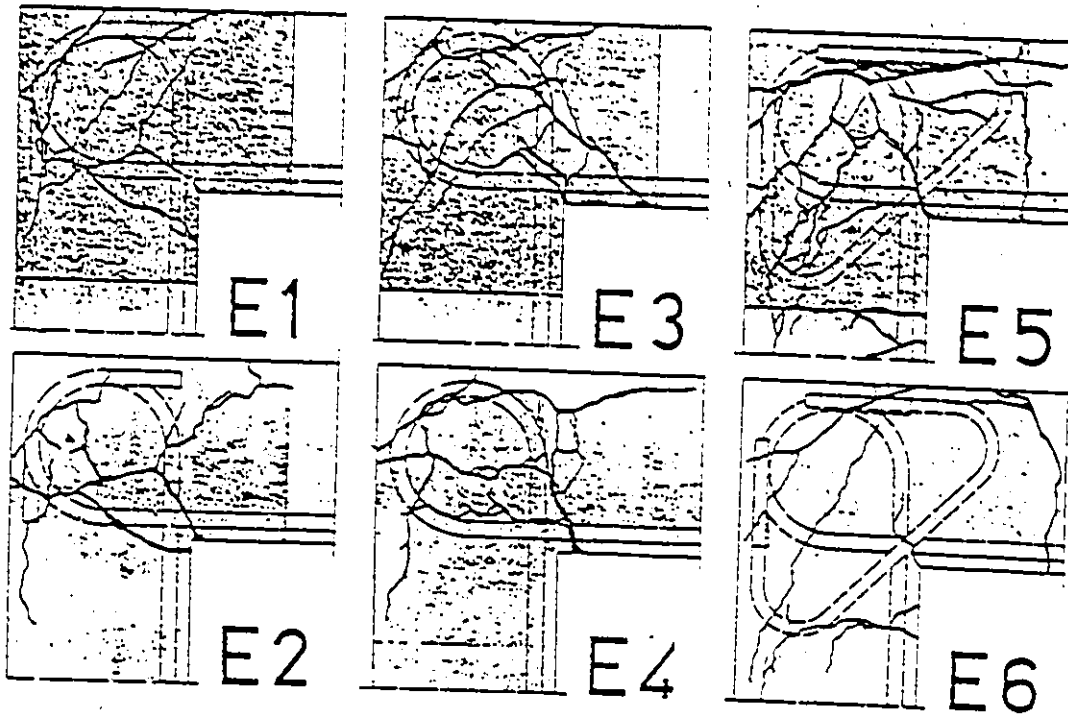
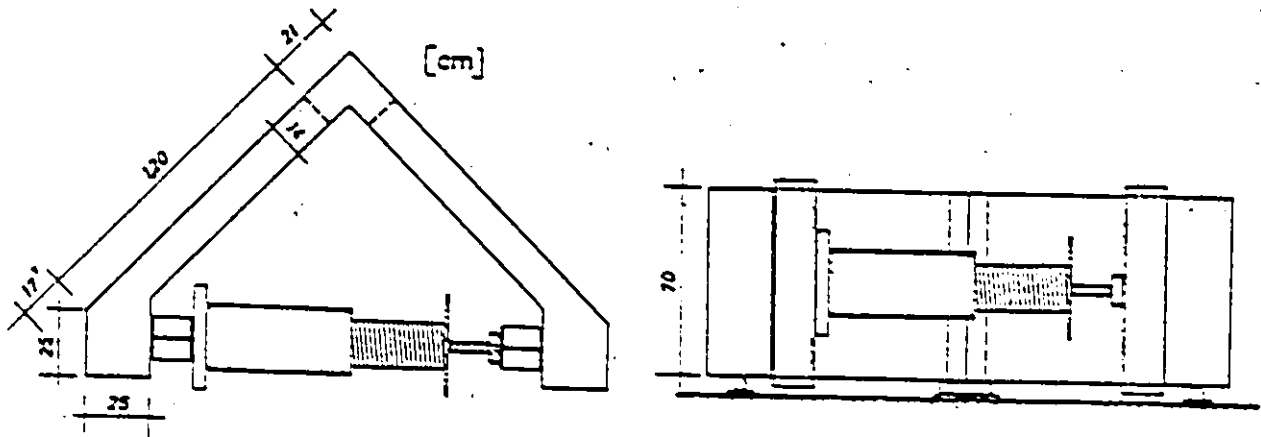
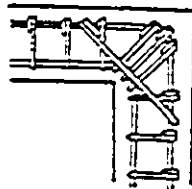


FIG. 20 TESTS BY KORDINA AND FUCHS (1970)  
(Ref. 16)



DETAIL 26

FIG. 21 TEST BY MAYFIELD ET AL (1972)  
(Ref. 5)

Similar tests were carried out on light weight concrete corners by Bennison et al in 1971 and 1972 (4,5). It was concluded that "the use of two sets of mutually perpendicular diagonal reinforcement was a promising method for developing flexural strength, reducing crack widths, and producing reasonably ductile behavior." However, in the report of May, 1971, after testing 48 reinforced light weight concrete corners, Bennison et al observed that, when the applied load opened the corner, none of the details tested developed the full strength of the bending members.

Of the 28 types of reinforcement detail tested, Bennison et al reported that detail 26, shown in Figure 21, gave the best performance. The diameter of the main reinforcement used in detail 26 was 0.39 in. (10 mm), which is equivalent to a steel ratio of 0.65 % (0.26 pb). For the diagonal reinforcement, the diameter of each of the stirrups and trimming bars was also 0.39 in. (10 mm); i.e. the corner was reinforced excessively with two mutually perpendicular diagonal bars. In addition, it was suggested that the three stirrups may be replaced by equal area reinforcement without significantly reducing the strength.

The work of Nilsson in 1973 (17,18) is especially worthwhile of note for the various types of joints tested. Nilsson compared the measured results with several coun-

tries' building design codes and commented that many countries did not put enough emphasis on the reinforcement detailing of corner joints. Only the codes of Germany and the U.S.S.R. state that special considerations be given to the failure criterion of joints, and recommend use of diagonal reinforcement and ties.

Nilsson catalogued the five modes of failure described earlier, namely, diagonal tension cracks in the corner, splitting crack failure, yielding of main reinforcement, anchorage failure and concrete compression failure. Reasonable results and also valuable conclusions can be drawn from Nilsson's study dealing with each of the criteria. In essence, Nilsson's conclusions and recommendations were related to the corners subjected to monotonic loading only; the laboratory tests were all conducted on the specimens simply by loading the corners to failure in one direction. It is, however, in the present study, recommended that considerations be given to the establishment of analyses of the corner joints under seismic loading, because, a corner joint will be subjected to opening moment and closing moment when the structure is subjected to earthquake motion.

Nilsson mentioned of the considerable influence on the efficiency of the corner by the reinforcement details and the flexural reinforcement percentage. For corners sub-

jected to opening moments, Nilsson proposed a reinforcing layout of the corner as in Figure 22, which consisted of reinforcement at the outside corner of compression zone and the inside diagonal steel. An area of approximately 50 % of that of the main steel was proposed for the trimming bars. In Nilsson's tests, the reinforcement percentage of the flexural member was chosen to be less than 1.2 %.

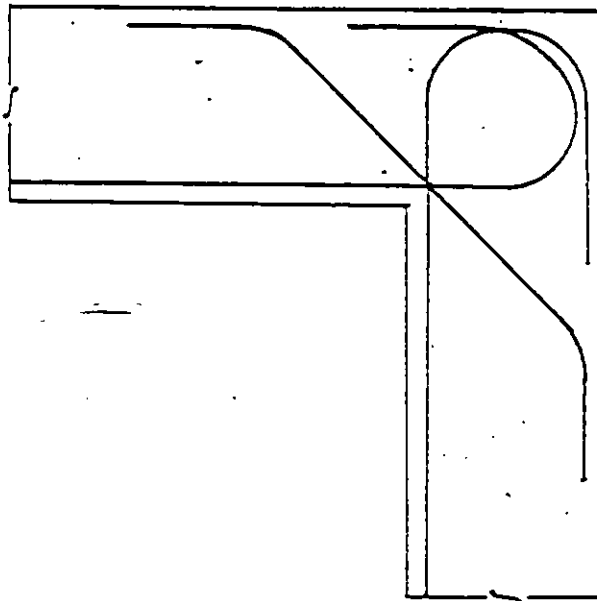


FIG. 22 CORNER DETAIL PROPOSED BY  
NILSSON (Ref. 18)

Nilsson concluded that the maximum reinforcement percentage should be limited to 1.2 % for reinforcing steel having a yield strength of 60,000 psi (413.7 MPa). The proposal for design of corners according to Nilsson, subjected to opening moment has been incorporated into the Bridge Specifications of the Swedish Road Board (Statens Vagverks Brobyggnade Anvisningar, 1969, Clause 13.322)

### 3.3 REVIEW OF BUILDING DESIGN CODES

Reinforcing details set by several buildings design codes are reviewed in this section, for corner joints subjected to opening moments.

Figure 23 shows the details considered by the Joint Committee of the Concrete Society and the Institution of Structural Engineers in 1970 (15), for the corner to resist a bending moment tending to open the joint. Of the three details shown, the committee agreed that detail 'a' with looped reinforcement should be avoided. However, it is evident that detail 'b' is never effective for the corner resisting the opening moment, the result of a test on a similar detail will be presented in a later chapter. Furthermore, detail 'c', similar to specimen # 5 in this study, does not appear to be capable of developing the full flexural strength when the joint is subjected to opening moment.

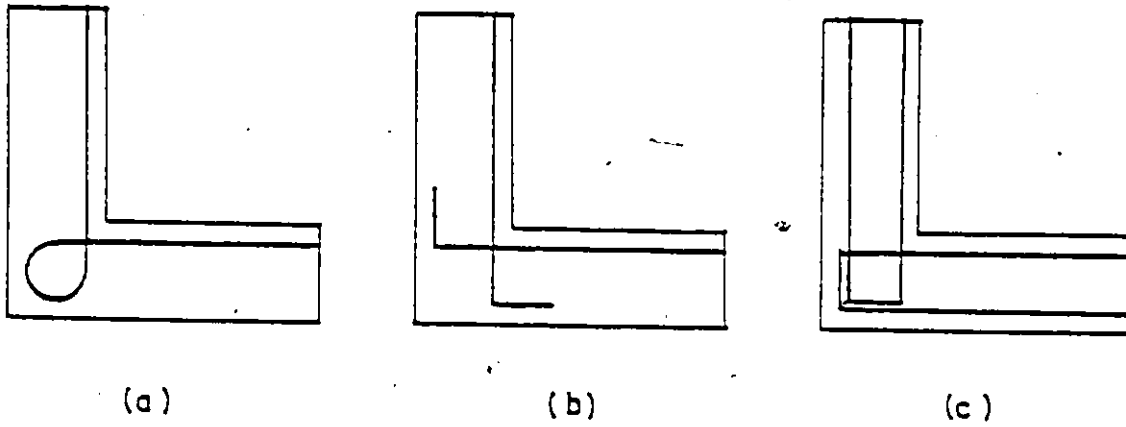


FIG. 23 DETAILS BY A BRITISH COMMITTEE  
(Ref. 15)

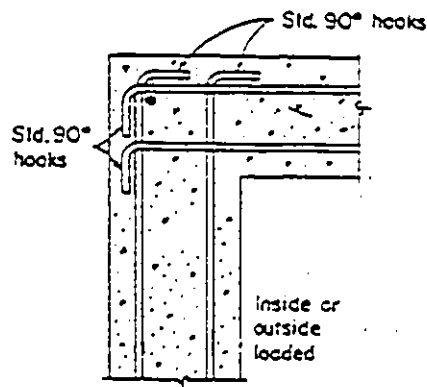


FIG. 24 CORNER DETAIL BY ACI 318-74  
(Ref. 1)

The American Concrete Institute (ACI 318-74) (1) developed a simple corner detail similar to Figure 24. It was shown on the "Proposed Revision of ACI 318-74 Manual of Standard Practice for Detailing Reinforcing Concrete Structures, 1970".

This particular detail does not attain the full flexural strength as a similar detail, specimen # 4, was tested in this study. Depending on the reinforcement percentage, the corner efficiency was in the range of 40 to 60 % with failure due to the excessive tensile stresses in the concrete core. The current building design code, ACI 318-77 does not mention the importance of nor the necessity of additional diagonal steel at a corner to resist the tensile stress produced in the concrete of joint.

On the contrary, as stated earlier, the German and Russian Building Codes do introduce diagonal tensile steel to the joints to carry the resulting tensile stresses. Figure 25 is the reinforcement detail commonly accepted in Germany (11), Nilsson reported that, the efficiency of  $M_{ut}/M_{uc}$  (ratio of the measured flexural moment capacity to the computed theoretical moment capacity) of such a detail was as low as 32 % without the diagonal stirrups, and 80 % with the stirrups. For detail 'b' in Figure 25, with reinforcement loops and without diagonal stirrups, the corner efficiency lay be-

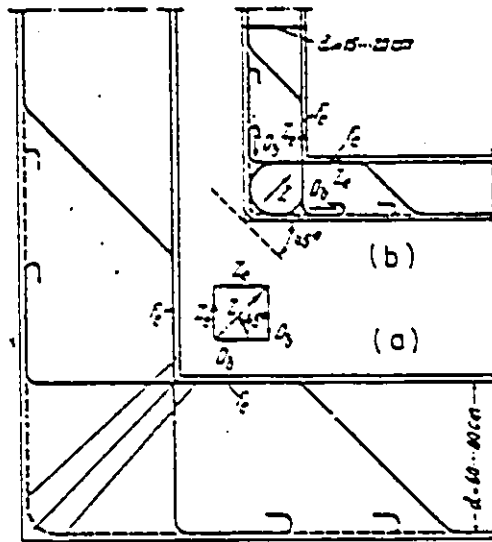


FIG. 25 STANDARD CORNER LAYOUT RECOMMENDED IN GERMAN BUILDING CODE (Ref. 11)

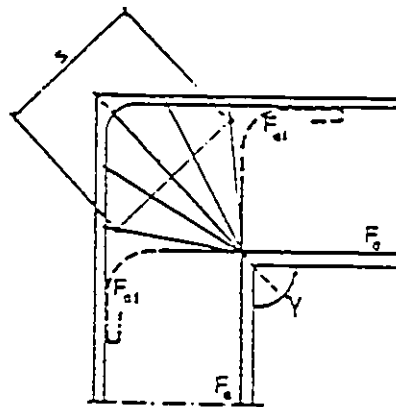


FIG. 26 STANDARD CORNER LAYOUT RECOMMENDED IN RUSSIAN BUILDING CODE (Ref. 6)

tween 30 to 77 %. Comparisons between the efficiencies did imply that the reinforcing detail with diagonal tensile stirrups gave more consistent and reliable performance.

For a corner subjected to opening moment, the Russian Building Design Code (\*) gives the solution shown in Figure 26. It is similar to detail 'a' of the Germany regulations, with an efficiency of 80 %. It was clearly stated that diagonal stirrups were introduced to carry the resultant diagonal force induced by the flexural reinforcement stresses.

#### 3.4 AIM OF THE INVESTIGATION

The object of this study was to investigate the behavior of beam-column corner connections of a reinforced concrete frame subjected to simulated earthquake loads, and to determine the joint requirements to ensure obtaining ultimate capacities for the beams and columns subjected to multi-reversals of loadings of major earthquake magnitude.

For this purpose, nine specimens were tested statically under various load schedules which were either monotonic or high-stress cyclic. The flexural reinforcement ratio, the arrangements of the reinforcing bars and the loads varied for each specimen, and the cracks and failure behavior of these connections are discussed for each specimen test.

## Chapter IV

### EXPERIMENTAL WORK AND INSTRUMENTATION

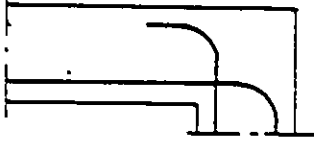
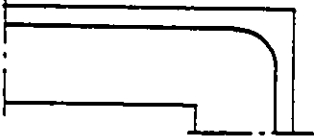
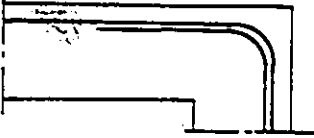
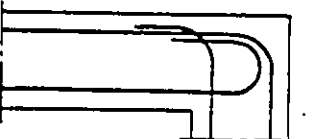
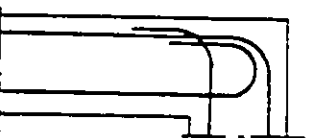

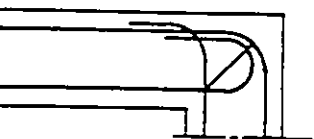
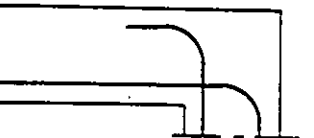
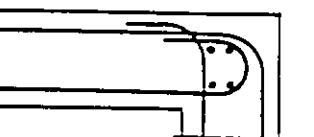
#### 4.1 GENERAL CONSIDERATION

The experimental investigation was conducted in the structural laboratory of the Department of Civil Engineering at the University of Ottawa. The basic concept of the investigation was to load to failure, under repeated and reversed loading, a number of corner joints with commonly used reinforcement details. Two series of tests were conducted on a total of nine reinforced concrete beam-column corners subjected to either uni-directional loading or static cyclic loading to simulate the effect of severe earthquake loading. Two different test set-ups, which will be discussed in detail later in the chapter, were used for the two series of tests. The schedule of specimens and the loading procedure are given in Table 1

In selecting the experimental systems, the member sections and the materials to be tested, the following aspects were considered :

1. All specimens had nominal beam and column cross section dimensions of 6.00 x 6.25 in. (152x158 mm)

TABLE 1  
Test Schedule

Specimen	Date(1980) of Cast	Flexural Steel Ratio (%)	Load Procedure	Main Steel Detail
1	June 11	1.27	opening	
2	June 20	1.27	closing	
3	Aug. 19	1.27	closing	
4	Sept. 3	1.27	cyclic	
5	Oct. 3	0.70	cyclic	
6	Oct. 29	1.27	cyclic	
7	Nov. 7	0.70	cyclic	
8	Nov. 21	1.27	opening	
9	Dec. 4	1.27	cyclic	

were reinforced with 60,000 psi (413.7 MPa) nominal yield reinforcing steel and a nominal concrete compressive strength of 5,000 psi (34.47 MPa). The section dimensions were chosen to give steel ratios of  $\rho_b/4$  and  $\rho_b/2$  with standard No.3 (9.5 mm diameter) and No.4 (13 mm diameter) reinforcing bar.

2. In designing the specimens, the current recommendations and procedures of ACI 318-77 Building Design Code was followed; namely, steel ratio less than  $\rho_b/2$ , tie spacings of  $d/2$  were chosen for the beam sections and six inches for the column sections, which is the smallest dimension of the column.
3. The load system for all tests was designed to give a bending moment distribution similar to that expected in a laterally loaded frame as shown in Figure 3.

#### 4.2 UNI-DIRECTIONAL LOADING

The first series of four specimen tests on #1, 2, 3 and 8, was preliminary. It was used to test and determine the problems in commonly used reinforcing details of corners and the problems in the testing procedure.

#### 4.2.1 Test Set-Up and Load Simulation

The specimens were tested on a large steel frame which supported the specimen at four points as shown in Figure 27

The supports were rollers or ball-joints which allowed rotation and horizontal translation. With this test frame, the first series of tests were made on three specimens, i.e. specimens # 1, 2 and 3 in which the loads were applied in one direction only using two 10-ton capacity Enerpac hydraulic jacks, connected to separate Enerpac pumps. Specimen # 1 was tested with load opening the corner and specimens # 2 and # 3 with load closing the corner. Tests of the first three specimens demonstrated that ball-jointed connections could be used efficiently between the load cells and the concrete sections; this eliminated the effects due to large deformations of the flexural members in keeping the load applied effectively to the members.

#### 4.2.2 Test Procedure

For all the tests, load supplied by the Enerpac pump was controlled manually with the load level measured by load cells. For the tests on specimens #1, 2, 3 and 8, the load was applied in several increments to collapse of the specimen. After each increment, the load was stabilized and

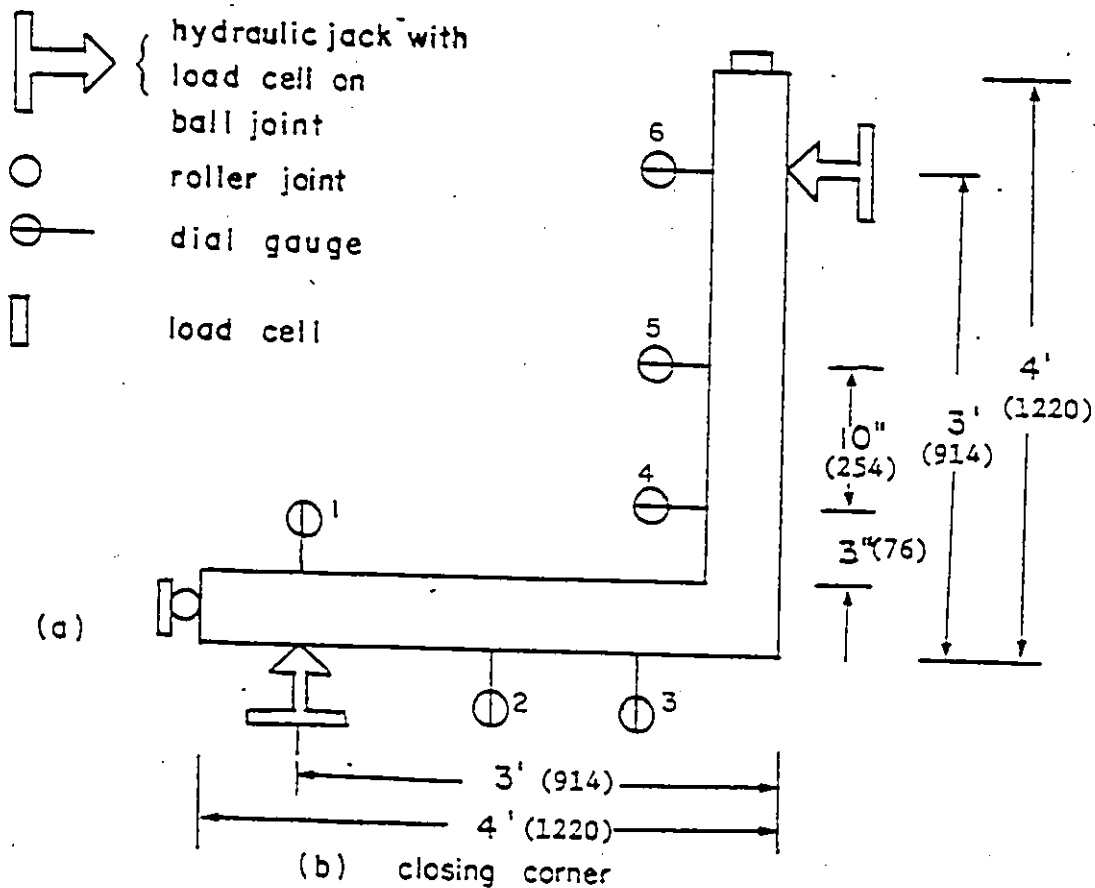
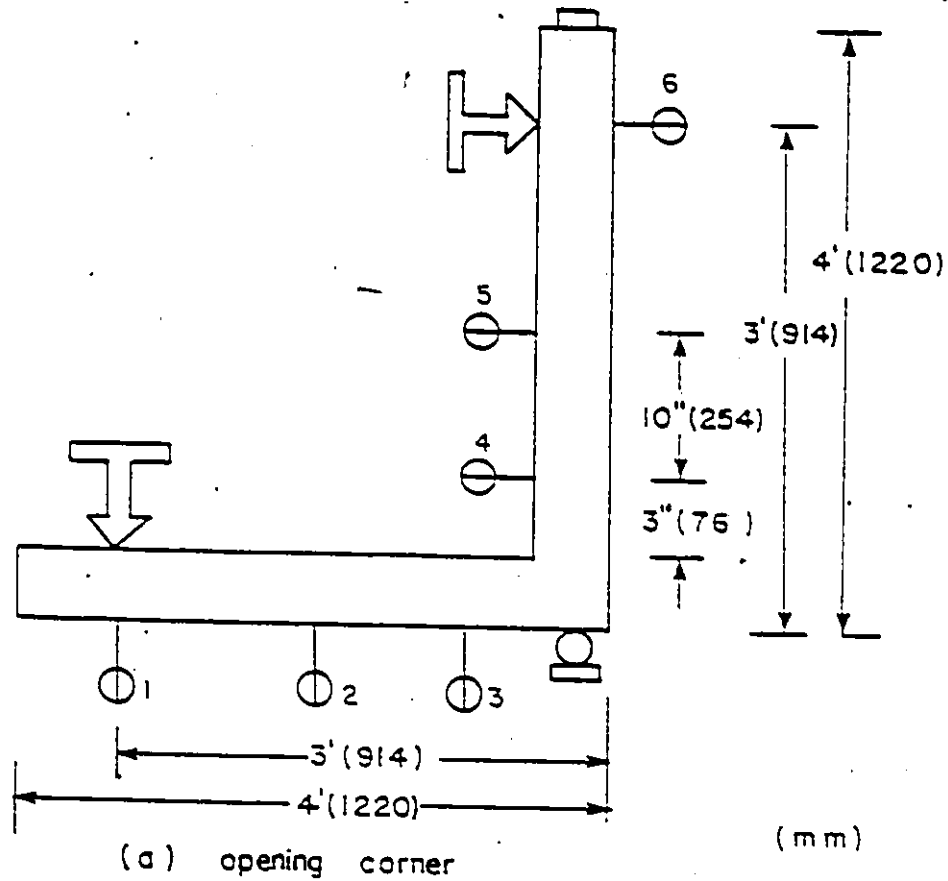


FIG. 27 TEST RIG FOR ONE-WAY LOADING

measurements were made of deflections, steel strains and concrete strains. In addition, the specimen was examined for crack formation.

#### 4.3 CYCLIC LOADING

The second series of four specimen tests on #4,5,6 and 7 was designed to determine the effect on the behavior under cyclic loading of the following variables; flexural steel ratio and modes of failure and to develop a reinforcing arrangement to increase the efficiency of the corner. The test on the last or the ninth specimen was to observe the influence of additional connecting beams to the corner; i.e., the difference of results between two-dimensional and three-dimensional specimens. The additional beams had cross-section dimensions of 6.25X6.25 in. (158X158 mm.)

##### 4.3.1 Test Set-Up and Load Simulation

The test set-up described in section 4.2.1 was impractical for cyclic loading so an alternative test rig was developed. The system consisted of clamping the column of the specimen to a strong floor and applying an inclined load to the end of the beam. Cyclic loading was achieved by reversing the pressures in the double acting jack, which has a capacity of 25 tons. Using a specially designed steel cage connected to the beam, loading to open or close the corner

was then possible without moving the specimens. The test rig which was used during the second series of test is shown in Figures 28, 29 and 30 .

The hydraulic ram used was a Miller model ph83b double acting hydraulic cylinder, 4-in. bore, 12-in stroke, service pressure of 5,000 psi (34.47 MPa). The load was applied at an angle of 45 degrees to the beam section as illustrated in Figure 30 .

The column was supported on a 2-ft. wide by 3-ft. long two-inch thick (610x1220x51 mm) steel plate by means of four 5x5x0.5 in. (127x127x13 mm) steel hollow box sections bolted to the base steel plate as shown in Figure 29 . The base plate itself was bolted to the laboratory floor by two 1.5 in. (38 mm) diameter threaded rods..

Figure 30 shows the load system. A load cage was attached to the beam section at a specified location as shown in Figure 30-b. The load cell, connected to the hydraulic ram, was bolted to the steel cage so that the loading force would be transmitted from the shaft to the beam through the steel cage. The hydraulic ram reacted against a large frame which had been assumed to remain steady and stable with concern to its size and the relatively low reaction by the hydraulic ram.

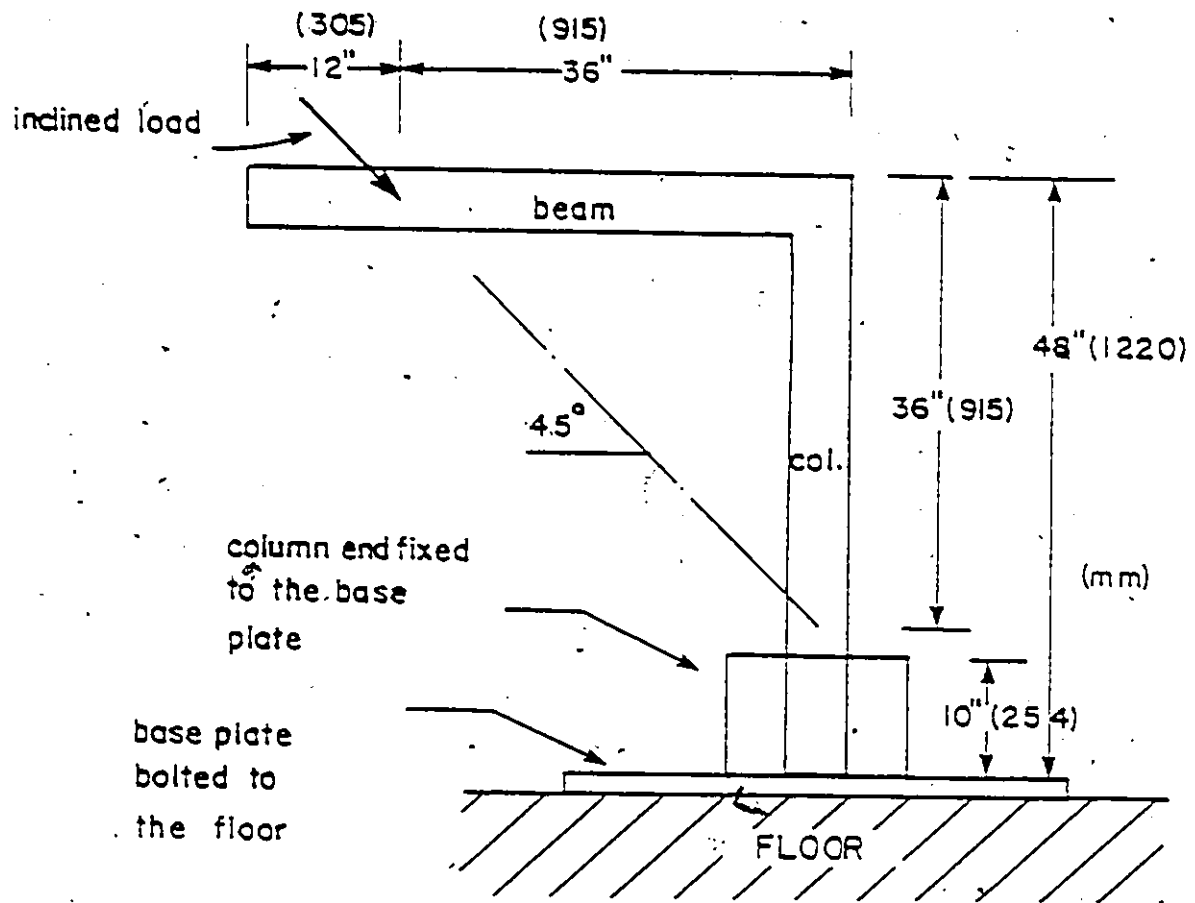


FIG. 28 TEST RIG FOR TWO-WAY LOADING

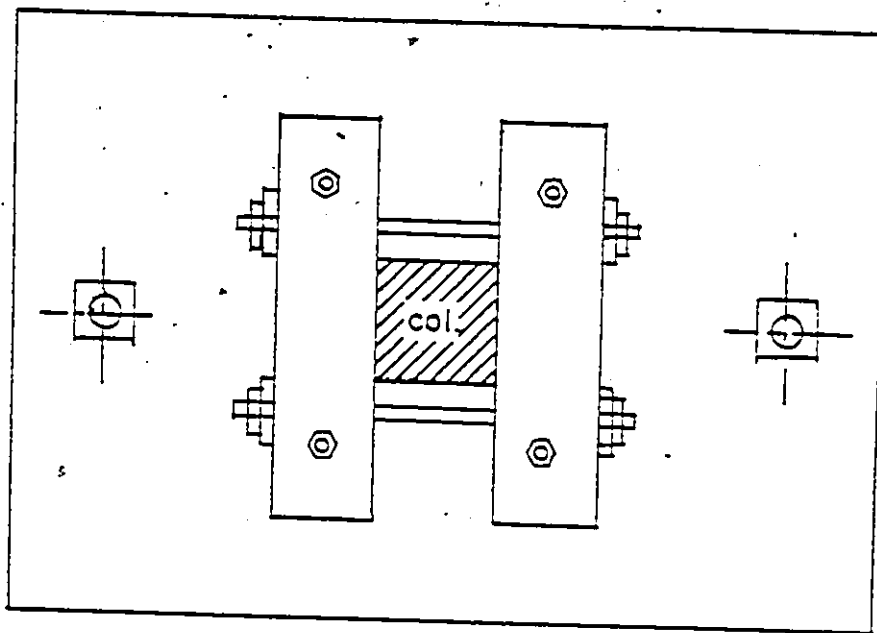
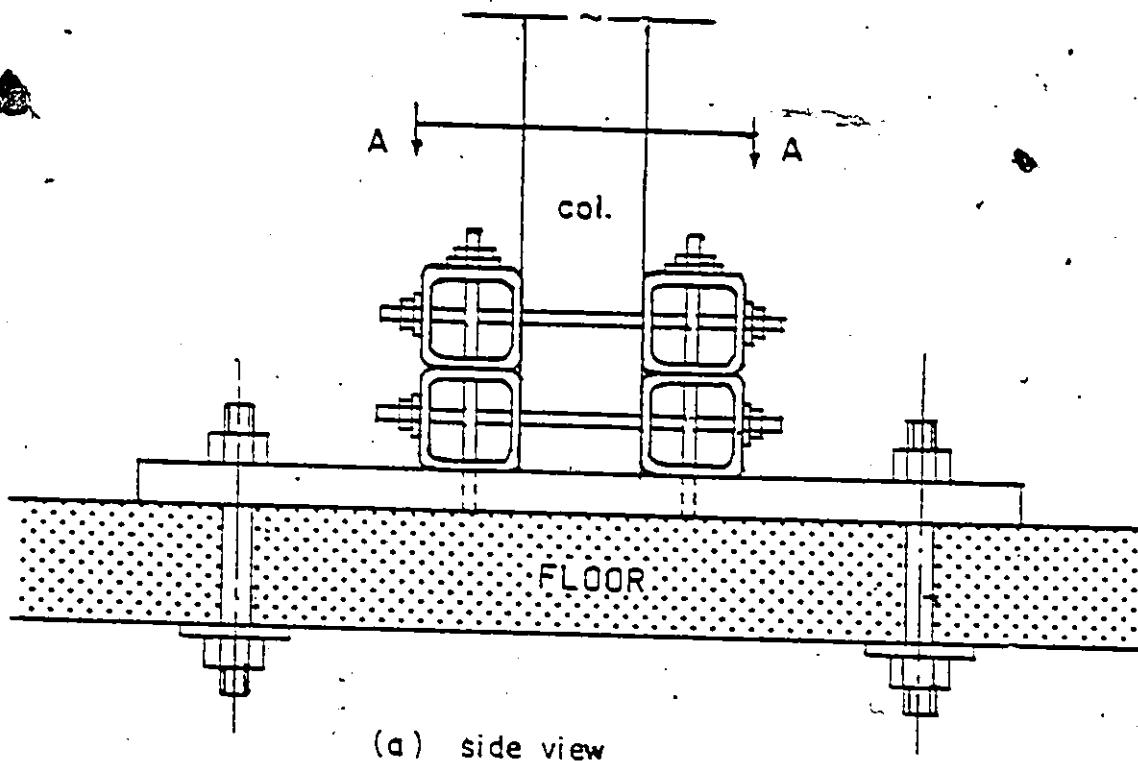
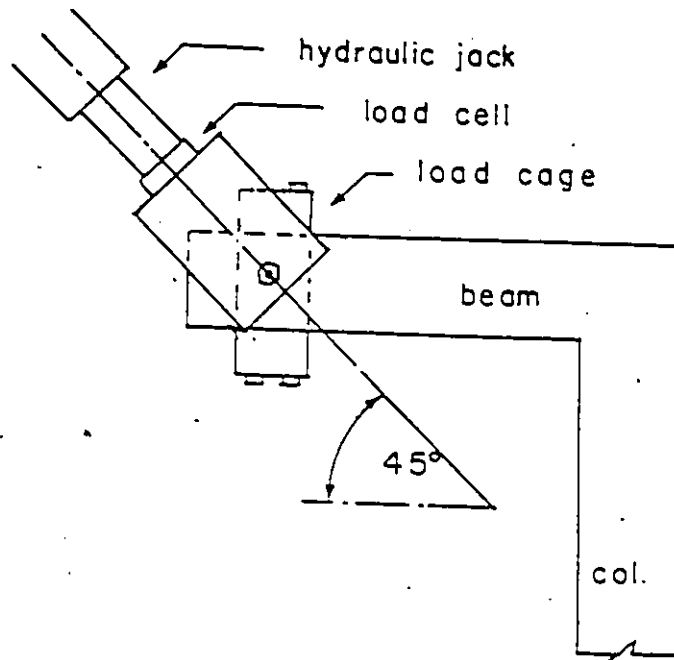
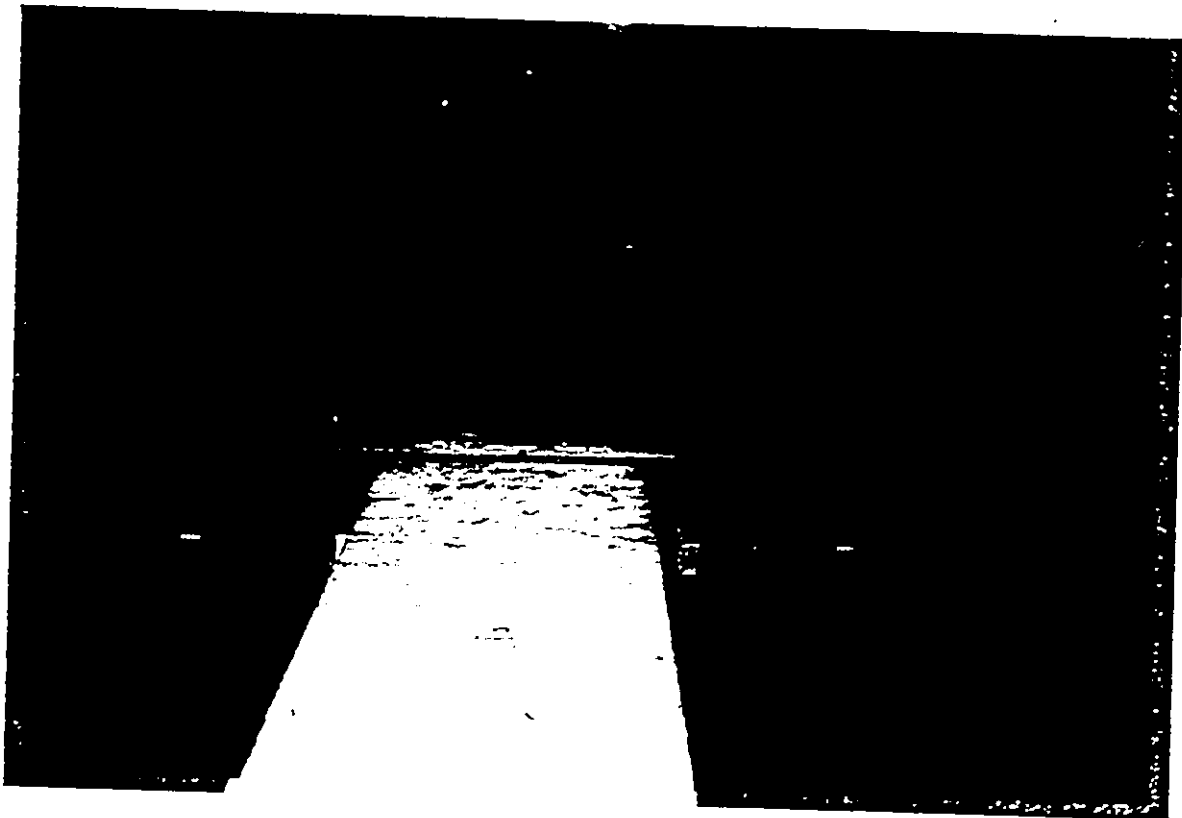


FIG. 29 BASE OF TEST RIG



(a) load set up



(b) load cage

FIG. 30 POINT LOAD SYSTEM AT BEAM SECTION

The applied moment, as in Figure 31, simulated the resulting moments of a corner joint when subjected to large lateral loads. - equivalent to the horizontal shear that would arise under seismic excitation, as presented earlier in Figures 3 and 6 .

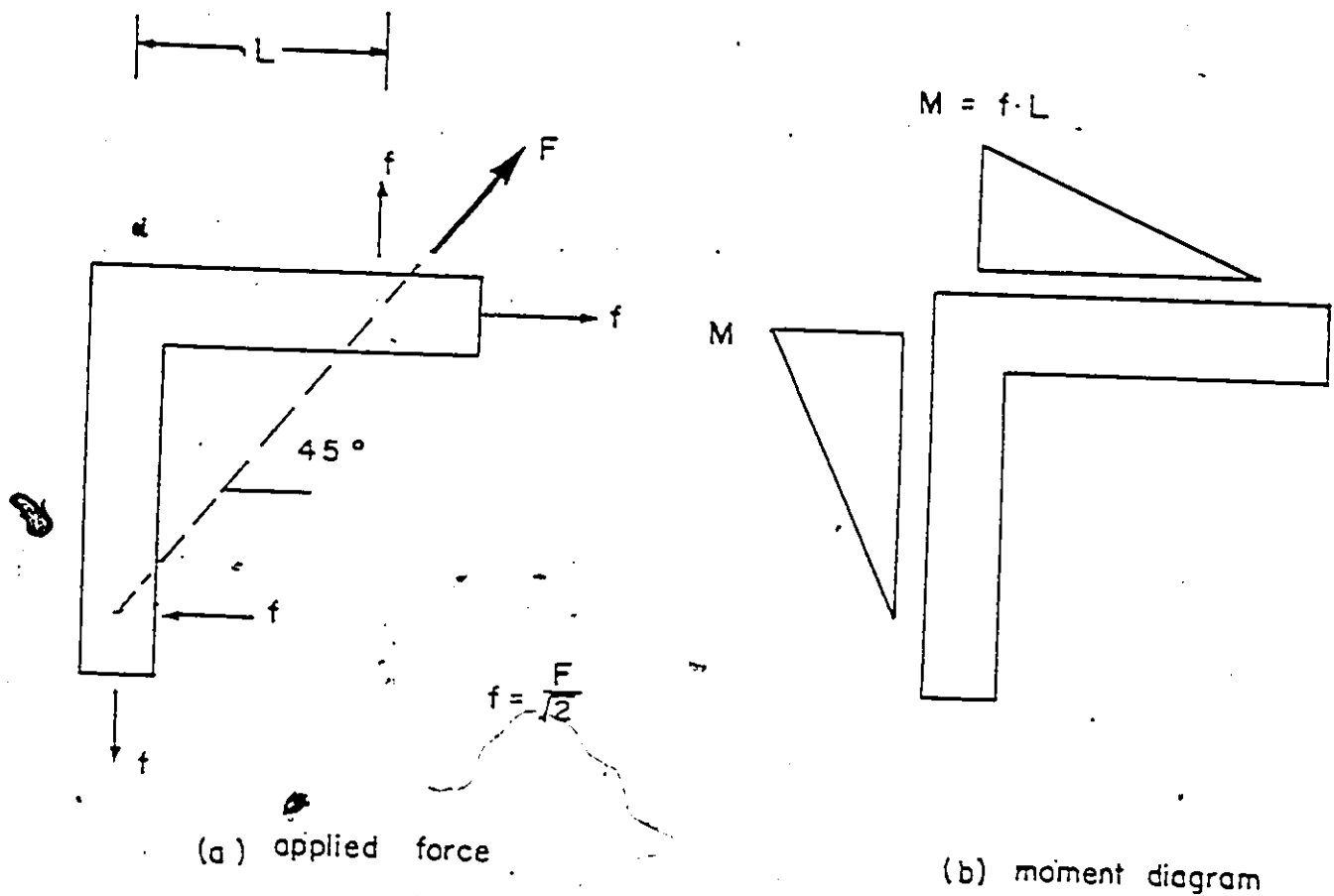


FIG. 31 SIMULATED MOMENTS

#### 4.3.2 Test Procedures

For the tests on specimens # 4,5,6,7 and 9, each test included five to six cycles of point load applied at 2.75 ft. (838 mm) from the centre line of the joint or one foot (305mm) from the beam end. Each cycle consisted of a complete reversal of loading with the load increasing until the full flexural strength of the beam was achieved. Ideally, each test should be continuous until destruction, with readings taken at regular timed intervals.

Great difficulties arose in deciding what loading history should be applied to represent simulated earthquake loads if load and deflection were considered. Arbitrarily, it was decided to test the specimens under a load sequence such that failure would occur in about five cycles as shown in Figure 32. Positive and negative values of the applied loads, deflections and strains corresponded to a closing moment and an opening moment respectively. Unfortunately, in some cases, the load obtained in one direction was not possible in the other direction in which case the displacement was limited to that obtained in the first direction.

The increments of load were varied to give approximately 25 to 55 increments or sets of readings, for each complete cycle of loading. One complete cycle consisted of loading the specimen up to a certain level, unloading to

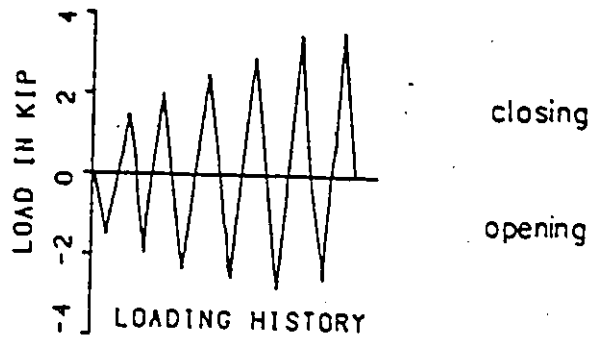


FIG. 32 TYPICAL LOADING HISTORY

zero, loading the specimen in the reverse sense and unloading to zero again. A single cycle of reversed loading took from two or four hours depending on the number of measurements to be taken.

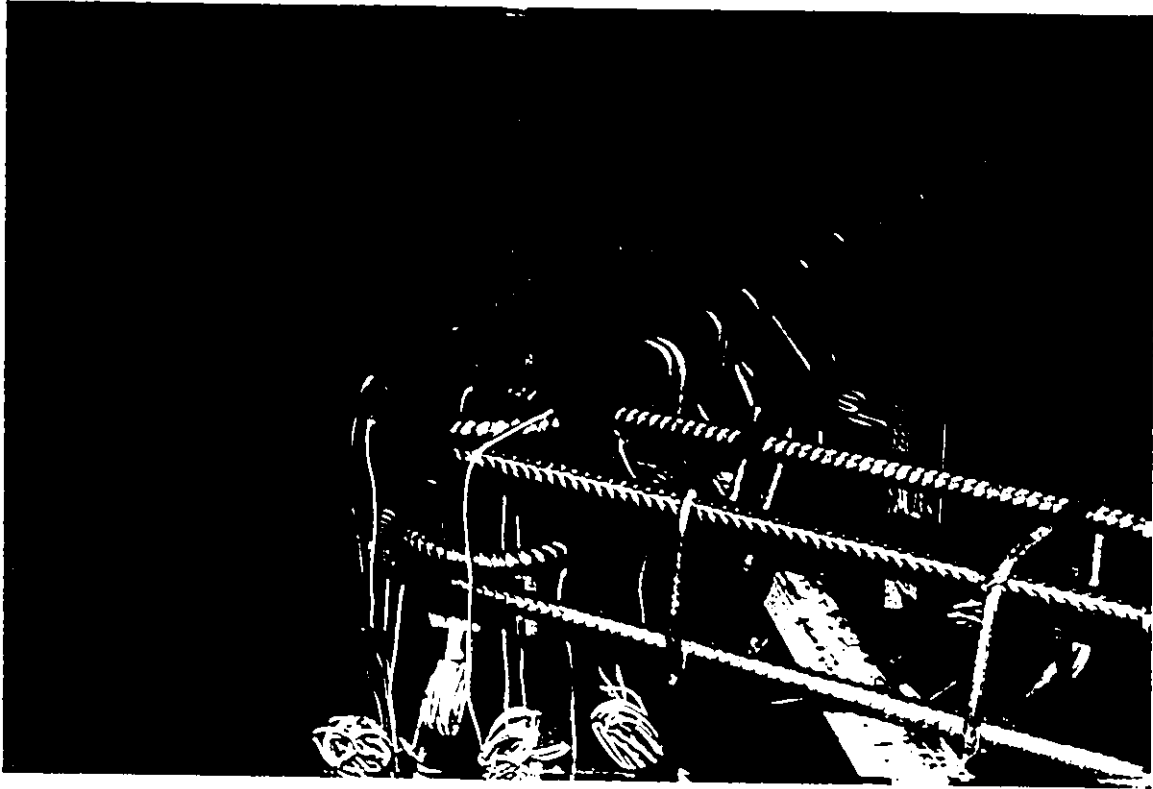
At loads close to the ultimate load, the load tended to drop off due to the yielding of the reinforcing steel whereas the deflections and strains remained constant. It was therefore decided that the load be recorded both at the time of starting to collect data of steel strains and deflections and after the collection of these data. Using the same procedure for each load increment should give reasonably accurate readings of the steel strains and deflections at load point as well as the rotation of the corner with respect to the averaged load levels.

All visible cracks were marked at the time they were discovered with two different color markers: when the load was applied to open the corner, red was used to mark the cracks, and when the load was reversed, the black ink marker was used.

#### 4.4 FORMWORK

Formwork made of steel channel sections was used for all specimens except for specimen # 9, which was cast in the steel form with additional plywood forms placed vertically above the joint as shown in Figure 33 and Figure 34 respectively. After the concrete was poured in the form, it was compacted by means of a high frequency vibrator. For at least the first three days, the beams and cylinders were cured under plastic at 70 degree F. The specimens were then stripped and were kept under wet sacking until one day before testing.

For the last specimen, #9, before casting the ready mixed concrete into the form, steel ties were wired to the vertical reinforcement cage to prevent the movement of the reinforcement relative to the form during the placement of the concrete.

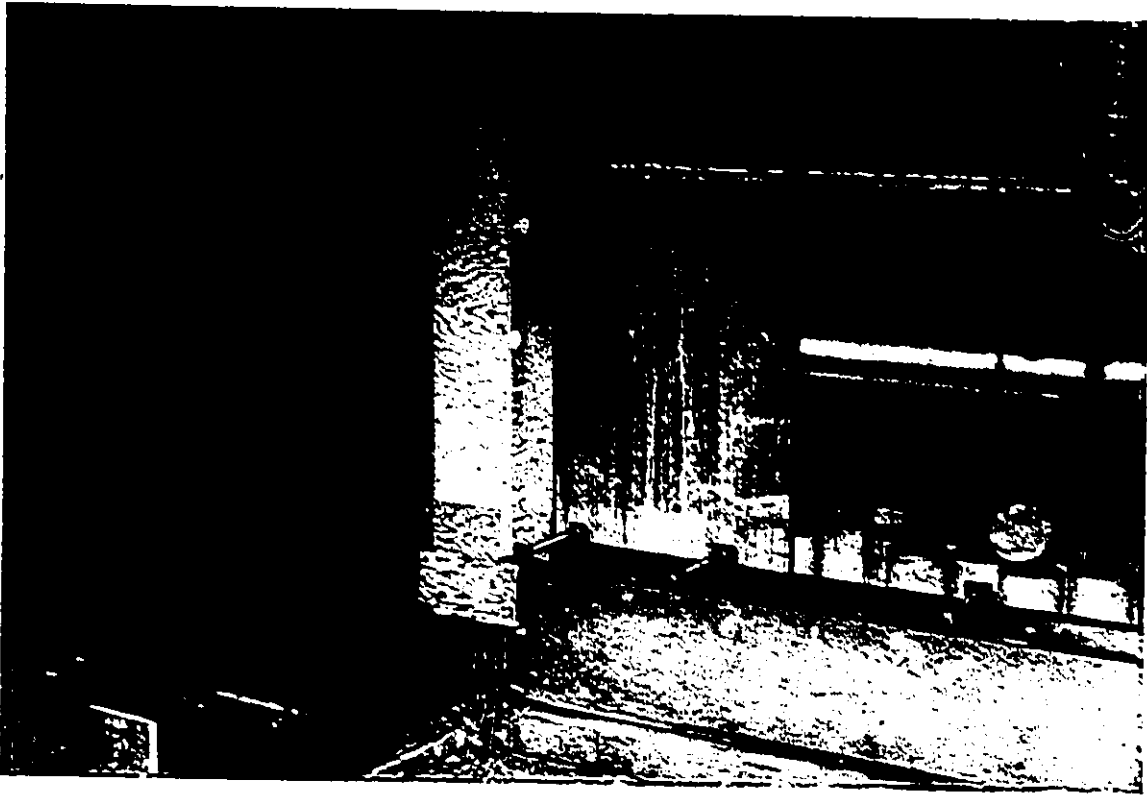


(a)

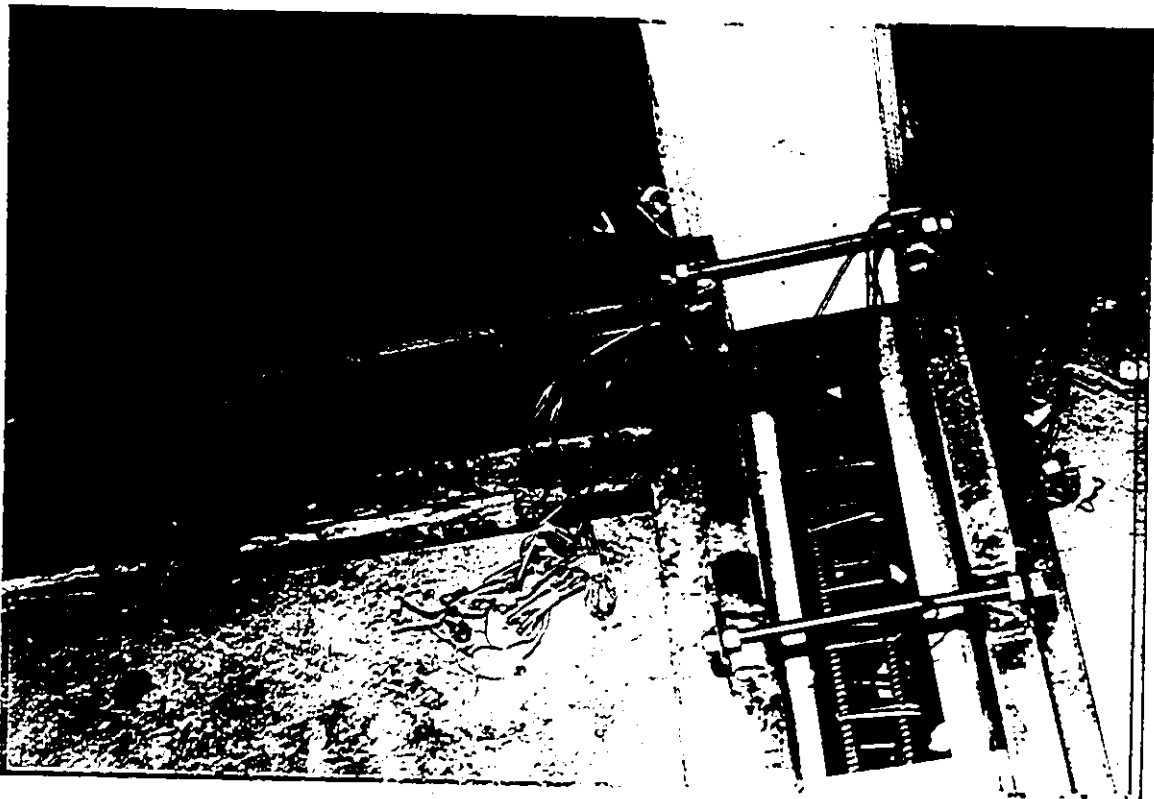


(b)

FIG. 33 PLANE FORMWORK



(a)



(b)

FIG. 34 THREE-DIMENSIONAL FORMWORK

#### 4.5 TEST SPECIMENS

The dimensions of the test specimens and the layout of reinforcement for the detail tests are presented in Figure 35 and Figure 36. In this investigation, the column and beam cross sections of 6x6.25 in. (152x158 mm) were kept constant for all tests and the length of both members was identical, 4-Ft. (1220 mm) as in Figure 36-a. However, in the last specimen, # 9, the additional beams on both sides at the corner were 6.25x6.25 in. (158x158 mm) section and 18 in. (457 mm) long as shown in Figure 36-b. Figures 37 to 44 in Appendix A and Table 2 in Appendix B show the specimen layout and properties in detail.

For the first series of test, only tension reinforcement was provided. For the second series of tests, in which specimens were subjected to repeated and reversed loadings, each test specimen had equal tensile and compressive reinforcement, or positive and negative moment tension reinforcement. The calculated ultimate moment capacities of the beams were virtually the same in both direction. For all tests, each test specimen consisted of similarly reinforced beams and columns.

Transverse reinforcement in the beams and columns consisted of # 2 (diameter 6.4mm) closed stirrups; for all tests, stirrups were spaced at 2.5 in. (64 mm) for the beams

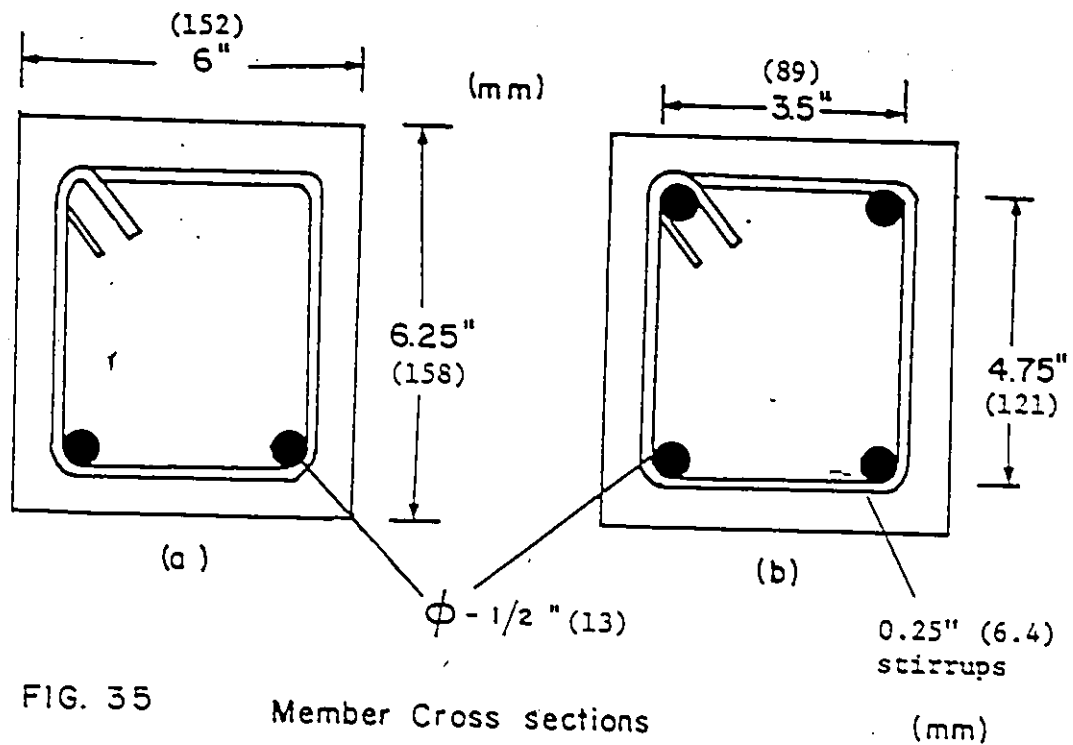


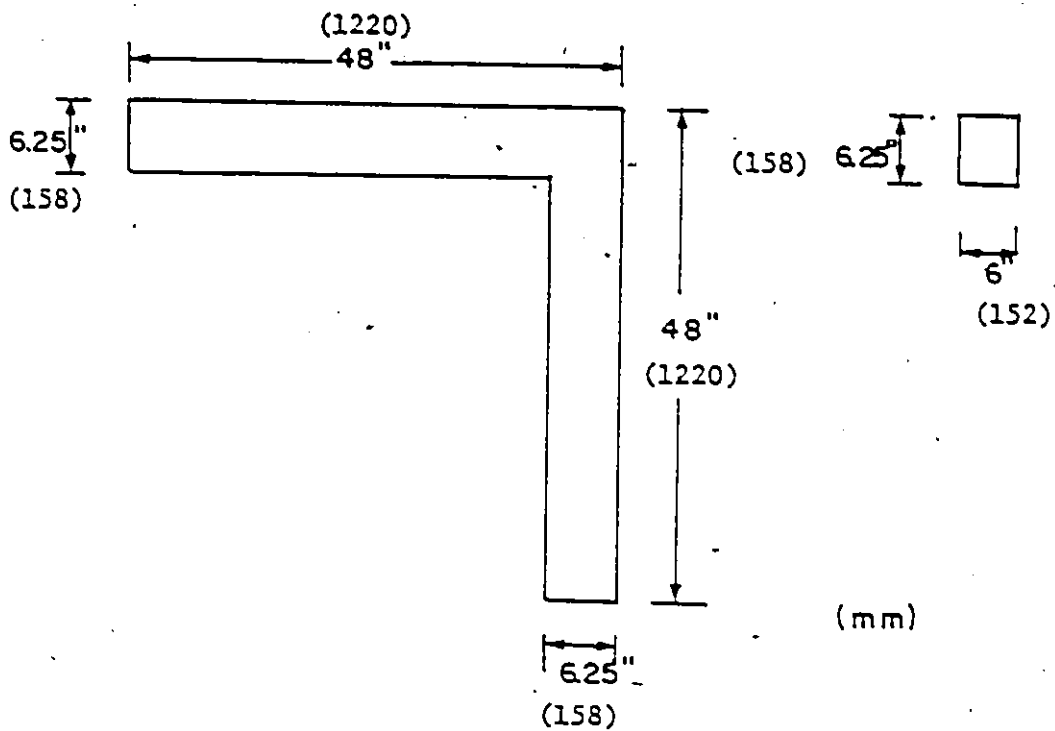
FIG. 35 Member Cross sections  
 (a) for monotonic loading  
 (b) for seismic loading

and 6 in. (152 mm) for the columns. Stirrups in the beams or columns were placed along the members and adjacent to the joint to minimize shear distress to the joint. Clear cover of the concrete was 0.5 in. (13 mm) to the stirrups minimum in all cases.

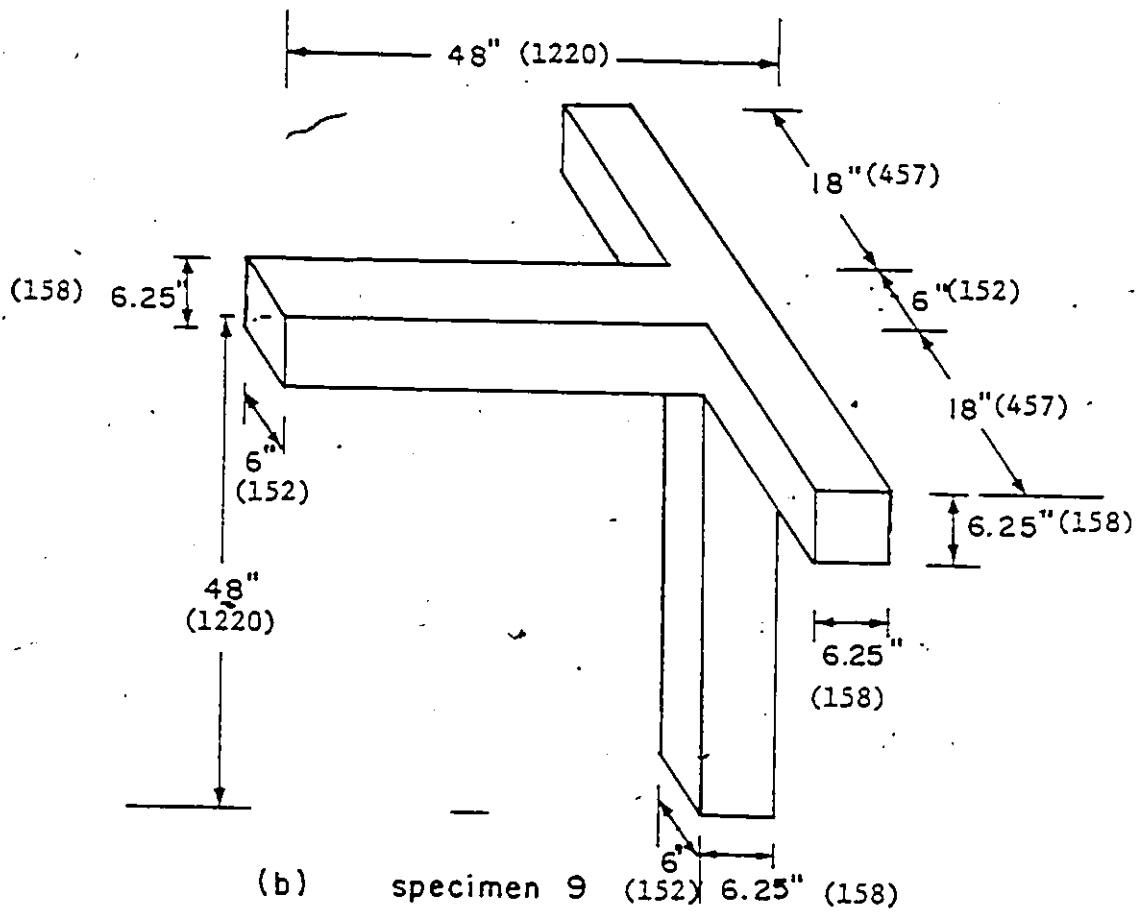
#### 4.6 MATERIAL PROPERTIES

##### 4.6.1 Concrete

The concrete mix was designed to provide a nominal cylinder strength of 5,000 psi (34.47 MPa) at 28 days and an



(a) specimens 1 - 8



(b) specimen 9 (152) 6.25" (158)

FIG. 36 DIMENSIONS OF SPECIMENS

average compressive strength of 4,000 psi (27.58 MPa) at 7 days.

Maximum aggregate size was 3/8 in. (9.5 mm) and the slump of the concrete was 3 in. (76 mm) except for specimen # 9 which had a slump of 1 in. (25.4 mm) for casting convenience. Standard 6 inch by 12 inch (152 x 305 mm) control cylinders were taken from each batch to obtain strengths at 7, 14 and 28 days respectively as well as the day of test. Average concrete strengths of the specimens on the day of test are listed in Table 2 and the compressive strengths of the specimens are plotted in Figure 45 against the age of the concrete.

Tests were normally conducted 7 to 10 days after casting to enable concrete to have a representative strength without expanding the duration of the test program unreasonably.

#### 4.6.2 Steel Reinforcement

All reinforcing steel for the specimens was Grade 60 with a nominal yield strength of 60,000 psi (413.7 MPa). For the beams, with flexural steel ratio of 1.27 %, No. 4 bars with a nominal diameter of 0.5 in. (13 mm) was used and No. 3 bars with a nominal diameter of 3/8 in. (9.5 mm) was used for 0.7 % steel ratio. Typical stress-strain diagrams

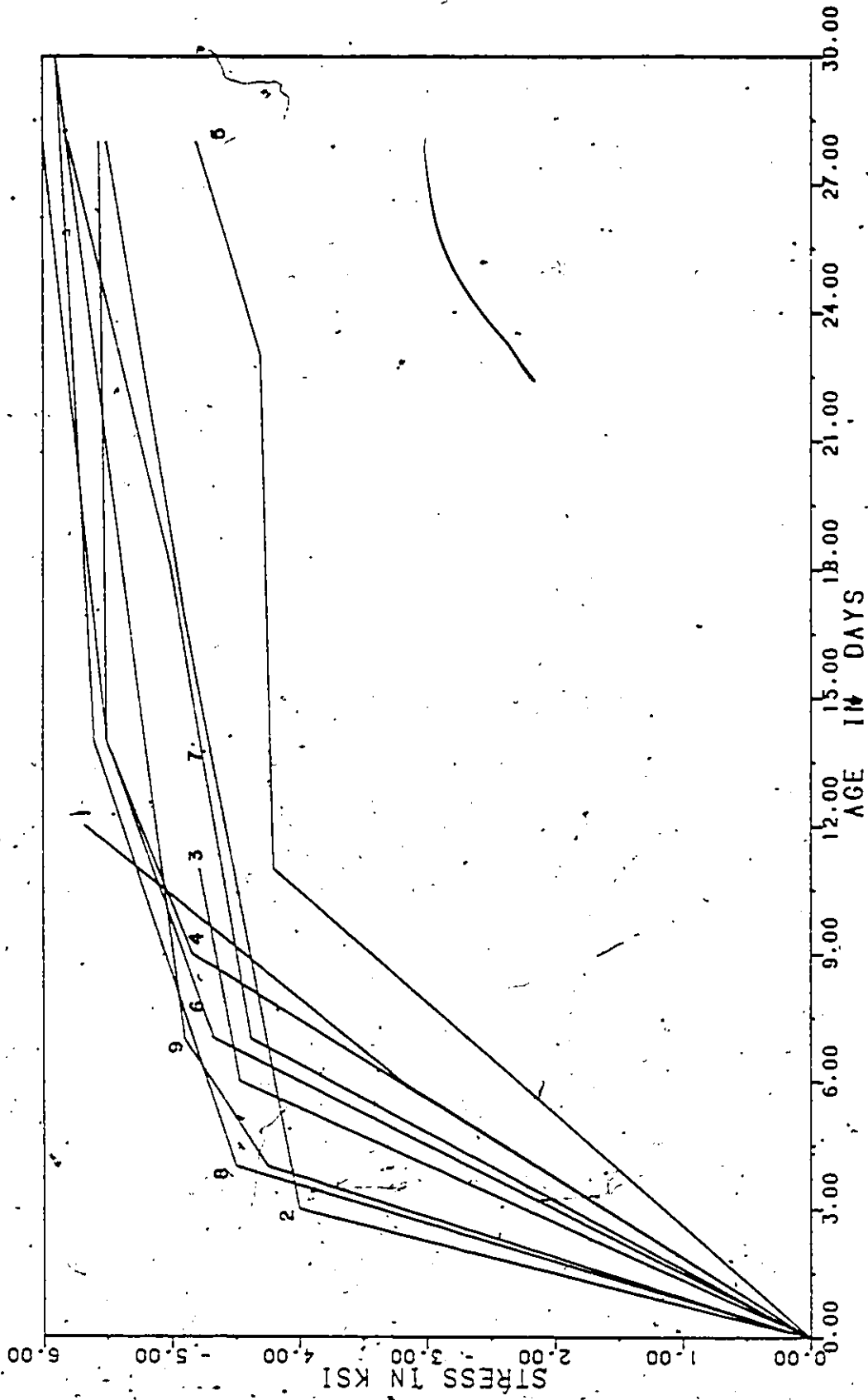


FIG.45 CONCRETE STRENGTH

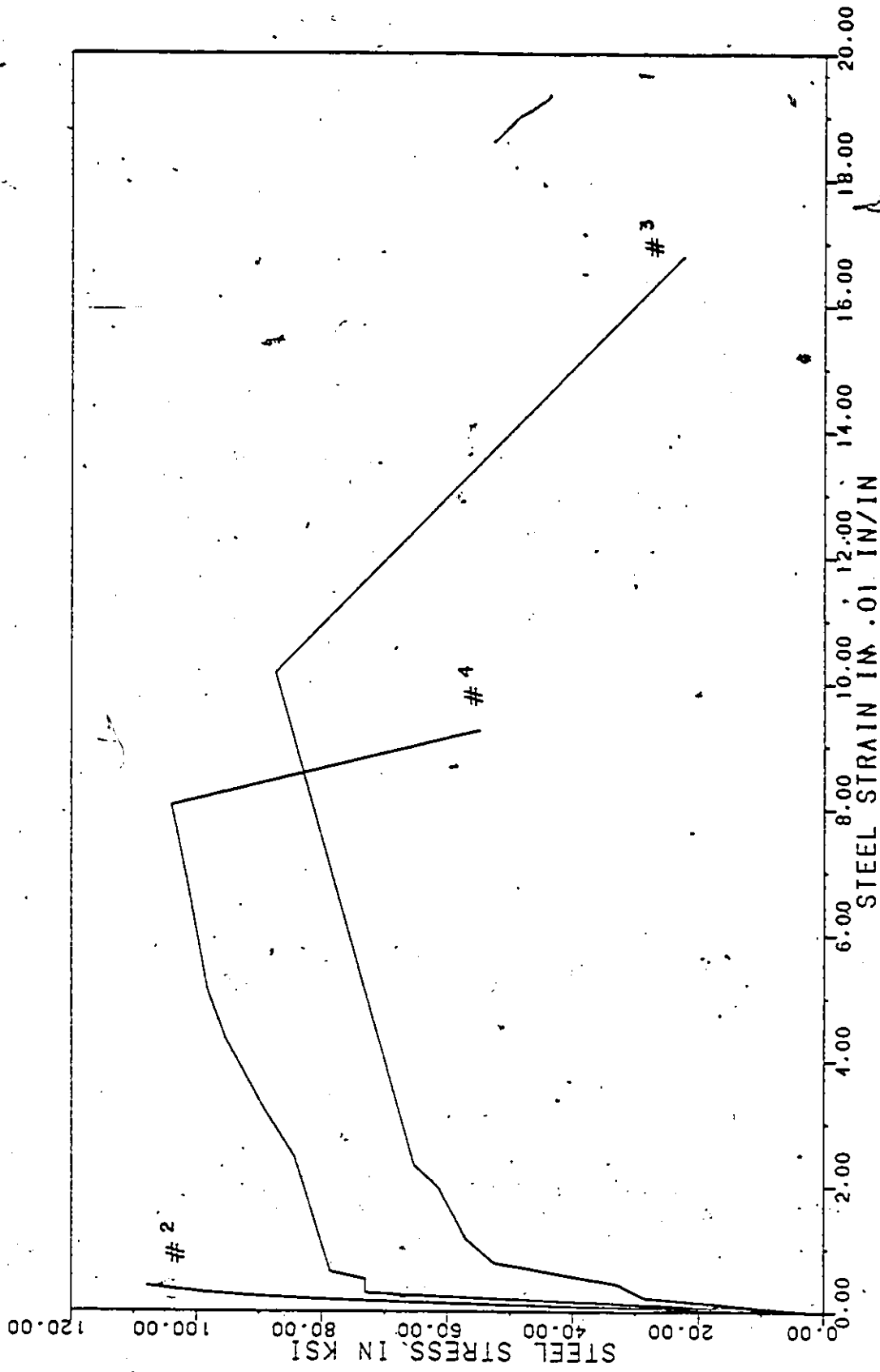


FIG.46 STRESS-STRAIN CURVES

for the No. 2, No. 3 and No. 4 reinforcing steel are shown in Figure 46 .

#### 4.7 INSTRUMENTATION

During each test, load level (P), deflection ( $\delta$ ), reinforcement strains ( $\epsilon_s$ ), concrete strains ( $\epsilon_c$ ) and corner rotations were measured.

1. Load Level : Universal Flat Load Cells, Strain-Sert model. FL25U-2SGKT were used to measure the applied load on the beam or the column. The load cells were connected to a BLH Electronics, portable Digital Strain Indicator, model 1200B.
2. Deflection : Tip deflections of the beam and deflections at other locations of the members were measured with precise dial gauges of 0.01 mm sensitivity. In the recording of the dial gauge readings, problems arose due to the friction between the plunges of the dial gauge and the rough surface of the concrete section. This was solved by glueing plastic pieces at the corresponding locations to the concrete to ensure a smooth surface to reduce the inefficiency by the slight movement of the dial gauge on the rough surface as a result of large deflection at load point.

3. Reinforcement Strains: At the locations specified on the bar, the surface of each location was machined and a groove was milled for installation of strain gauges; the gauges used were Kyowa Strain Gauges, type KFC-5C1-11. The gauges were cemented in the base of the groove and waterproofed.

Almost half of the number of strain gauges were located at the corner region such that details of the behavior of the reinforcement at the corner could be examined. The locations of the strain gauges of the specimens are specified in Figures 37 to 44 in Appendix A.

#### 4.7.1 Concrete Strain

For several specimens, #1 to #5, electrical resistance gauges were mounted on the surface of the concrete at the joint. For the others, two-inch (51 mm) Demec gauges were used. The former gave the concrete strains before cracking at several specified locations only, whilst the latter gave measurements of concrete strains even after cracking occurred at the joint but with less accuracy due to the fact that the measurements were made mechanically.

#### 4.7.2 Corner Rotations

The rotations of the corner were measured for each specimen. This was done by means of two dial gauges mounted as shown in Figure 47. The rotation of the corner was calculated from the measured deflections of the beam at the two specified locations with the distance between the locations of the two dial gauges kept constant at 10 in. (254 mm).

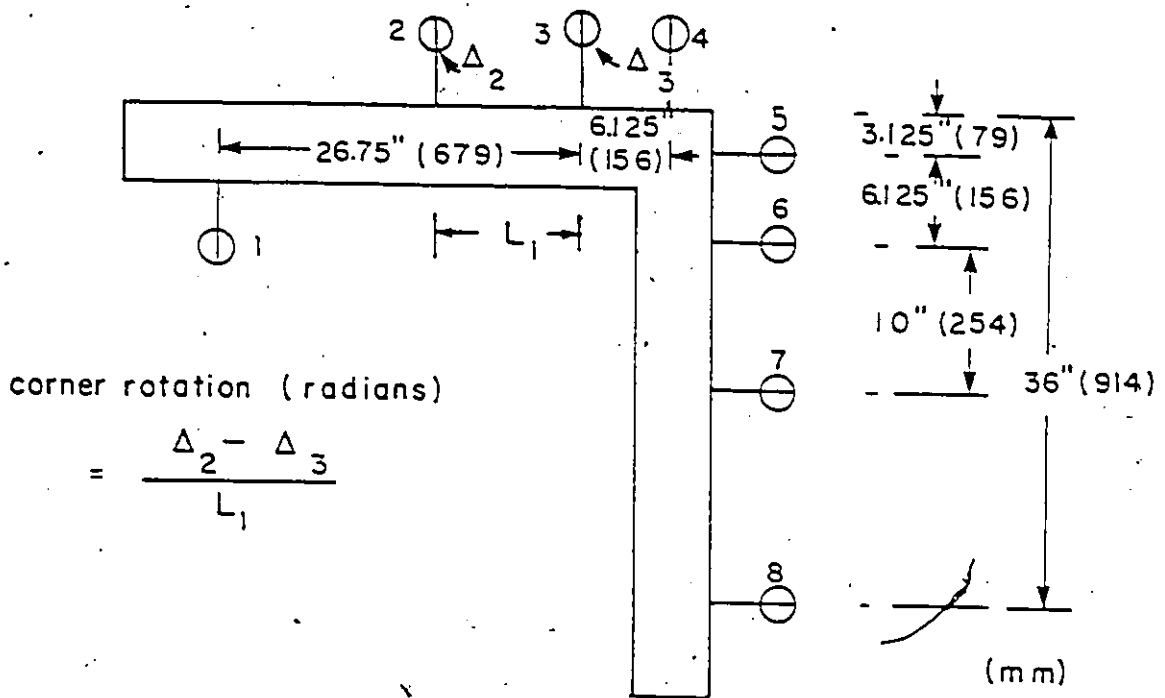


FIG. 47 ROTATION MEASUREMENT

The rotations of the corner can be computed with the following expression:

$$\text{rotation} = \frac{\Delta_2 - \Delta_3}{L_1} \quad \text{mm/mm}$$

where  $L_1$  is equal to 10 inches or 254 mm.

## Chapter V

### PRESENTATION AND DISCUSSION OF RESULTS

#### 5.1 INTRODUCTION

This chapter presents the results of the two series of tests on nine specimens simulating corner joints in a reinforced concrete structure under different types of loading so as to study the behavior of the joints with different reinforcing details. The presentation and discussion reported here are designed to improve the understanding of how reinforced concrete beam-column connections respond to either monotonic or cyclic loading.

##### 5.1.1 Load-Deflection Curves

It has been assumed that the ratio between the deflection at the first yield and at the ultimate load can be taken as a measure of the ductility of the member. In all the tests, the axial deformation of the column at the joint contributed less than 3 % to the overall displacement of the beam; only the deflection at the load point on the beam is then of main concern about the load-deflection relationship of the member.

Results of measured deflection at load point versus the load/moment are shown in Figures 48 to 56 for individual specimen accordingly with the discussion of the curves presented later in the chapter.

### 5.1.2 Moment-Rotation Curves

Rotation of the beam gives appropriate measurements of the corner angle rotations which in turn reflects the stiffness of the corner joint. In a framed structure, most of the work done in the course of the lateral deflection of the structure is due to energy absorption at the joints. Thus, the area under the moment-rotation curves of a joint gives a good measure of the energy absorbing capacity of a reinforced concrete section subjected to earthquake effects.

Figures 48 to 56 present a family of curves that illustrate the behavior of the corner rotation with respect to the applied moment.

### 5.1.3 Steel Strain-Load Curves

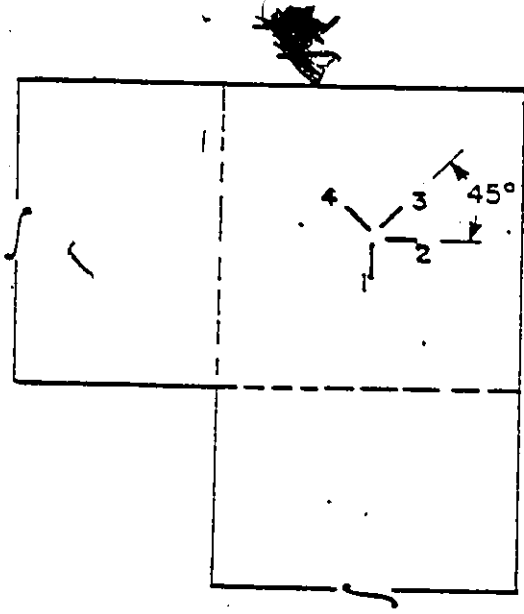
Strains in the reinforcement were measured with strain gauges which were mounted at specified locations on the reinforcement in every specimen. The readings of the gauges were expected to give the necessary information about the reinforcement behavior at various stages as well as at the ultimate load conditions.

Because of the fact that the electrical resistance strain gauges could have been damaged anytime during the test, the measurements of the steel strain were not necessarily accurate. Furthermore, the strain gauges were installed only at certain locations, and it was understood that using two gauges at every location always gave a more reliable indication of the behavior of the steel during the test. In addition, although calibration tests had been made to ensure that there was little influence by the bending of the steel to the actual readings of gauges on the indicator, the measured values of the steel strain were expected to have included a very small percentage of the bending strain of the reinforcement.

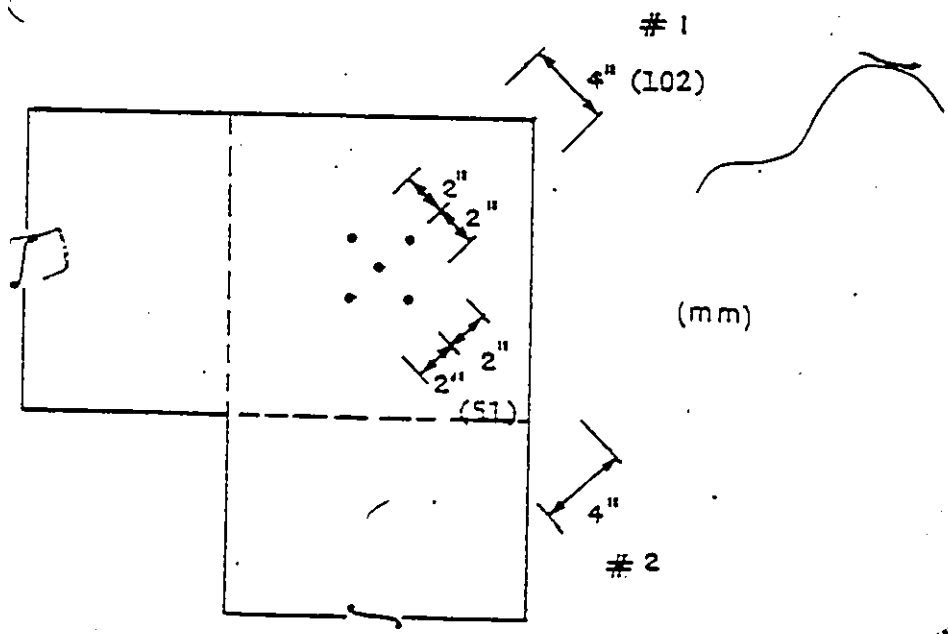
#### 5.1.4 Concrete Strain-Moment Curves

The tensile and compressive strains in the concrete at the core were also measured by electrical resistance strain gauges. For specimens # 1 to # 5, four gauges were mounted on the face of the concrete corner as shown in Figure 57-a. It was obvious that gauges could be damaged anytime there was a crack at the vicinity of the corner and the readings would be meaningful only at the most until just before cracks developed in the corner.

In specimens # 6, # 7 and # 8, the concrete strains at the corner were measured by means of Demec Strain gauges;



(a) strain gauges on concrete surface



(b) demec strain gauges

FIG. 57 CONCRETE STRAINS MEASUREMENTS

four Demec measurements were made as shown in Figure 57-b, for each two-inch (51 mm) distance. The surface strain measurements from the Demec readings were used to give an insight into the bond stresses of the bars in the joint. In specimen # 7, after the main reinforcement yielded, high strain measurements were recorded on the concrete indicating that in some areas, very high bond stresses were expected due to and resulting from the bond deterioration and as a result, intersecting diagonal cracks got wider and extended in length.

Due to the fact that the measurements made with the Demec strain gauges gave only reasonably accurate readings and that only specimen # 7 performed effectively under the cyclic load schedule, only the measurements for specimen # 7 will be shown in Figures 54-k and 54-l.

## 5.2 PRESENTATION OF RESULTS

### 5.2.1 Monotonic Loading

#### 5.2.1.1 Specimen # 1

This was the first test conducted during this study of corner joints. As a result of badly chosen load increments, the corner failed soon after the test started and no pertinent data was collected.

Early cracks, at a load of 900 lb. (4,000 N) occurred at the inside of the corner due to the stress concentration at that region. During the next load increment of 1099 lb. (4.98 KN), another diagonal crack continued along the bent main reinforcement out towards the compression zone until the corner zone became detached. Before there was any visible flexural crack, the corner failed due to this diagonal crack causing sudden failure. Figure 48-a shows the diagonal crack following the main reinforcement. In Figure 48-a, the outside corner was removed to show that there was no bond failure nor anchorage slippage. Because the concrete could not resist the resulting tensile force in the corner, the corner failed with an efficiency of only 30 % of the maximum flexural strength with a maximum load of 1040 lb. (4.6 KN).

#### 5.2.1.2 Specimen # 2

The first test under closing moment was successful with full flexural strength developed. The load-deflection curves and the load-steel strain curves are shown in Figures 49-a/d. At ultimate load, the deflection at load point was 17 mm., i.e. the member developed high ductility when subjected to closing moment. As shown in Figure 49-c, the main reinforcement yielded before reaching the maximum load, and at failure, there was crushing of the inner concrete.

First crack was visible at the inner corner at a load of 950 lb. (4.23 KN) whilst the first flexural crack was first observed adjacent to the joint region at a load of 1640 lb. (7.38 KN). As the load increased, both the inner corner cracks and the flexural cracks extended towards each other and consequently, they joined together at failure of the joint. The corner failed when the load reached 3,600 lb. (16.20 KN) which is more than 100 % of the calculated beam flexural capacity. /

In the construction of most reinforced concrete members, this mode of failure, designed to have yielding of main flexural reinforcement before crushing of the concrete to avoid sudden failure, is desirable.

#### 5.2.1.3 Specimen # 3

The specimen was reinforced to resist closing moment, but instead of having continuous main reinforcement for the beam and the column as in specimen # 2, the column bars were anchored into the beam and vice versa. Again, full flexural strength was obtained and the mechanism of failure was identical to specimen # 2, with crushing of the corner concrete after the yielding of main reinforcement of the beam at failure.

Because the beam end was not provided with a ball-joint in this test, deflection at load point was obviously low and an unreasonable deflection of only 3 mm. was recorded as shown in Figure 50-b. Figure 50-c shows the reinforcement strains during the test, the steel yielded before the ultimate moment was obtained.

There were no major differences between the behaviors of specimens # 2 and # 3 during the tests, and it is certain that the corner can develop full flexural strength of the framing members when the corner is subjected to closing moment.

#### 5.2.1.4 Specimen # 8

The reinforcing details of this specimen were the same as those of specimen # 1. It failed at a load of only 1049 lb. (4.72 KN) which is equivalent to only 30 % of the flexural strength of the beam. Diagonal cracking was the reason why the corner failed so early and at failure, the maximum steel strain was only 0.08 % (Figure 55-d) which is equivalent to 24,000 psi (165.5 MPa) of the steel stress.

Figures 55-b/c shows the load-deflection and moment-rotation relationships of the specimen. The corner failed when the deflection was a little more than 7 mm. which is low in the consideration of energy dissipation. As shown in

Figure 55-b/c, the energy absorbing capacity was not effective since the maximum rotation was less than 0.009 radians at failure. In spite of sufficient anchorage capacity, specimen # 8 did not show reasonable behavior against a moment which tended to open the corner.

With the comparison of test results of specimens # 1 and # 8, it is evident that the reinforced concrete corner joint did not develop the full strength when it is subjected to opening moments whilst little difficulty was encountered in the case of closing moment.

Study of the latter test results will give a better understanding of the behavior of the corners under repeated reversal loadings in which both opening and closing moments are included.

### 5.2.2 Cyclic Loading

#### 5.2.2.1 Specimen # 4

Figures 51-a to 51-e show the relationships between moment-deflection, moment-rotation and moment-steel strains of specimen # 4 respectively. Failure was at a load of 3280 lb. (14.76 KN) and a deflection at load point of 14.4 mm during the fourth cycle of closing moment, disintegration of the concrete in the corner over the full width of the column and beam just at the region of the corner core was accompanied

by spalling of the corner region due to the bearing failure at the reinforcement bend.

As the load increased during the first and second cycles, flexural cracks developed but did not extend or propagate rapidly. Crack at the inner corner occurred at a load of 1095 lb. (4.96 KN) during the first opening cycle and the first diagonal tension crack occurred when the load was 1473 lb. (6.63 KN) of the third opening cycle. Flexural cracks extended and widened obviously after the third cycle of closing moment in which the applied moment reached 3206 lb. (14.4 KN) with a maximum deflection of 11.28 mm.

Bond degradation under repeated cyclic loadings led to the pulling out and pushing in simultaneously of the same bars at the face of the column and this accelerated the total slippage of the beam reinforcement causing large fixed-end rotations between the beam and the column. The concrete deterioration produces unstable hysteresis loops which decreased the moment capacity from one cycle to the next, resulting in continually changing structural response characteristics.

When the specimen was loaded to failure under closing moment in cycle # 4, yielding of main reinforcement was recorded at the corner of the column region and as a result of

bond and bearing failure at the corner, wide cracks were visible after the termination of the tests. This in turn caused the strength, stiffness, and energy dissipation of the members to diminish substantially, as indicated by the rapid drop of the slopes of the moment-rotation and moment-deflection curves in Figures 51-b/c.

Throughout the test, relatively few flexural cracks were marked when opening moment was applied. This was simply because the corner could not develop enough resistance after the load had reached 1600 lb. (7.20 KN), and as a result, the applied load was reversed using displacement as a control regardless of the low load level attained.

#### 5.2.2.2 Specimen # 5

This specimen consisted of the same reinforcement detail as specimen # 4 but with a lower reinforcement ratio, 0.7 % instead of 1.27 % for specimen # 4. The specimen failed during the fifth cycle of closing moment at a load of 2700 lb. (6.75 KN) and a deflection at load point of 18.40 mm.

Inner corner crack occurred at a load of 944 lb. (4.47 KN) together with the first diagonal tension crack at 1187 lb. (5.34 KN) of the second cycle of opening moment. Flexural cracks close to the joint region developed and extended

Shortly after the discovery of the diagonal tension cracks but they were not serious until the fifth cycle of loading in which the corner was loaded to failure in closing moment at its maximum capacity.

The overall response of the corner was better than that of specimen # 4, and the corresponding relationships between load, deflection, steel strains, and rotations are presented in Figures 52-a to e. It was found that the corner exhibited better ductility characteristics than specimen # 4. Besides, specimen # 5 indicated higher efficiency of the corner subjected to cyclic load reversals, due to the reduction of the stresses concentrated at the joint by using lower flexural reinforcement ratio.

Due to the damage of the joint by tensile and compressive yielding, rapid decrease of the strength and stiffness of the specimen were obvious; especially, when they were subjected to reversal loadings. However, it is easily to notice that, as compared to Figures 52-b/c and Figures 51-b/c, the drop of the slopes of the moment-deflection and the moment-rotation curves in specimen # 5 were much less than that in specimen # 4.

Again, a similar mode of failure to specimen # 4 was observed, in this case, the concrete under the bend of the

beam steel failed in bearing and spalled off the side of the joint. Under cyclic loading, the bond of reinforcement within the joint was expected to deteriorate under alternating loads.

#### 5.2.2.3 Specimen # 6

Specimen # 6 was tested with the same reinforcing detail and reinforcement ratio as specimen # 4 except that in specimen # 6, diagonal reinforcement was provided at the corner to resist the resulting tensile force at that region. The behavior of specimens # 4 and # 6 were dramatically different, as can be seen by comparing the two series of curves in Figures 53 and Figures 51. Yielding of the members occurred in specimen # 6 at a larger displacement and larger load than in specimen # 4. This was due to some stiffness degradation of the joint in the earlier cycles in which specimen # 4 was subjected to lower loads with the absence of the supplementary reinforcement.

Inner corner crack was first observed at a load of 776 lb. (3.49 KN) of the first cycle of opening moment. After the third cycle of opening moment, more flexural cracks were discovered after a load of 1191 lb. (5.36 KN) and sudden diagonal tension cracks appeared at a load of 2045 lb. (9.2 KN). Before the corner failed at a load of 2000 lb. (9.0 KN) and deflection at load point of 29.63 mm in the fifth cycle

of opening moment, many more flexural cracks were found but the previously developed flexural cracks did not get wider or extend. After the corner joint failed in the fifth cycle of opening moment, many of the strain gauges had been damaged and were not functioning during the rest of the test.

Although there might be some difference in the concrete strengths of the two specimens, it is believed that the main reason for the observed difference is the bond deterioration at the joint caused by cyclic loading, if no diagonal reinforcement is provided.

A noticeable drop in stiffness occurred only during the sixth cycle of opening moment after the failure of the corner as shown by the decrease in the slope of the curves in Figure 53-b. Nevertheless, it should be pointed that there was no significant change in the slopes of the curves when the moment tended to close the corner, even after the corner failed at the previous cycle of loading.

For curves in Figures 53-d to j, the fact that the tensile strains in the main reinforcement or the diagonal bar never recovered explains why the width of the diagonal cracks increased with progressive cyclic loading. At this stage of opening moment, the hysteretic curves had become so pinched that the amount of energy being dissipated by the

subassemblage, determined by the area enclosed by the moment-rotation curves, had decreased cycle by cycle very rapidly to only small percentage of the peak moment which occurred during the previous cycle, # 5. When the moment closed the corner, it can be shown from Figures 53-b/c that, after the corner failed at cycle # 5 of opening moment, the behavior of the corner did change from the previous cycle # 4 of closing moment, and the change of behavior remained unchanged for the following cycles, i.e. cycles # 5 and # 6, as indicated by the last loops of curves in the first quadrant of the graphs.

For the beam-column joints with relatively high reinforcement ratio, the overall response of specimen # 6 to the slow-reversed loading was better than that of specimen # 4, although it did develop only 60 % of the full strength of the joint, it performed considerably better when diagonal steel was installed, which proved to increase the strength of the joint and the energy dissipating capacity very efficiently. Diagonal reinforcement limited the bearing stress induced at the bent of the main reinforcement; however, slippage was expected to have happened along the cracks as crushing occurred.

In Figures 53-b/c, it can be observed that diagonal cracks developed and enlarged rapidly after the corner

failed in opening moment of cycle # 5. Bond conditions for the column may become too severe for the reinforcement to participate in the column moment transfer, since the stress induced is proportional to the bar size. Moreover, the spalling of the cover concrete may extend beyond the joint area and significantly reduce the flexural strength of the columns.

#### 5.2.2.4 Specimen # 7

This specimen gave the overall best results against the simulated earthquake loadings, with an efficiency very close to 100 % of the flexural strength of the framing members i.e. the joint developed its full strength against repeated and reversed loading before the failure of the beam. The relationships between the loads, deflections, rotations, steel strains and concrete strains are illustrated in Figures 54-a to 1 respectively.

At a load of 990 lb. (4.45 KN) of the first cycle of opening moment, first crack at the inner corner was discovered. First flexural cracks appeared very close to the column and joint boundary at a load of 421 lb. (1.90 KN) of the first cycle of closing moment. More flexural cracks developed but the propagation of these cracks was not obvious before the occurrence of the first diagonal tension crack at a load of 1264 lb. (5.69 KN) in the third cycle of opening mo-

ment. When the corner failed during the fifth cycle of opening moment, the ultimate load attained was 1950 lb. (8.78 KN) at a deflection at load point of 31.80 mm.

The flexural yielding of the beam predominated over other modes of failure; the corner joints showed favorable deformation characteristics even in the range of large deformation as shown in Figures 54-b/c.

When the joint developed diagonal cracks, the opening sides of the joint continued to enlarge as increments of deflection were applied to the beam but the joint remained stiff under closing moment. Figures 54-a/b as well as the moment-concrete strain curves in Figures 54-k/l show that the diagonal cracks had developed and interconnected over the core of the corner which weakens the joint in response to repeated cyclic loading. The diagonal bars, by their ability to yield in tension and compression, contributed very much to the shear resistance of the joint, it can be seen from Figures 54-b/c and Figures 53-b/c that the diagonal cracks developed in the corner core were not as critical in specimen # 7 as that in specimen # 6.

From the results, it can be said that, very high beam rotations were observed and this, too may possibly be explained by the yielding of the steel at the joint. In the

last load cycle of opening moment, the corner joint had been badly damaged at the end of the beam section and subsequently the beam could barely sustain more load, which resulted in the deflection at load point reaching as high as 26 mm. with the load capacity at this stage only 40% of its designed capacity.

Although the maximum load levels attained were different for specimens # 6 and # 7, the summation of the maximum displacements in opening moment and closing moment of the fifth cycle were both equal to 67 mm. This indicated that specimen # 7 developed a relatively high ductility whilst specimen # 5 demonstrated its stiffness due to the higher reinforcement ratio.

Figures 54-j/k show that the concrete strains remained elastic at very low load before the development of diagonal cracks which intersected each other during successive cycles of loading. The last major crack formed was the inclined crack in the column in the joint zone.

In conclusion, additional diagonal reinforcement did increase the strength, stiffness and the ductility of the corner. Use of a higher reinforcement ratio did increase the strength of the corner but only a mere 20%, and the use of lower reinforcement ratio increased the ductility by more

than 50 % which is more desirable in the design of reinforced concrete members under earthquake actions.

#### 5.2.2.5 Specimen # 9

It was observed that the stiffness and the strength of the connections were improved by the intersecting beams, and Figures 56 show the relationships between load, moment, steel strains, rotation and deflection at load points for the test. For this specimen, # 9, although no diagonal steel was used, satisfactory results were recorded and the results obtained were definitely better than those for specimen # 4 which had identical reinforcement layout as specimen # 9 but without the additional intersecting beams. As illustrated in Figures 56-c of M-0 curves, the slopes of the curves were almost identical from cycle to cycle even after the corner failed in opening moment of load cycle # 5.

When the specimen was loaded to failure in the fifth cycle of opening moment, the maximum load reached 2824 lb. (12.7 KN) and the maximum beam deflection at load point was 26.78 mm. After the failure of the corner subjected to opening moment, when the load reversed to close the corner, the corner still could carry a load of 3488 lb. (15.7 KN), which is the flexural strength of the beam, and the maximum tip deflection of the beam reached 11.12 mm. It was interesting to note that, during the sixth cycle of closing mo-

ment, the response of the corner was consistent in that the ultimate applied load was 3588 lb. (16.11 KN) with a deflection at load point of only 12.72 mm.

Due to the high main reinforcement percentage used, the specimen did not illustrate better ductility than specimen # 6 as compared Figures 56 to Figures 53. When the corner was subjected to opening moment, specimens #9 and #6 developed maximum displacements of 26.87 mm and 29.63 mm respectively; the corresponding maximum displacements were 11.12 mm and 32.65 mm for specimens #9 and #6 in the case of a closing moment.

On the basis of the comparison of test results of specimens # 4, # 6 and # 9, it can be concluded that the results of tests on two-dimensional specimens are expected to be conservative; for the sake of convenience in the test programme, laboratory tests on two-dimensional members are preferable as the test results are on the safe side.

### 5.3 DISCUSSION OF RESULTS

For all the specimens, the first crack was at the inner corner under both opening and closing moments. In an opening corner, the first crack was a flexural crack and in a closing corner, it was the crushing of concrete at the inner corner. Flexural cracks at the junction of the members ap-

peared shortly after these first cracks and after this, the flexural behavior of the specimens was normal until the diagonal cracking moment of the joint was reached. When the joint developed diagonal cracks due to the opening moment, the cracks continued to open as increments of load were applied to the beam. It is reasonable to say that, in most cases, failure was produced by side splitting of the joint and not by pullout of the hooked bar.

For the five specimens, # 4, 5, 6, 7 and 9, under slow reversal loading, it was observed that the failure of specimens # 4 and # 5 was due to the slippage of reinforcement or bond failure together with the bearing failure at the bend which resulted splitting and spalling of the concrete at the corner, and the maximum loads of these tests were well below the desirable strength of the corner.

Flexural cracks in the connection appeared in all four specimens # 4, 5, 6, and 7, during the first loading cycle, and moreover, before the beam or column reinforcement yielded at subsequent cycle loadings. The cracks were visible first at only 20 % of the ultimate load and the cracks widened and extended as the load increased, but the propagation of these cracks was not serious under incrementally increasing cyclic loading.

At the corner, bond failure started at cracks and resulted in splitting of the concrete along the bars, either in vertical planes or in horizontal planes. In addition, the bars at the inside corner, being in tension when the joint was subjected to a closing moment, tended to straighten and pulled through the concrete cover.

Generally, anchorage conditions at the corner joints are less critical than at the interior beam-column joints because the corner joint absorbs actions from one beam only and beam bars can be anchored more favorably by bending them toward the core beyond the face of the column. However, high radial stresses, exerted by bends where large diameter bars bear against core concrete that has been damaged by intersecting diagonal cracks, may lead to excessive hoop deformations and consequent slip. The concrete cover over these column bars tends to spall relatively easily, particularly when heavy reinforcement is used.

### 5.3.1 Monotonic Loading

#### 5.3.1.1 Specimens # 1, 8

Initially, a set of three tests on specimens # 1, 2 and 3 were conducted to study the response of the corner joints with generally proposed reinforcing details, subjected to opening or closing moments; In the first test, specimen # 1, due to the specimen failing at a low load, very little

information was obtained, and a duplicate specimen, specimen # 8, cast identically to specimen # 1, was tested by loading the corner to failure unidirectionally. Specimen # 1 was subjected to monotonic opening moment only. The reinforcement consisted of opening corner steel and stirrups as detailed in Figure 37, with a main steel reinforcement ratio of 1.27 %. Specimen # 8 was a duplicate of specimen # 1 and was to be loaded under monotonic corner opening moment. The failure mode of diagonal tension cracks can be clearly seen in Figures 48-a and 55-a for both specimens. In both tests on specimens #1 and #8, the load-steel strain curves show that the measured steel strains did not exceed the yield strain.

It was seen that, even during monotonic loading, the specimens # 1 and # 8 subjected to opening moment never reached the desired strength of the corner. Actually, a mere 30 % efficiency of the corner was attained, which was mainly associated with the diagonal tension cracks developed. The failure was sudden, with the entire outside corner spalled away and load dropping immediately and rapidly to a very low level.

#### 5.3.1.2 Specimens # 2, 3

It was demonstrated that, from the test results of specimens # 2 and # 3, corner joints subjected to closing moments encountered no difficulty. The two specimens did

develop full flexural strength. At failure, the main reinforcement yielded with splitting and bearing cracks as the consequences. The relevant test results are recorded in Table 2 in Appendix B.

As might be expected, the shear developed in the beam was low and the transverse stirrups provided excellent crack control.

### 5.3.2 Cyclic Loading

#### 5.3.2.1 Specimens # 4, 5

Based on the previous test results on opening moments, it was noted that the concrete in the corner did not provide enough resistance for the resulting diagonal tensile force developed across from the inner to the outer corner. Before considering providing tensile resistance by means of supplementary reinforcement to the corner, tests on specimens # 4 and # 5 were carried out to study the behavior of the corner when subjected to slow reversal loading, two different reinforcement ratios were used, 1.27 % for specimen # 4 and 0.7 % for specimen # 5.

It was observed that, during the test, the behavior of the joint of both specimens was not desirable if the applied moment was to open the corner. Both specimens were loaded to failure in closing moment, and the failure mode of these

joints was by splitting cracks and crushing of the concrete struts between the cracks after the main reinforcement yielded at the previous cycle.

Although the flexural cracks along the beams and into the core never widened or extended progressively, the cyclic loading was seen to reduce the strength of the joint core due to the development of the intersecting diagonal cracks. With more steel in the corner, larger forces will be generated diagonally and eventually diagonal tensile cracks will develop and significantly reduce the energy dissipation; in other words, the ductility of the member is not directly proportional to the amount of the tensile reinforcement used. It can be observed that the decrease in main reinforcement ratio does not eliminate the necessity of the diagonal steel to attain the required strength or the ductility of the structure.

The slopes taken from load-deflection curves can be used as a measure of the stiffness of the beam at various stages during the tests. The slopes of the load-deflection curves in Figures 51-b and 52-b reflect the gradual reduction in stiffness of the member with increasing damage prior to failure. A rapid decrease in the slopes of load-deflection curves, after the corner was loaded to failure in the previous cycle of loading, indicate that the beam lost its

stiffness significantly as the stress of reinforcing bar reached well beyond the yield point and cracks progressed. However, the reduction in the slopes of the load-deflection curves for specimen #5 with lower reinforcement ratio was less serious than that for specimen #4 with higher reinforcement ratio.

According to the test results, it can be concluded that the previously proposed reinforcing details needed to be modified with respect to the diagonal tensile force to decrease or eliminate the failure at the joint. The problem of diagonal failure at joints could be solved in a general manner by an addition of reinforcement sufficient to resist the tensile forces produced in the concrete.

#### 5.3.2.2 Specimens # 6 , 7

Tests were conducted on specimens # 6 and # 7, with identical reinforcement ratio and reinforcing details as specimens # 4 and # 5 but with the installation of supplementary reinforcement, equal in area to the main steel which was expected to allow greater rotational capacity of the corner to attain equivalent moment capacities so as to absorb the induced energy due to the ground motion. The fact that, specimens # 6 and # 7 performed effectively under the simulated earthquake loadings indicated the effectiveness of the additional diagonal reinforcement.

The additional diagonal steel was proved to have increased the concrete compressive and tensile resistance at the corner, the rotational capacity of the corner, the confinement of concrete in the corner as well as that of the reinforcement of the core. The results of these two tests were listed in Table 2 in Appendix B. It must be noted these specimens were heavily reinforced against diagonal tension failure, with the result that the concrete was constrained more than if the transverse steel had been the optimum in preventing the diagonal tension failure of the joint. It was interesting to note that the connection could develop its capacity in one direction after having developed it in the opposite direction.

With reference to Figures 53-b and 54-b, it is clear that a gradual decrease in slopes of the load-deflection curves was observed due to the cracking of the concrete. Again, after the failure of the corner in the fifth cycle of opening moment, the rapid decrease in slopes of the load-deflection curves was more serious for specimen #6 with higher reinforcement ratio than that for specimen #7 with lower reinforcement ratio.

These specimens failed due to the bond deterioration after the yielding of the main reinforcement as a result of reversed and repeated loading. Large flexural cracks were

obvious but there was no spalling of the corner concrete when the test was terminated. For specimen # 7, the corner failed at a load level very close to the ultimate flexural strength (97.5 %) of the beam section, and the reinforcement details are believed to be acceptable.

#### 5.3.2.3 Specimen # 9

The last specimen, # 9, with identical reinforcement details as specimen # 4 i.e. reinforcement ratio of 1.27 %, but with additional connecting beams at the joint was tested against reversed loading. Although no diagonal steel was used, the specimen gave as high as 80 % efficiency of the corner joint when failed in opening moment simply due to the confinement of the joint by the connecting beams and the greater area of concrete to resist the diagonal tensile force.

#### 5.4 COMPARISON OF RESULTS

In the tests reported in previous sections, the efficiency to which each specimen performed varies and is shown in Table 2 in Appendix B. In nearly every case, the measured values of ultimate load were less than those computed. Only specimen # 7 developed moment capacity relatively close to the calculated considering both the opening moment and the closing moment.

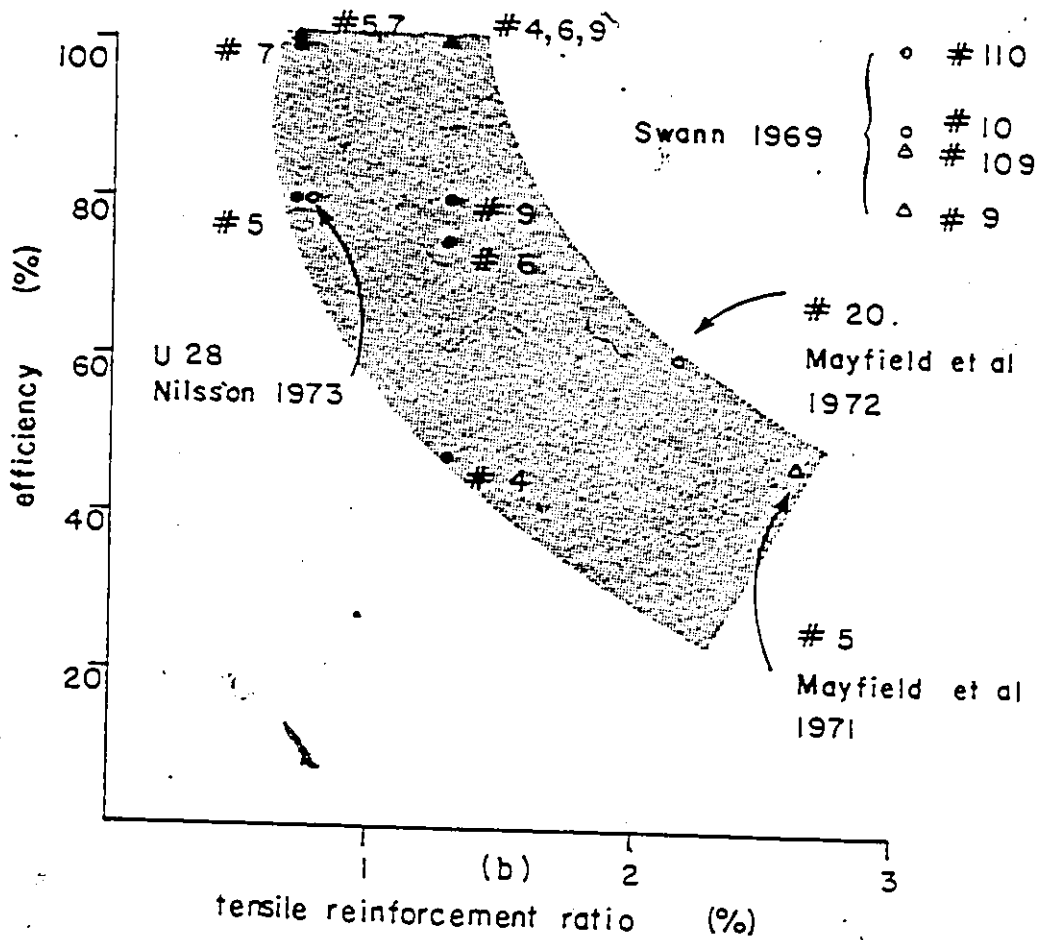
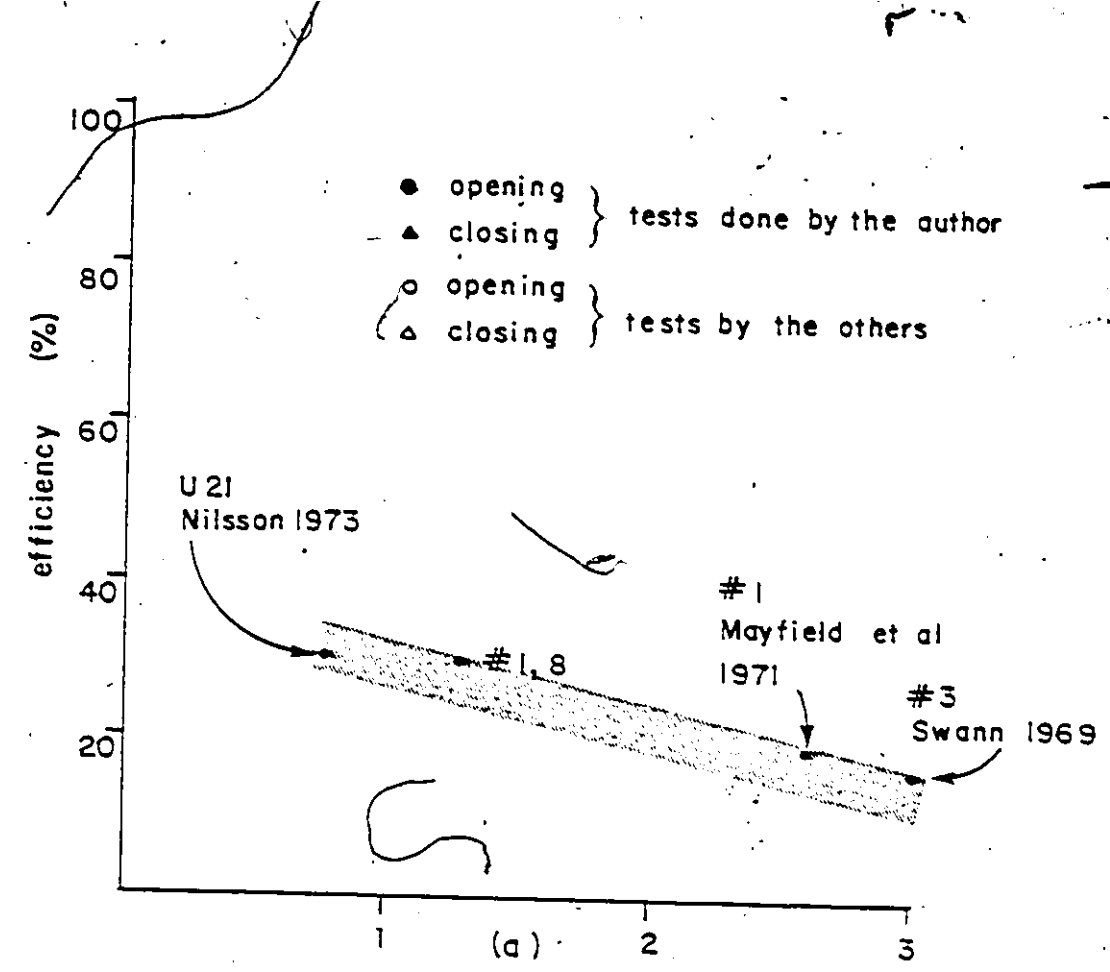


FIG. 58 COMPARISON OF RESULTS

One of the most significant differences is that the corners with lower steel ratio exhibited considerably more rotational capacity and relatively higher efficiency than the corners with higher ratio; for instance, the applied load reached 75 % of the ultimate flexural strength for the section with reinforcement ratio of 0.7 % and only 47 % for the section with ratio of 1.27 %. This agrees well with that concluded by the other investigators as the comparisons of the results are shown in Figure 58 .

As stated by Swann, and also according to the reinforcement details adapted in Germany and Russia, the trimming bar had been shown to be of little advantage. In the report of Nilsson, without diagonal tensile steel, corner efficiency of 100 % was attained simply because of the use of low reinforcement ratios of 0.5 %, 0.75 % and 1.2 % respectively. In this study, for the reinforcement details without diagonal steel, the efficiency was found to be 80 % for a steel ratio of 0.7 % and only 50 % for a steel ratio of 1.27 %. It is also believed that the load history affects the behavior of the reinforced concrete members. The difference in behavior indicates that the response under monotonic loading cannot be used to predict the response under cyclic loading. A comparison of the results of this study with respect to the reinforcement percentages are shown in Figure 58 and Table 2 .

## Chapter VI

### CONCLUSION AND RECOMMENDATION

#### 6.1 CONCLUSION

Based on the few experimental results presented here, several conclusions can be drawn for detailing practices related to the design and construction of reinforced concrete corner joints in a structure.

1. Generally, there is no problem encountered with a corner joint subjected to closing moment.
2. For the corner joints, the method of anchorage of beam bars recommended in the ACI 318-77 code appears to be adequate providing the joint region remains intact.
3. The energy dissipated by specimens 1 and 8 was very small compared to the amount for specimen 4. The difference lies in the two different loading histories applied to the specimens, namely, monotonic loading to specimens # 1 and # 8 with cyclic loading to specimen # 4.
4. When excessive amounts of beam steel are required to be carried into the joint and anchored,

- the joint zone may not be able to provide the potential strength of the members framing into it.
5. It is essential that the applied force simulates to some extent the forces acting on the corner joints of a structure under ground motions by earthquake.
  6. The characteristics of the loading history have a marked effect on the bond deterioration and the mode of failure. As a result of the gradual bond deterioration, the energy absorption diminishes but the additional secondary reinforcement seemed to have constrained the hook movements.
  7. Cycles of loading after the yielding of the main reinforcement produce concrete deterioration and modified steel properties causing changes in the cyclic energy absorption and the load-deflection curves. Cyclic reversed loading induces a progressive deterioration of bond between concrete and reinforcing bars.
  8. It is seen that good agreement exists between the observed results of the study and those of previous studies; namely, an increase in main reinforcement decreases the efficiency of the corners.

9. Size of main bars and patterns of arrangement are shown to be a critical aspect of joint performance. The styles of confinement and joint detailing are important. Good reinforcement layout at the corner assures satisfactory behavior.
10. In the current study, same size of reinforcing bars had been used for the flexural and diagonal reinforcement. It is evident that the addition of diagonal reinforcement did improve the behavior of the corner subjected to earthquake ground motion.
11. Higher reinforcement ratios generate higher stresses in the corner core; the diagonal reinforcement of specimen #6 reached a higher stress than that of specimen #7 with lower reinforcement ratio.
12. The assumption of a rigid joint is not accurate at large ductilities and at the yield levels under both monotonic and cyclic loading.

## 6.2 RECOMMENDATION

The following recommendations are for proportioning and detailing reinforced concrete corner joints in structures and are based on laboratory experience together with the previous investigation results.

It is, however, important that these recommendations be suitable to corners of equal column and beam width and though it appears to be conservative to the design of corners with wider column sections, corresponding valuable researches are needed.

1. The principal aim of the proposed design details should be to increase the resistance of the concrete in the core to resist the diagonal tensile forces developed when the joint is subjected to opening moment.
2. The intention of the design should ensure that no tensile cracks at the joint caused the failure.
3. Low reinforcement ratio and the application of diagonal steel should be designed to resist the diagonal cracks to ensure a desirable ductility and hence the response of the structure to the seismic loading.
4. The size of the diagonal reinforcement varies; but at least half of the main reinforcement area is recommended.
5. Stirrups are required for the whole length of both the beam and the column and adjacent to the corner joint to minimize the distress at the joint.

6. Main bar sizes should be severely restricted if their slippage is to be avoided.
7. Effect of inclined trimming reinforcement could be neglected.
8. For a corner joint subjected to closing moment, the equations in the ACI 318-77 Building Design Code can be used to meet the flexural requirements.
9. From a wider point of view, a frame type arrangement of the reinforcing bars at the joint seems to be capable of restraining the corner joint from failure due to either moments closing the joint or opening the joint.
10. In the present study, the objective had been aimed to improve the response of the corner joints to seismic loading so that the corner would not fail before reaching the ultimate flexural strength of the connecting beam, i.e. failure at the corner was allowed after reaching the ultimate load of the beam. To ensure that the hinging of members occurs at the beams so as to maintain the integrity of the structures by means of the columns, it is advisable that strong-column-weak-beam philosophy be followed, namely, on the basis of

using low steel ratios, the reinforcement ratio should be less for the beams than for the columns.

11. An idealized reinforcement detailing may be thought of as the set up similar to that in Figure 42 with the possibility that both the column and beam bars will be in the form as specimen # 7 and thus, the detailings can also be applicable when dealing with a column slab joint or a retaining wall.

It is not possible here to develop a complete and sound reinforcement detailing of the corner joints, the main point of the above conclusion and recommendation can just be treated as guidelines to the construction design of the joints. Definitely, more efforts have to be put in the researches on both the construction design of structures and the causes and prediction of earthquake, because after all, earthquake-resistant structure is never earthquake proof.

## BIBLIOGRAPHY

1. American Concrete Institute (ACI) "Manual of Standard Practice for Detailing Reinforced Concrete Structures", Proposed Revisions of ACI 315-65 and 315-74, ACI, Detroit, 1970 and 1974
2. ACI-ASCE Committee 352 "Recommendations for Design for Beam-Column Joints in Monolithic Reinforced Concrete Structures", ACI Jr., July, 1976
3. ACI Standard 318-77 "Building Code Requirements for Reinforced Concrete", ACI 318-77, Detroit, 1977
4. Bannison A, Kong F.K., and Mayfield B. "Corner Joint Details in Structural Lightweight Concrete", A.C.I. Jr. May 1971
5. Bannison A, Kong F.K., and Mayfield B. "Strength and Stiffness of Lightweight Concrete", A.C.I. Jr. July 1972
6. Betonniye i Zhelezobetonniye Konstruktsii, Norm'i Protektirovaniya. SNIIP II-B 1-62. Gosudarstvenn'ii Komitet Sovyeta Ministrov SSSR po Delam Stroitel'stva. Stroitel'niye Norm'i "ravila. Moscow 1962 Building Codes and Recommendations for Concrete and Reinforced Concrete Structures
7. Blume J.A., Corning L.H., and Newmark N.M. "Design of Multistory Reinforced Concrete Buildings for Earthquake Motions", Portland Cement Association, 1961
8. Clarke J.L. and Taylor H.P.J. "Some Detailing Problems in Concrete Detailing Problems in Concrete Frame Structures", The Structural Engineer, V.54 No.1, Jan. 1976
9. Clough R.W. and Penzien J. "Dynamics of Structures" McGraw Hill Book Company, 1975.
10. Conner H.W. and Hanson N.W. "Seismic Resistance of Reinforced Concrete Beam-Column Joints", Jr. of the Structural Division, Proc. A.S.C.E., Oct. 1967

11. DIN 4224 Bemessung im Stahlbetonbau. DIN-Taschenbuch 37 . Baunormen. Beton- and Stahlbetonbau. Published by Deutschen Normenausschuss (DNA), Berlin 30. Beuth-Vertrieb GmbH, 1972
12. Fintel M. "Handbook of Concrete Engineering" , Van Nostrand Reinhold Company, N.Y., 1974
13. Gumensky D.B. "Concrete Corners in Tension" , Engineering News Record, V. 123, New York , September 1939
14. Hall A.S., Rangan B.V. and Warner R.F. "Reinforced Concrete" , Pitman, Australia 1977
15. Joint Committee of the Concrete Society and the Institution of Structural Engineers, "Standard Method of Detailing of Reinforced Concrete", London, 1970
16. Kordina K. and Fuchs G. "Untersuchungen zur Anwendung von hakenformigen Uebergreifungs stossen in Rahmenecken", Vorlaufiger Abschlussbericht. Institut fur Baustoffkunde und Stahlbetonbau. Der Technischen Universitat Braunschweig. Braunschweig, Januar 1970
17. Nilsson I.H.E. "Reinforced Concrete Frame Joints Subjected to Positive Moment" , National Swedish Building Research Summaries 1969
18. Nilsson I.H.E. "Reinforced Concrete Corners and Joints Subjected to Bending Moment" , National Swedish Building Research, D-7, 1973
19. Ostlund L. "Inverkan av bockningsradier och tackande betongskikt hos kamstal pa spjalkningsrisken for armerade betongkonstruktioner" , (The Influence of the Bending Radius and Concrete Cover for Deformed Bars on the Risk of Splitting Failure in Reinforced Concrete Structures) (Stencil). The Royal Institute of Technology (KTH). Stockholm 1963
20. Paduart A. "Etude des tensions regnant dans les angles de portiques en beton arme". Bulletin de la Societe Royale Belge des Ingenieurs et des Industriels. No.3, Bruxelles 1940
21. Park R. and Paulay T. "Reinforced Concrete Structures" , John Wiley and Sons, New York, 1975
22. Posey C.J. and Kofoid O. "Reinforced Concrete Corners in Tension" , Jr. A.C.I., Proc. V.40 Detroit, September 1943

23. Ryan J. "Reinforced Concrete Beam-Column Connections" , Concrete Mag. March 1977
24. Sandbye P. and Nicolajsen J.S. "Rammehjorner af jernbeton. Planlaegning af forsogsserie" , (Frame Corners in Reinforced Concrete. Planning of Test Series. In Danish.) , Danmarks Ingeniorakademi, Bygningsafdelingen. Rapport 67/35, Copenhagen, Dec. 1967
25. Sandbye P. and Fangel M. "Rammehjorner af jernbeton 1969. Planlaegning af forsogsserie" , (Frame Corners in Reinforced Concrete. Planning of Test Series. In Danish.) Denmarks Ingeniorakademi, Bygningsafdelingen. Rapport 68/27, Copenhagen, Nov. 1968
26. Sandbye P. "Rammehjorner af jernbeton 1970. Planlaegning af forsogsserie." , (Frame Corners in Reinforced Concrete. Planning of Test Series. In Danish ) Denmarks Ingeniorakademi, Bygningsafdelingen. Rapport 70/1, Copenhagen, Jan. 1970
27. Statens Betongkommitte (National Concrete Committee), "Bestammelser for betongkonstruktioner - Allmanna Konstruktionsbestammelser (Building Code for Concrete Structures, in Swedish), Publication B6, AB Svensk Byggtjanst, Stockholm, 1968.
28. Swann R.A. "Flexural Strength of Corners of Reinforced Concrete Portal Frames" , Cement and Concrete Association, London, Technical Report TRA 434, Nov. 1969.
29. Wastlund G. "Untersuchungen uber die Festigkeit von Beton bei Belastungen, welche ortlich auf die Oberflache sowie an Schleifen and Abbiegungen von Bewehrungseisen Wirken" , Dissertation presented to The Royal Institute of Technology (KTH) in Stockholm in fulfilment of the requirements for the Degree of Doctor of Technology (teknologie doktorsgrad). Tryckeri Aktiebolaget Thule, Stockholm 1934
30. Weigel R.L. "Earthquake Engineering" , Prentice-Hall Inc., Englewood Cliffs, N.J. 1970
31. Zienkiewics O.C. "The Finite Element Method in Engineering Science" , McGraw-Hill, London 1971

Appendix A  
LAYOUT OF SPECIMENS

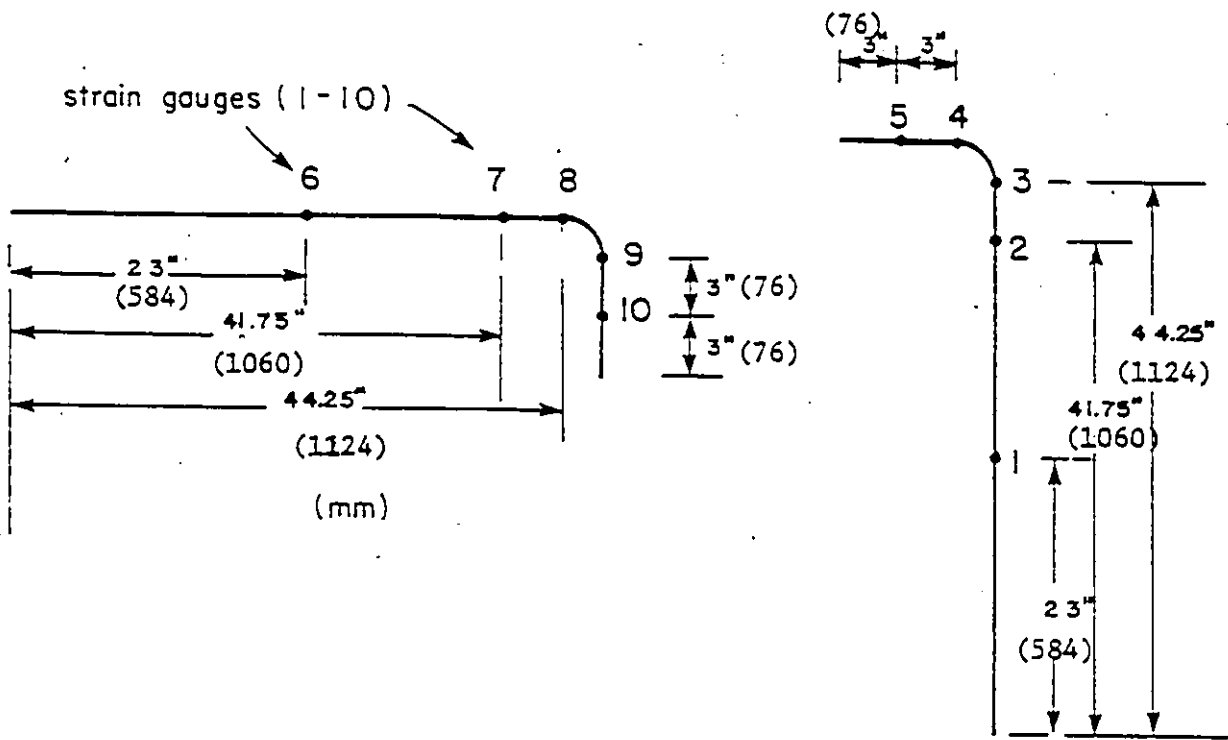
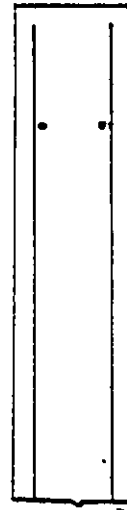
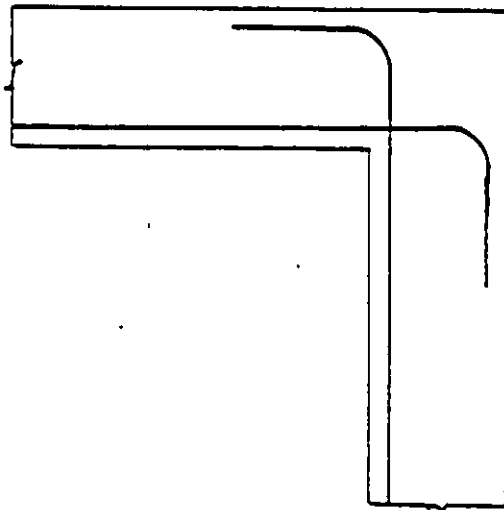
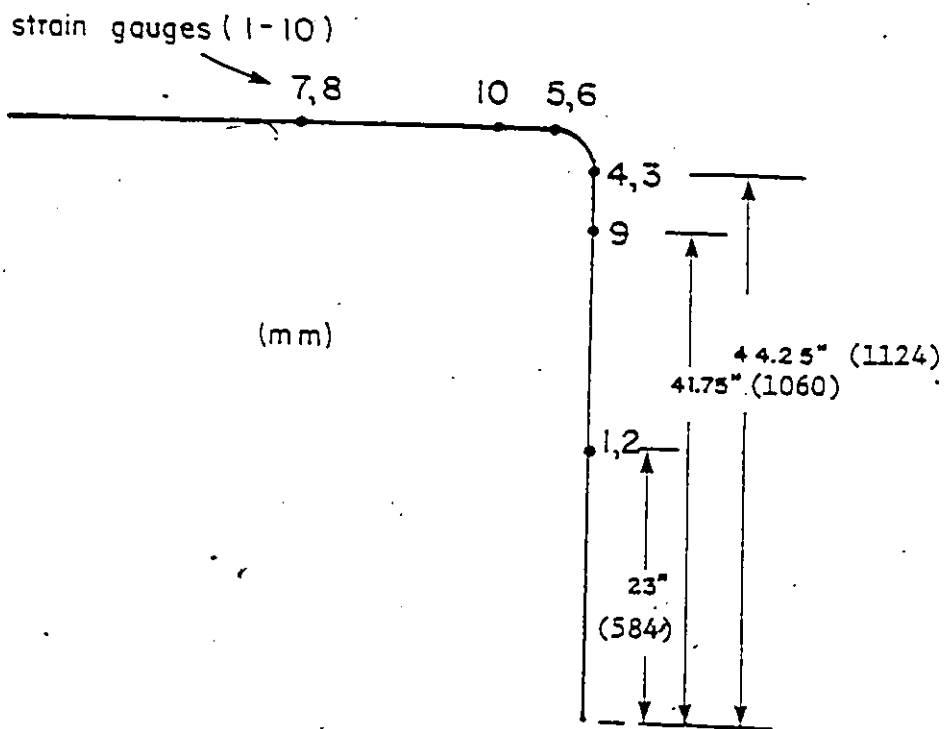
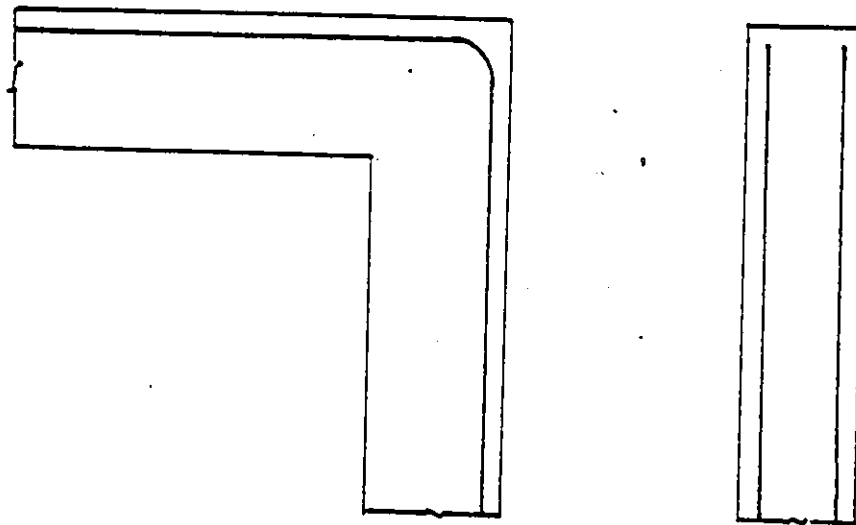


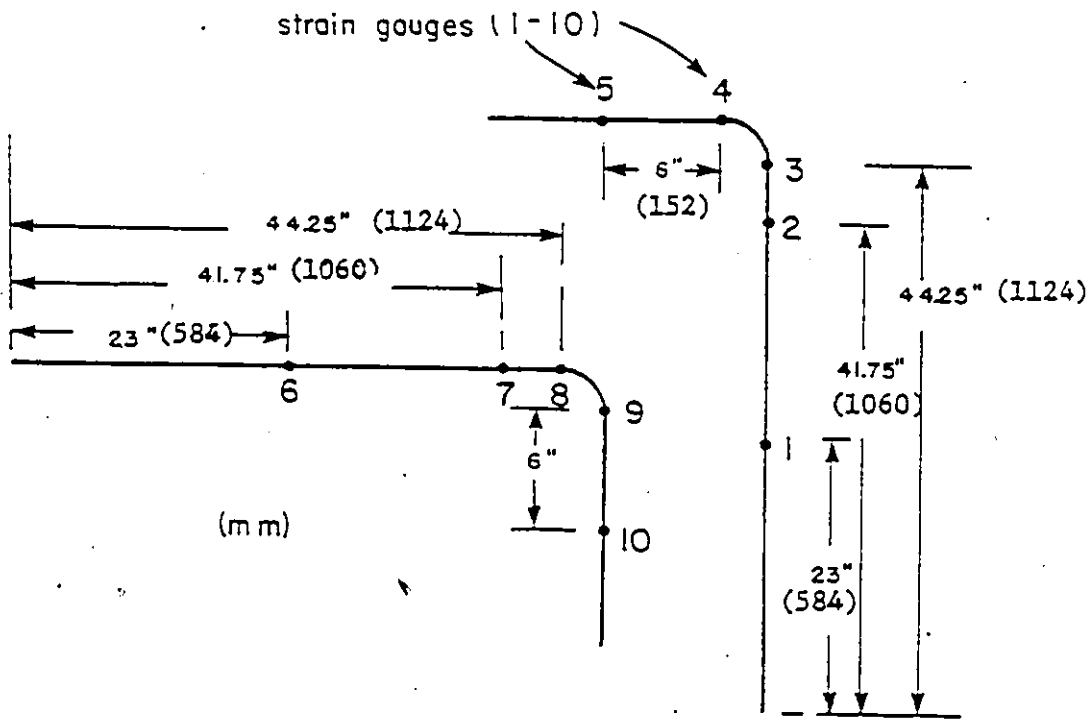
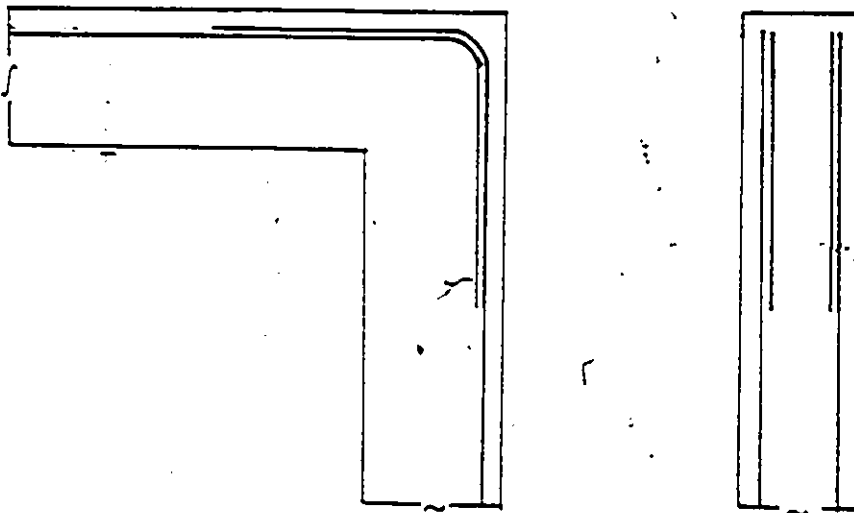
FIG. 37 REINFORCEMENT LAYOUT



specimen 2

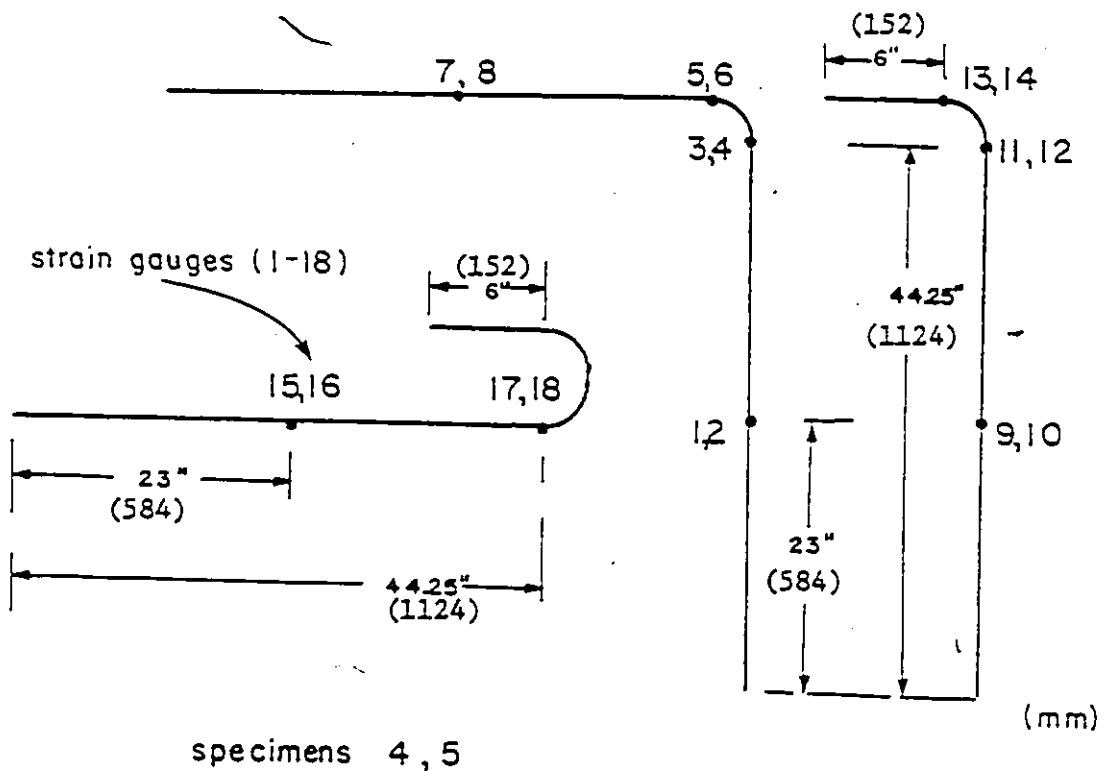
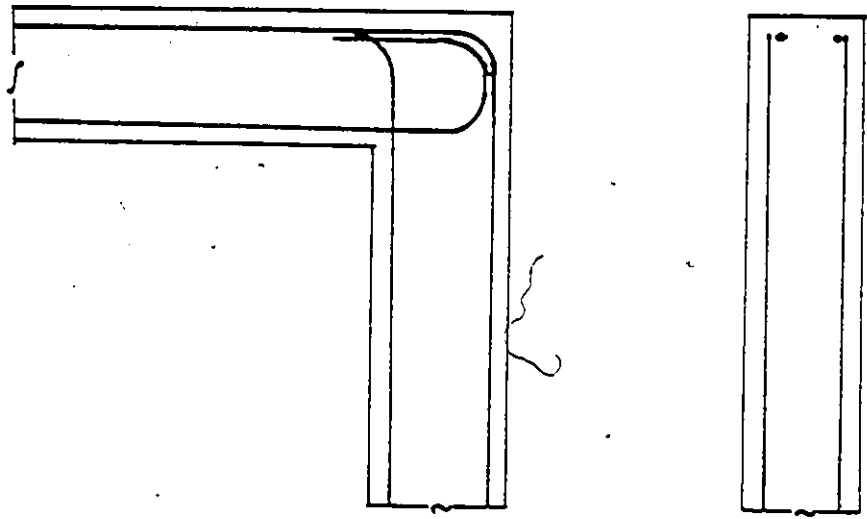
FIG. 38

REINFORCEMENT LAYOUT



specimen 3

FIG. 39 REINFORCEMENT LAYOUT



specimens 4, 5

FIG. 40 REINFORCEMENT LAYOUT





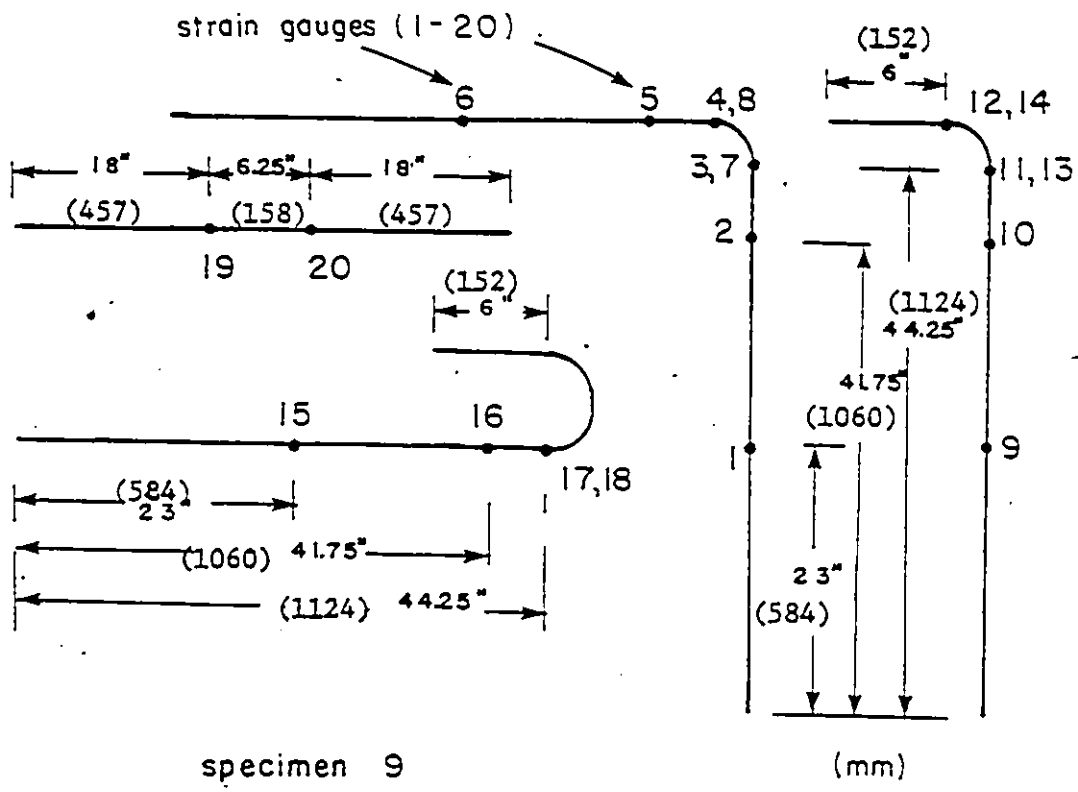
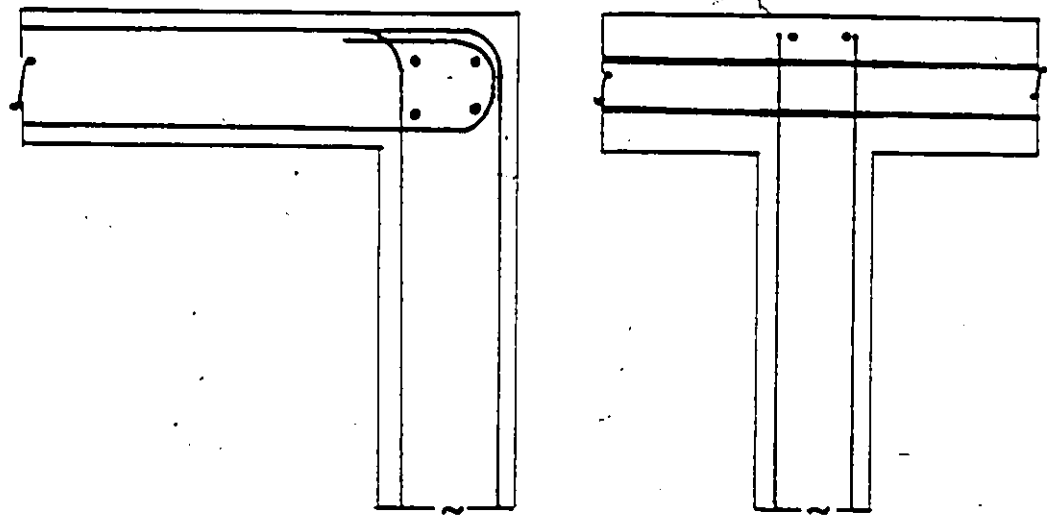


FIG. 43 REINFORCEMENT LAYOUT

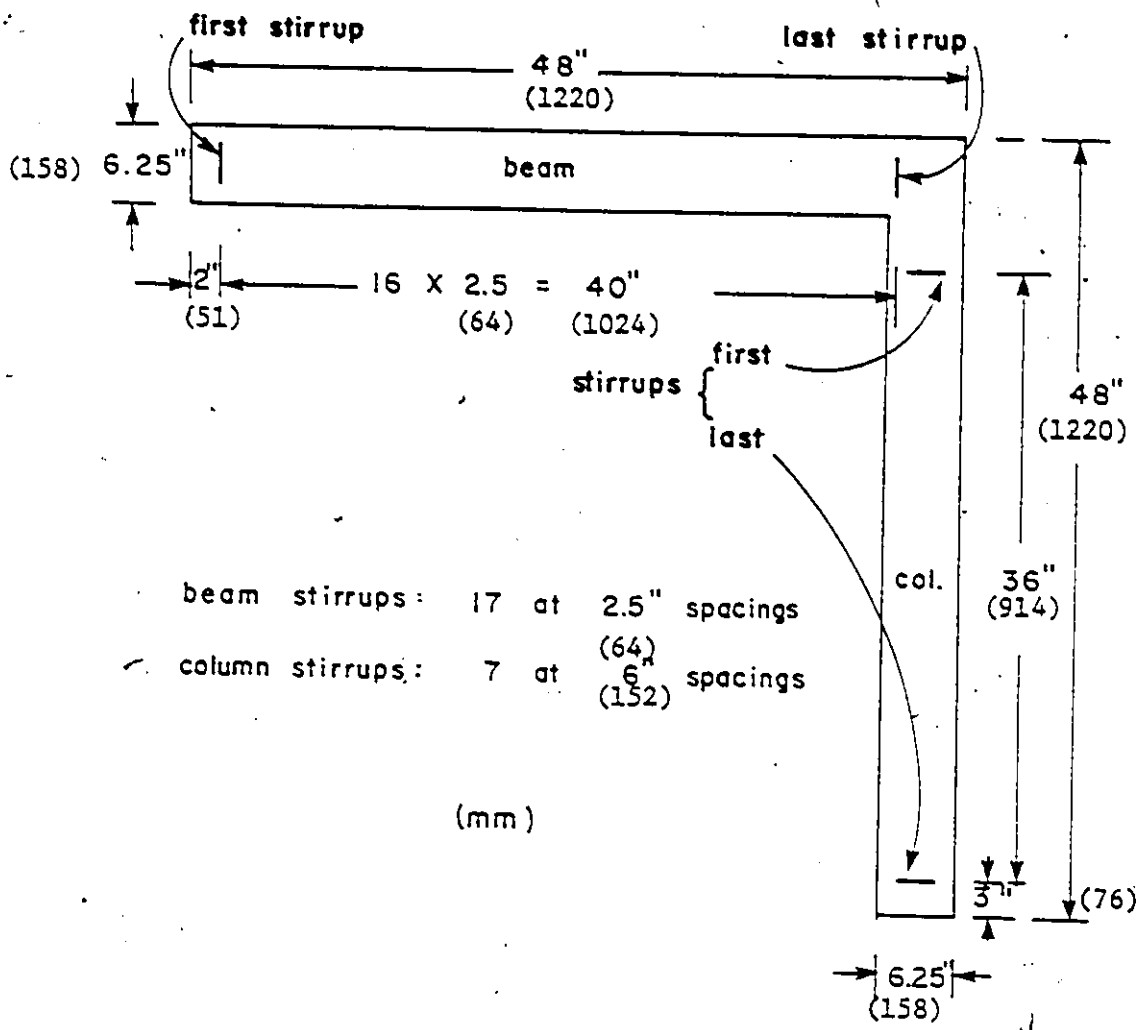


FIG. 44 MEMBER STIRRUPS

## Appendix B

TABLE 2

## Specimens Properties and Test Results

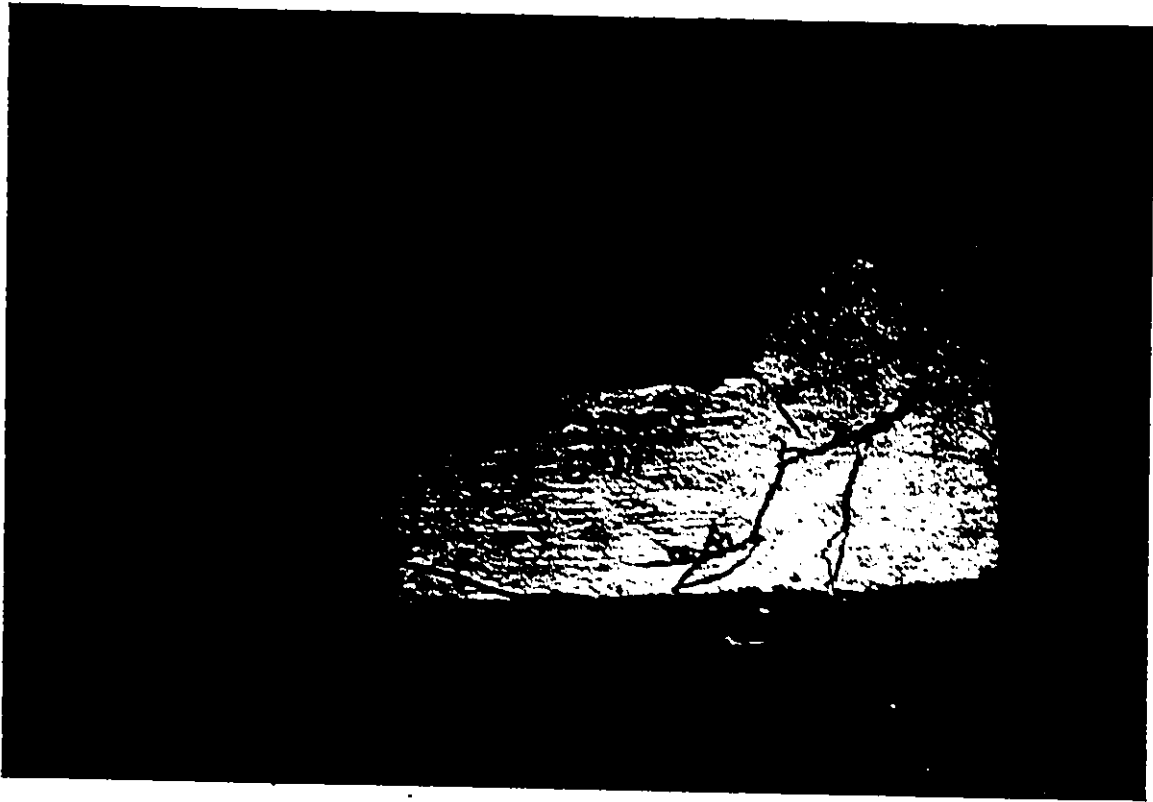
Specimen	Diameter of Main Bars (mm)	Nominal Yield Strength (MPa)	Concrete Strength At Test (MPa)	Type of Moment at Failure	Efficiency attained (closing) (%)	Efficiency attained (opening) (%)
1	13	413.7	39.3	opening	—	30
2	13	413.7	33.8	closing	100	—
3	13	413.7	31.0	closing	100	—
4	13	413.7	38.6	closing	100	47
5	9.5	413.7	29.6	closing	100	80
6	13	413.7	37.9	opening	100	75
7	9.5	413.7	34.5	opening	100	97.5
8	13	413.7	31.0	opening	—	30
9	13	413.7	34.5	opening	100	80

Appendix C

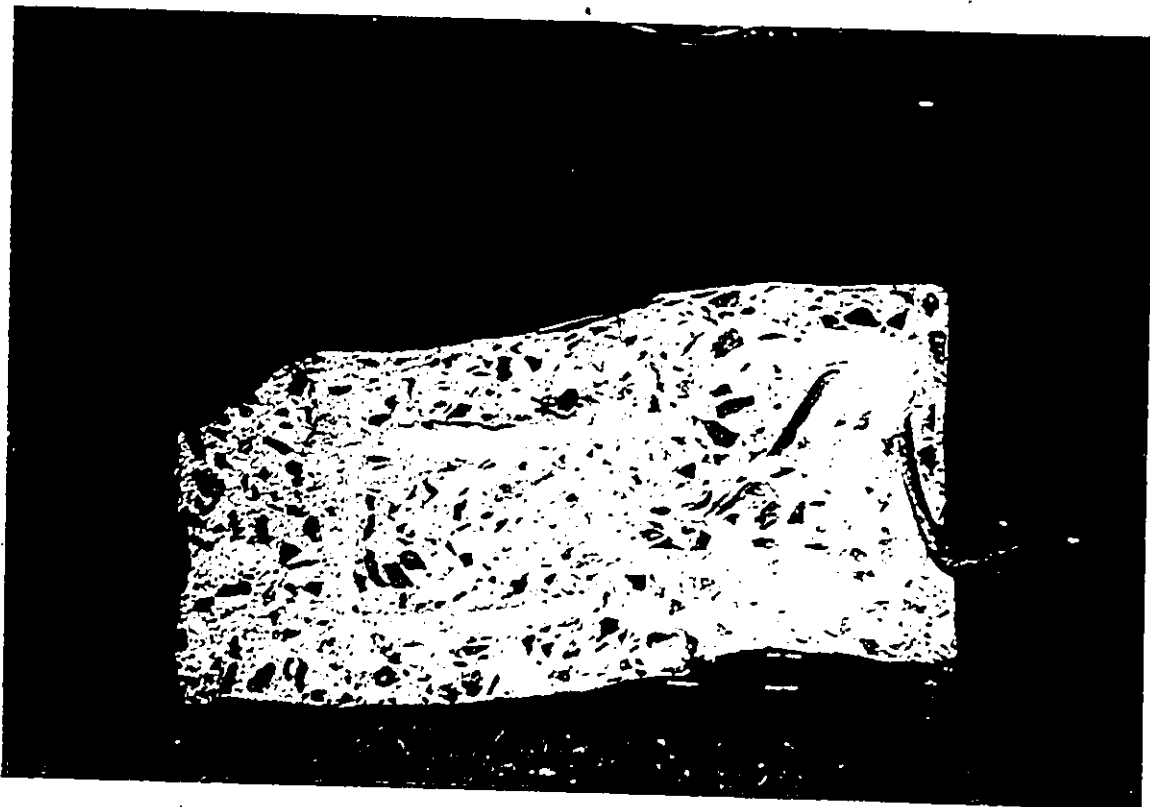
RESULTS

6

2



(i)



(ii)

(a) illustration of specimen when test was terminated

FIG. 48 TEST RESULTS - SPECIMEN I

COLOURED PICTURES



(a)

(a) illustration of specimen when test was terminated

FIG. 49 TEST RESULTS - SPESIMEN 2

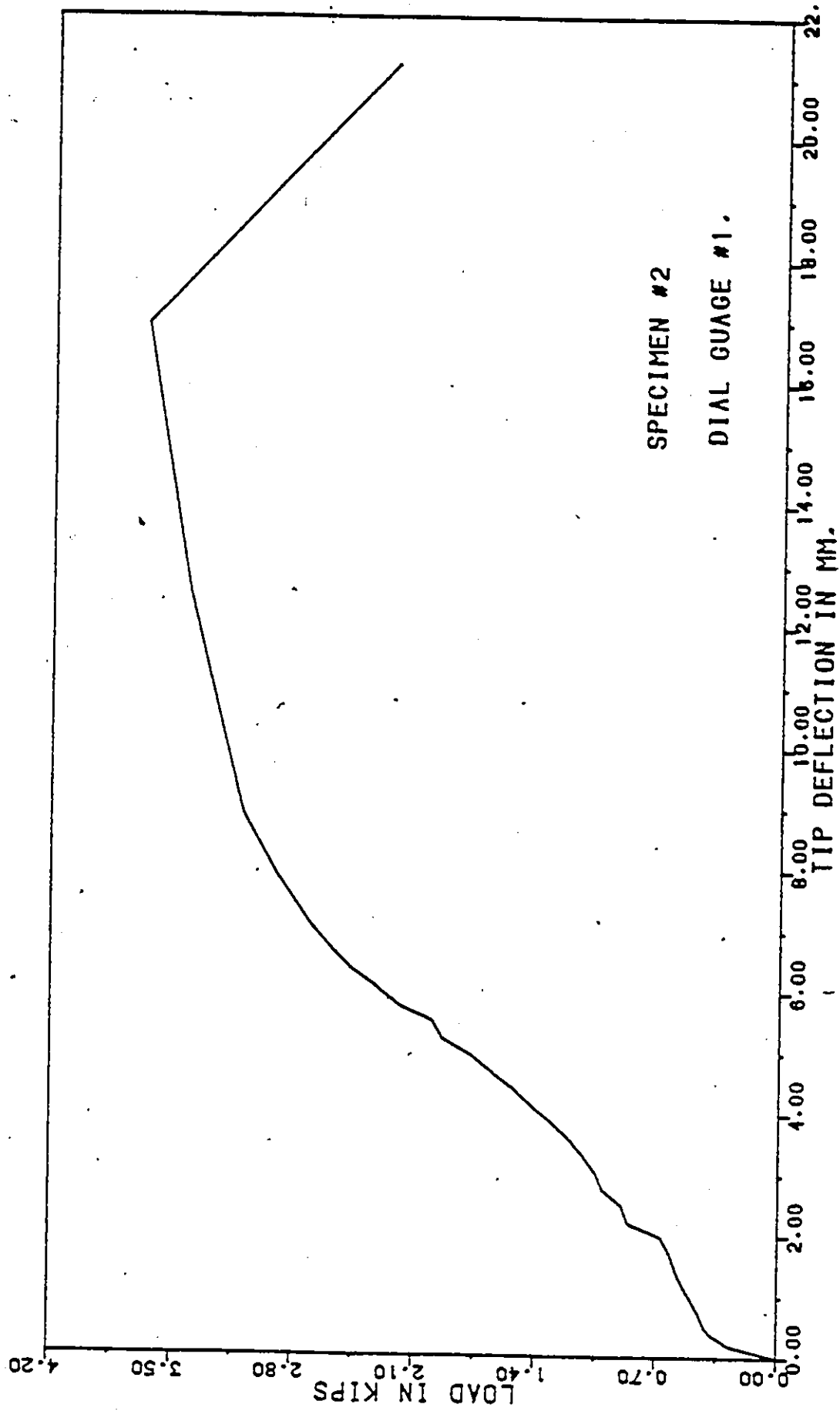


FIG. 49-b LOAD DEFLECTION CURVE

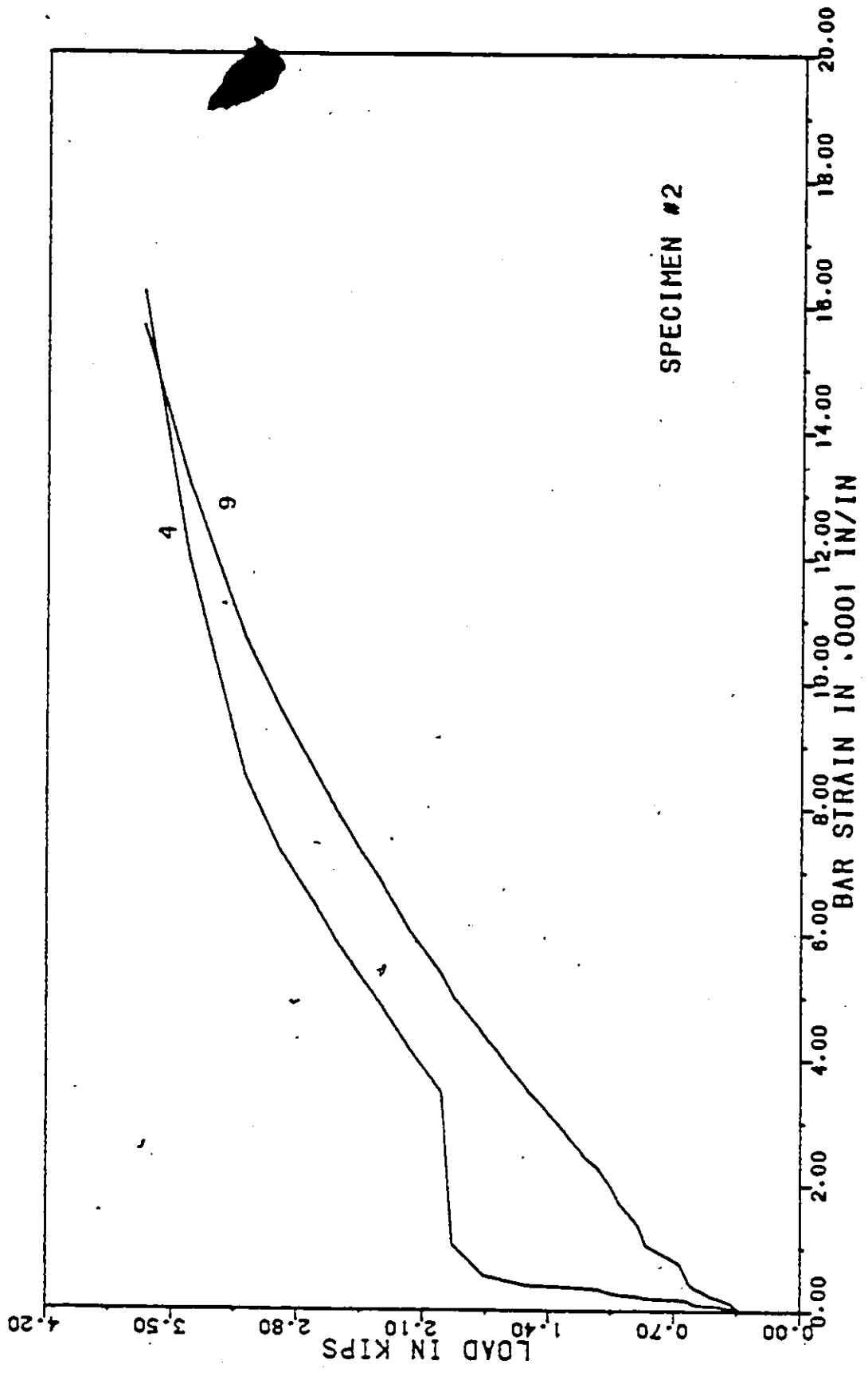


FIG. 49-c . LOAD - STRAIN CURVES

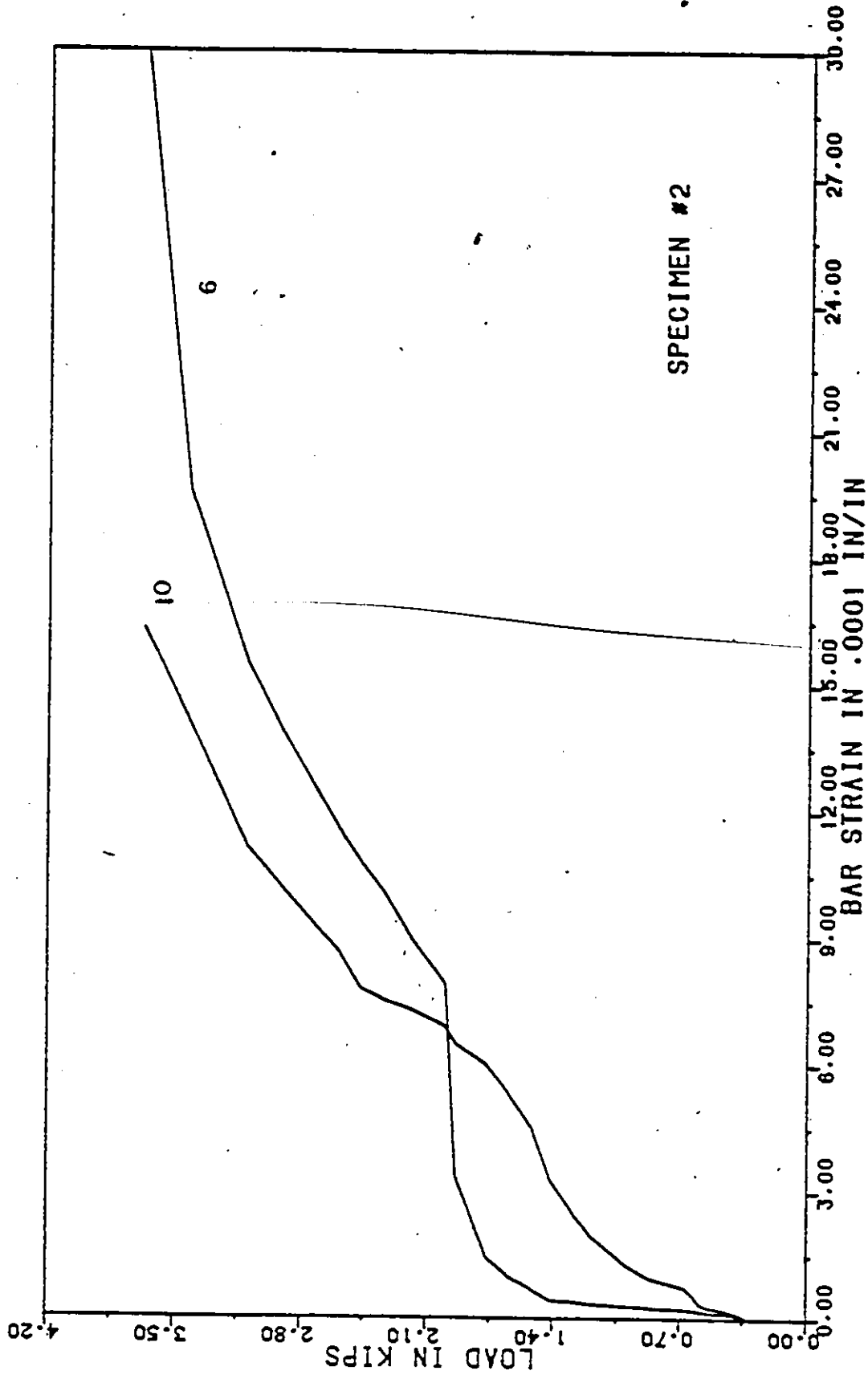
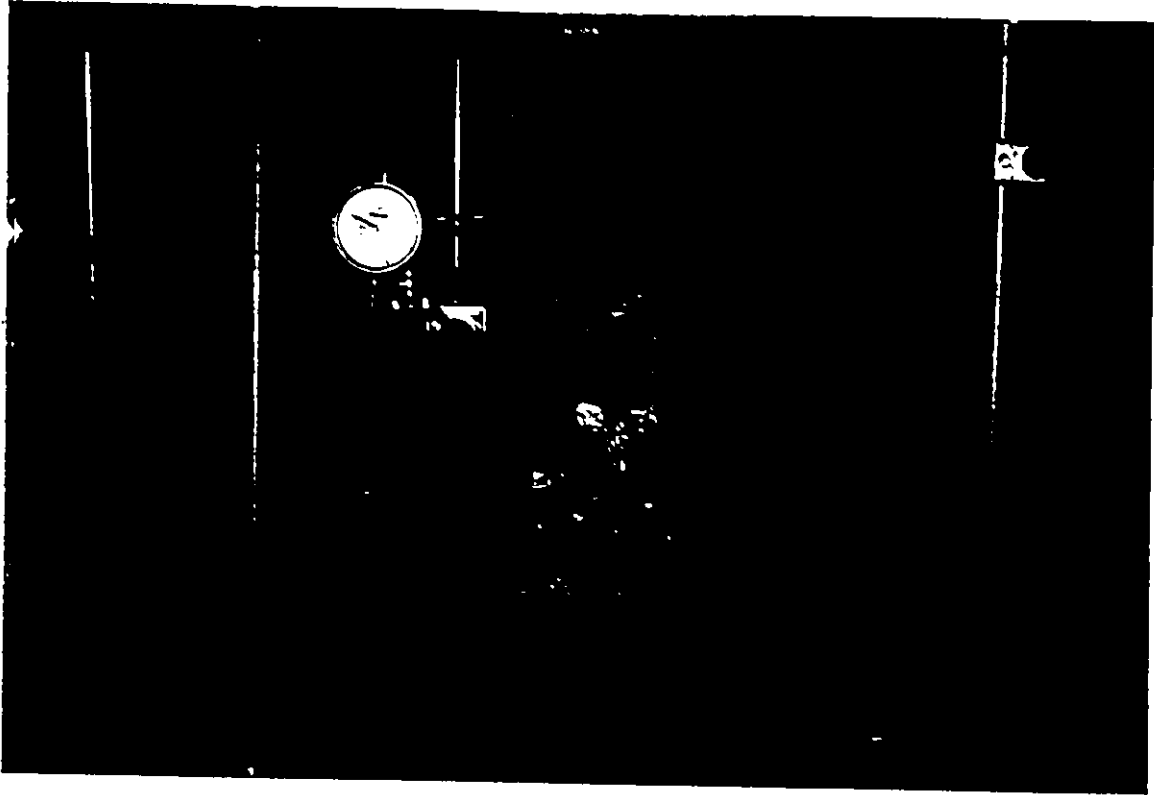


FIG. 49-d LOAD-STRAIN CURVES



(a) illustration of specimen when test was terminated

FIG. 50 TEST RESULTS - SPECIMEN 3

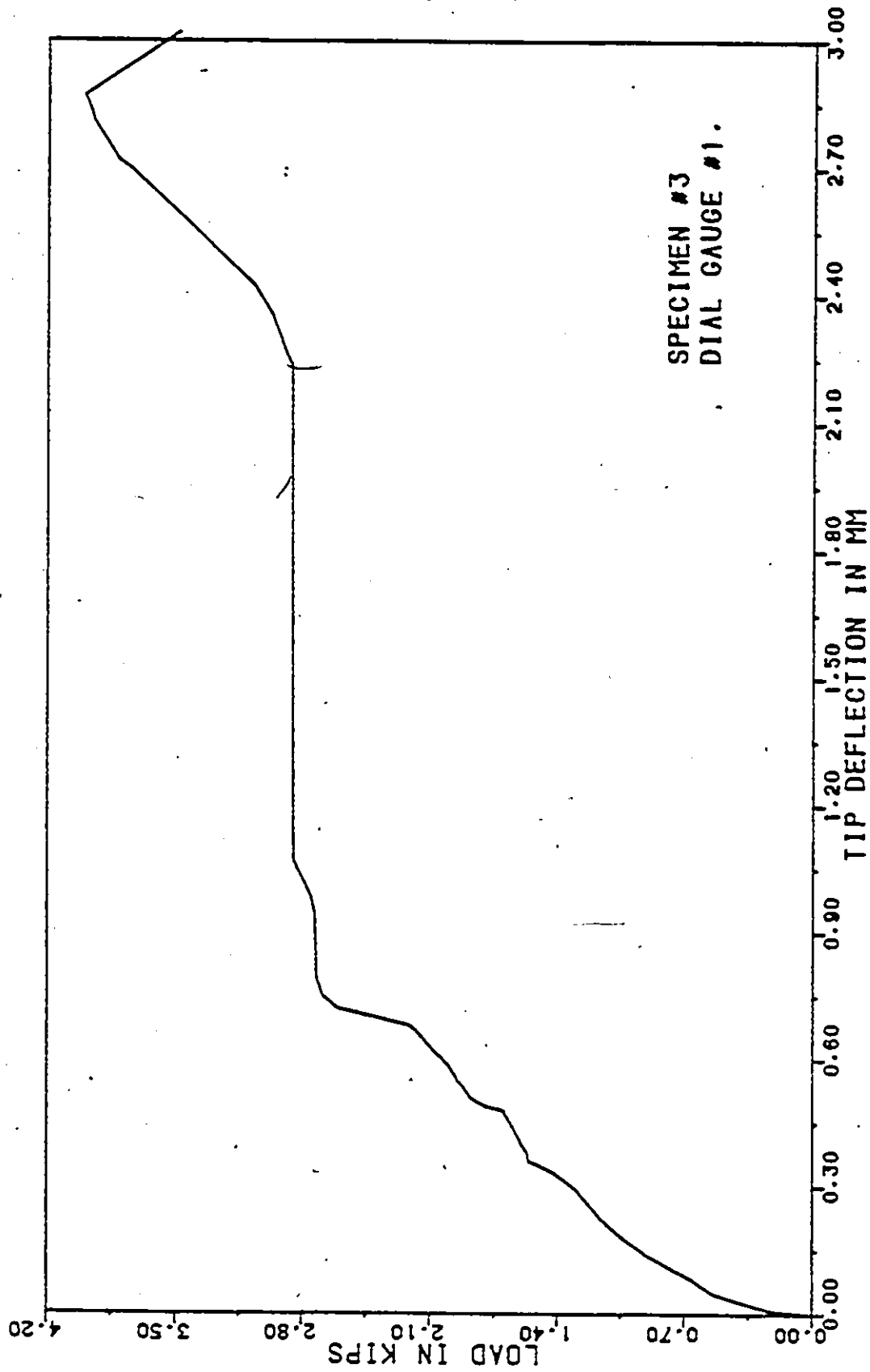


FIG. 50 - b LOAD-DEFLECTION CURVE

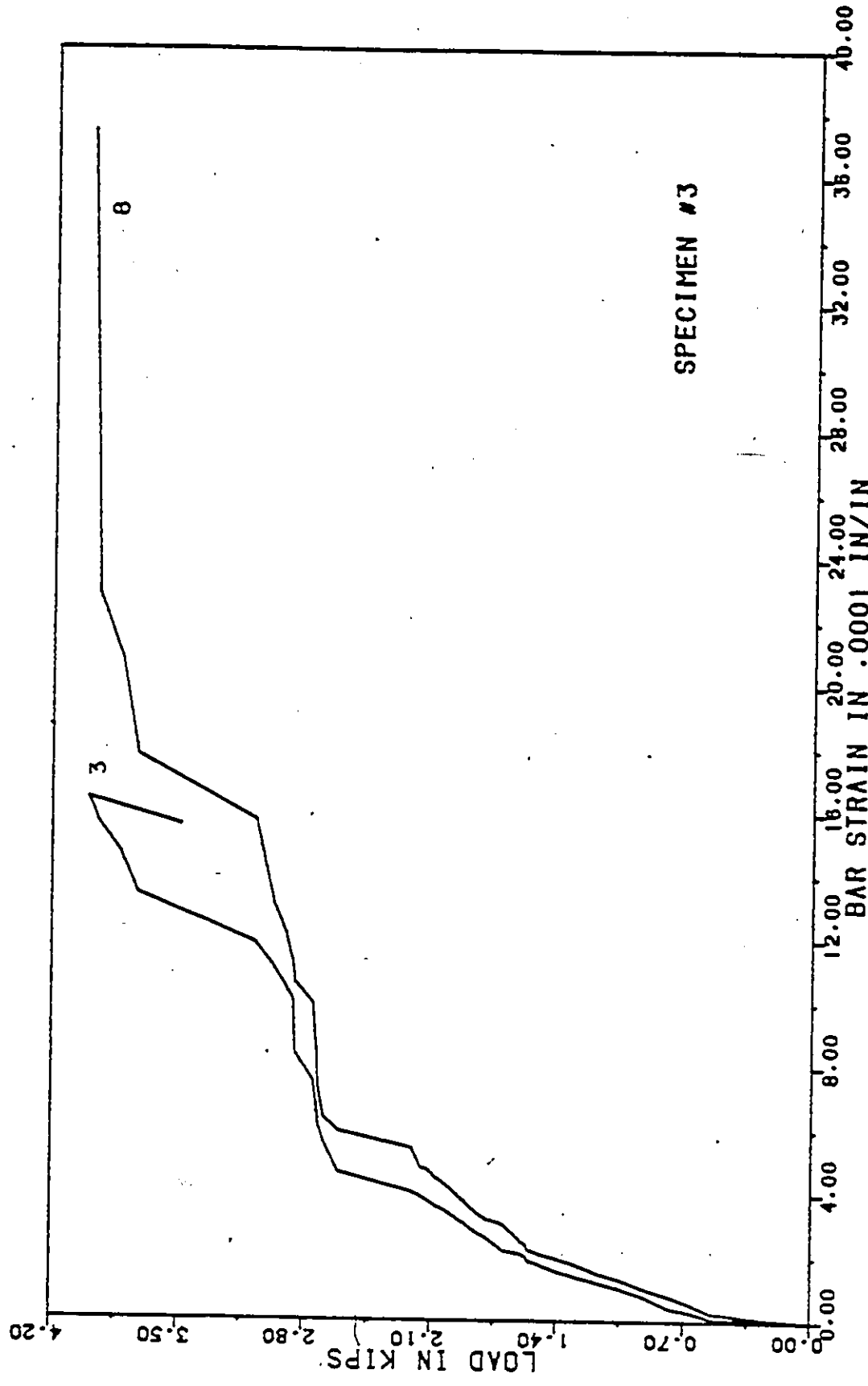


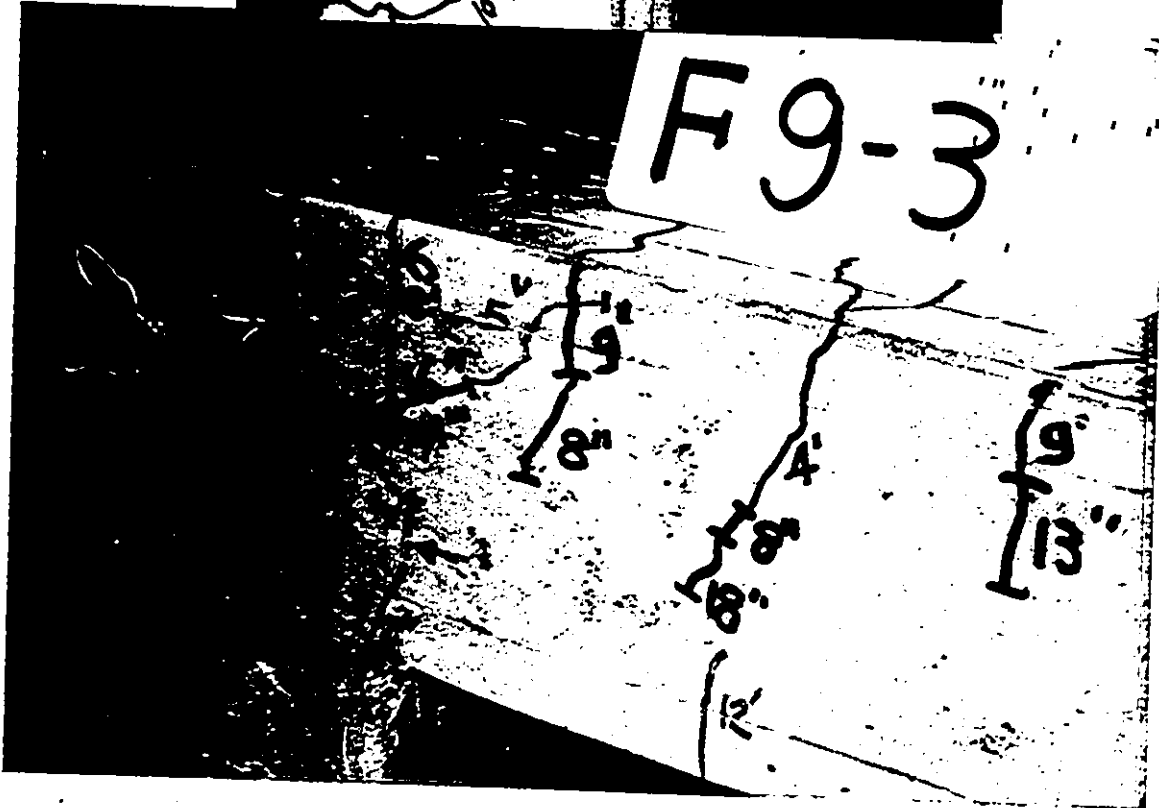
FIG. 50-c LOAD-STRAIN CURVES

F9-3



(i)

F9-3



(ii)

(a) illustration of specimen when test was terminated  
FIG. 51 TEST RESULTS - SPECIMEN 4

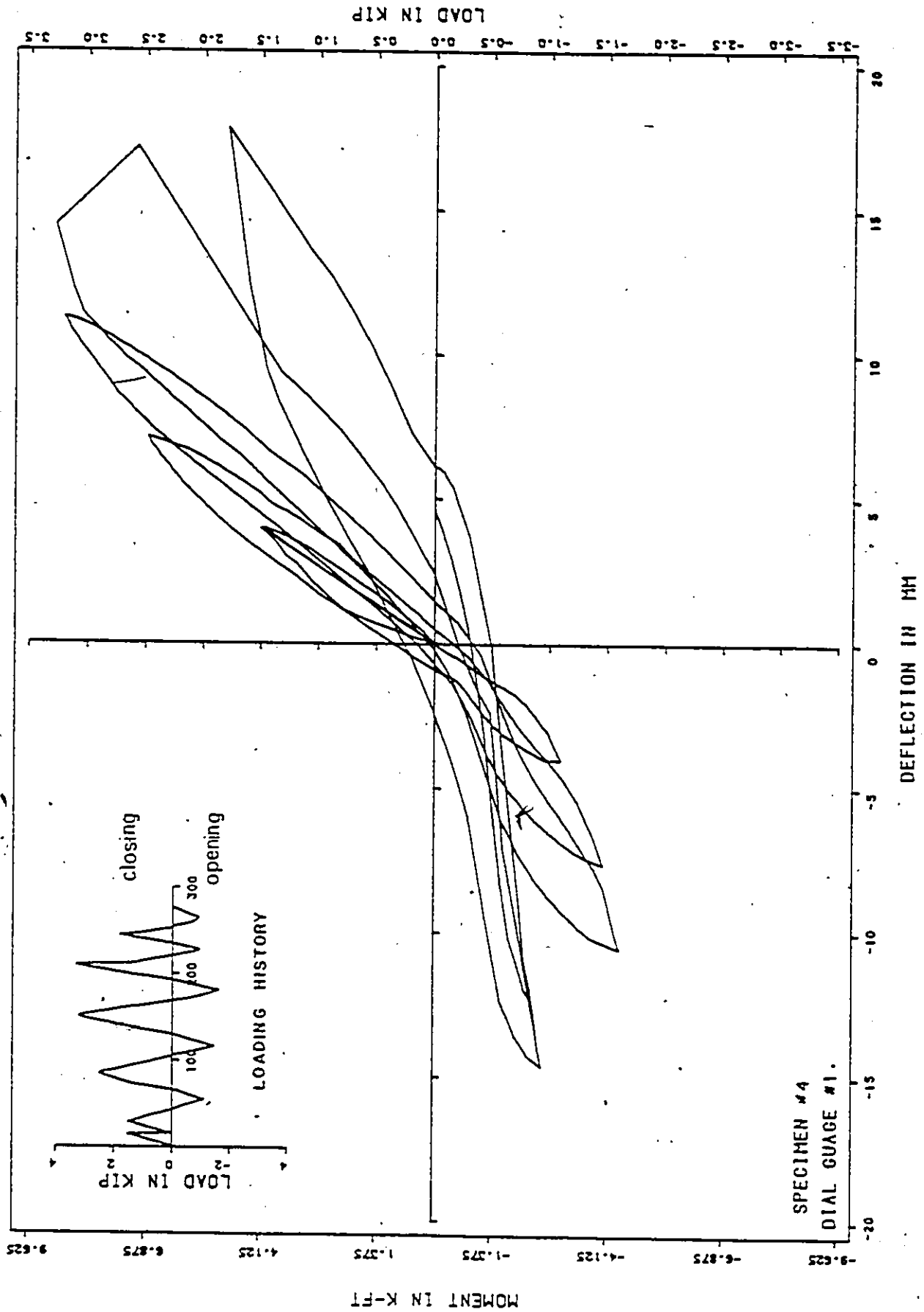
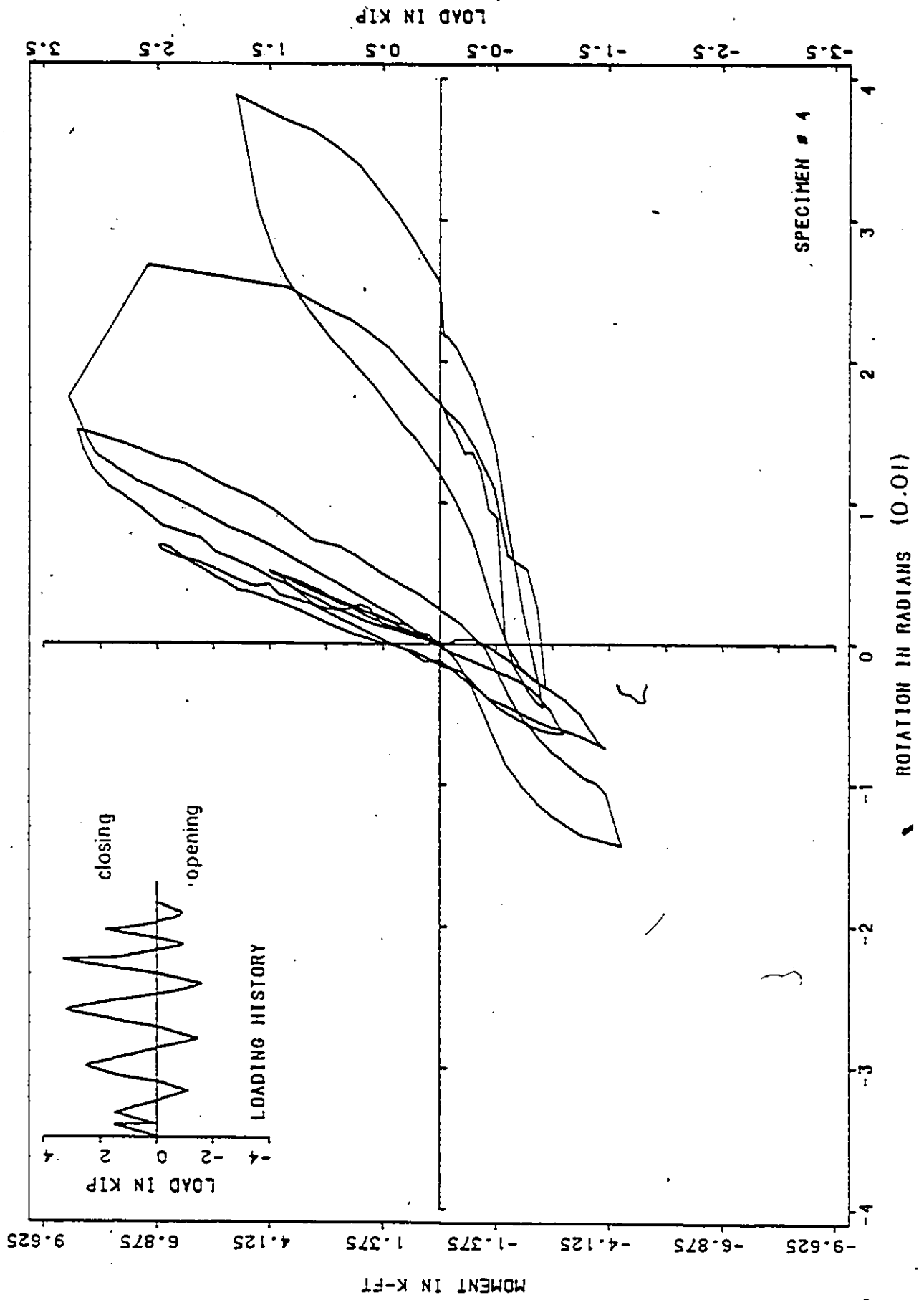


FIG. 51-b MOMENT-DEFLECTION CURVE



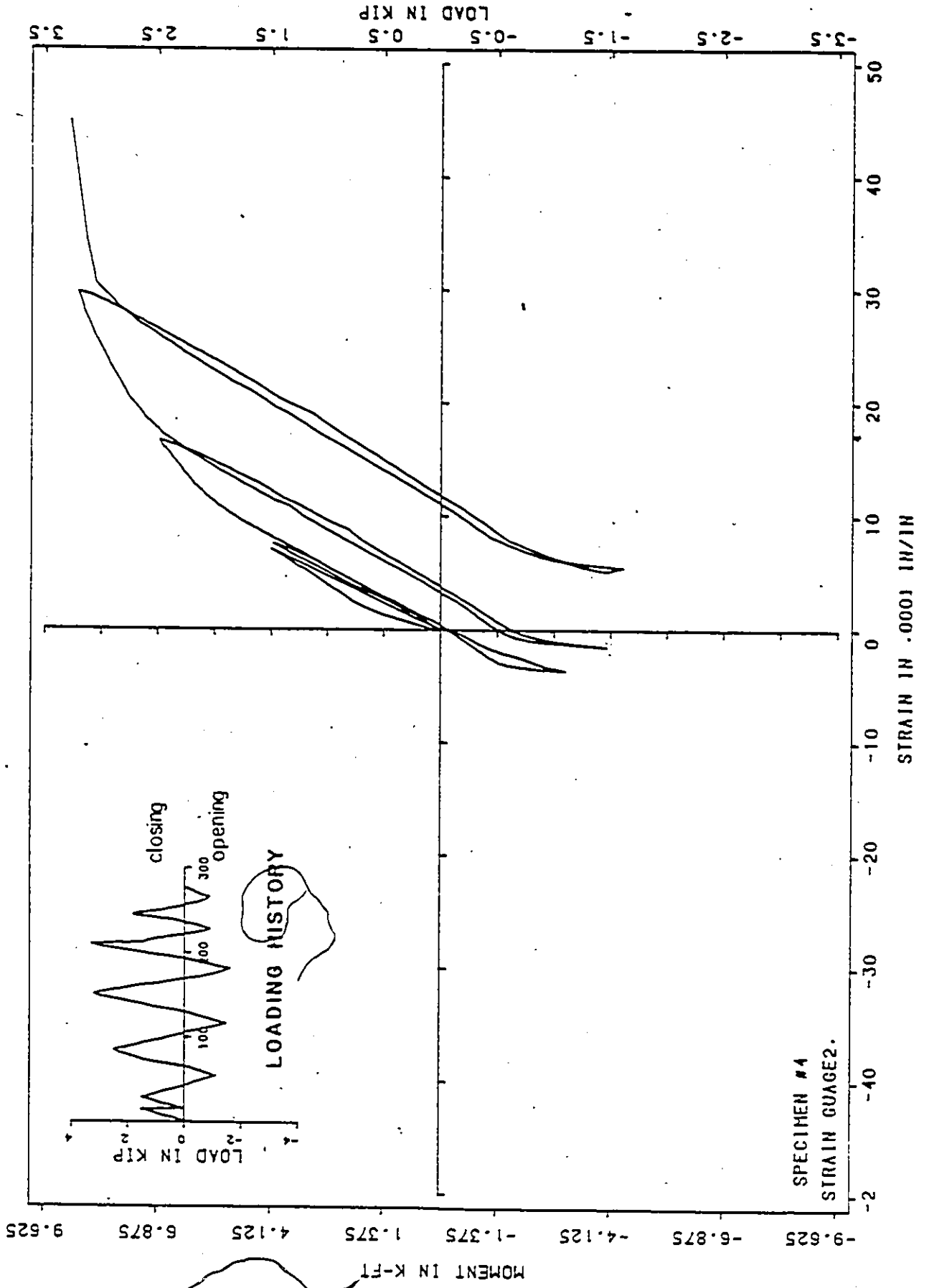


FIG. 5I-d MOMENT-STRAIN CURVE

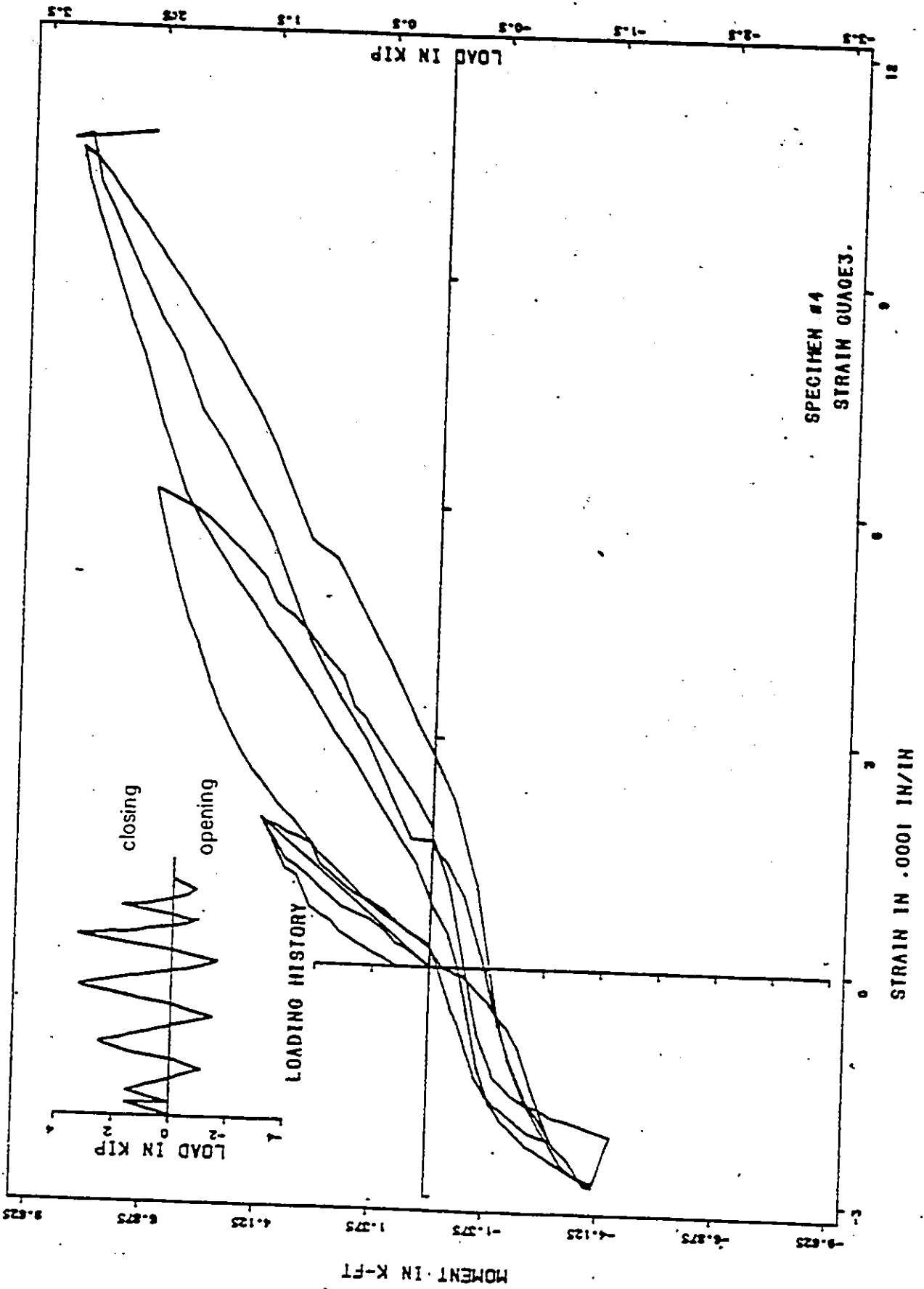
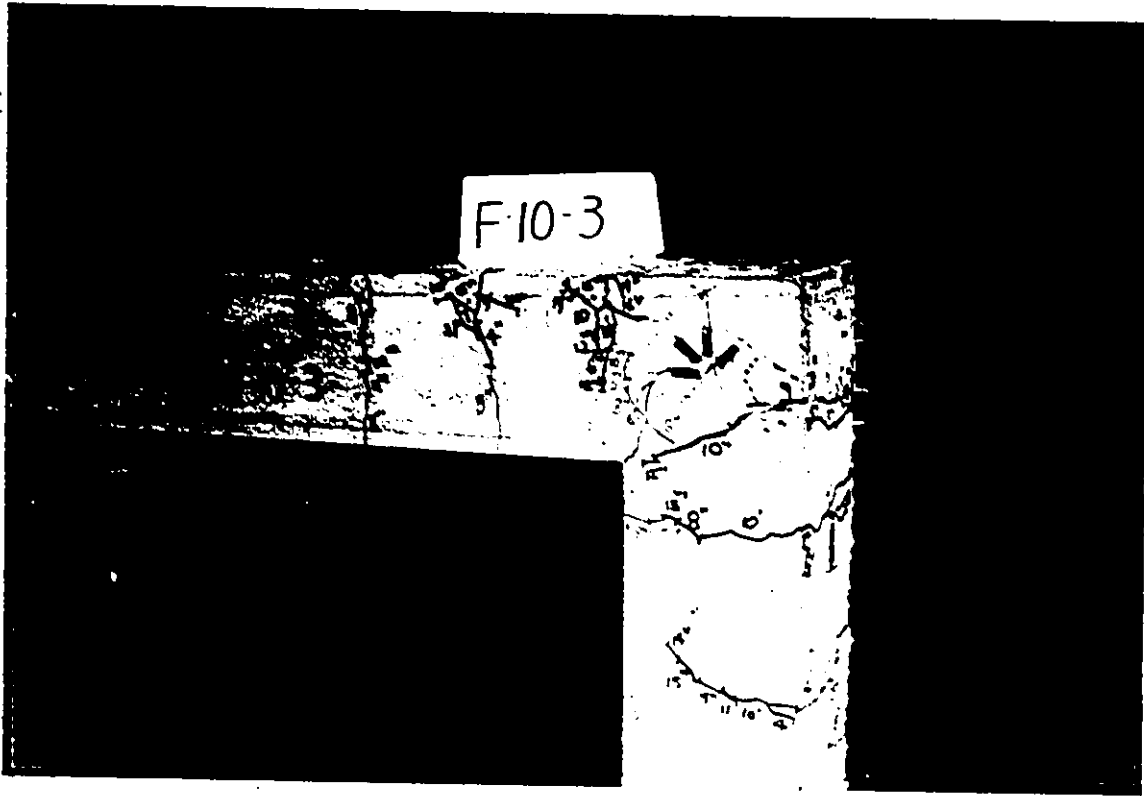
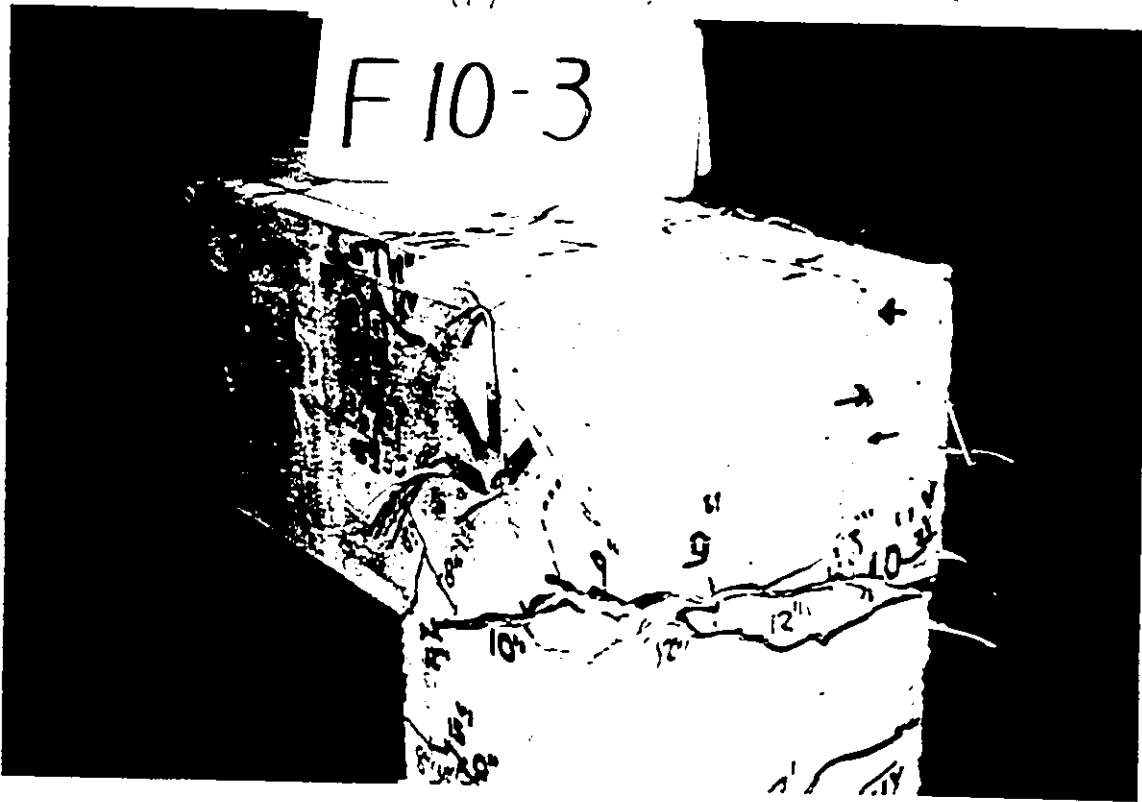


FIG. 51-e MOMENT-STRAIN CURVE



(i)



(ii)

(a) illustration of specimen when test was terminated

FIG. 52 TEST RESULTS - SPECIMEN 5

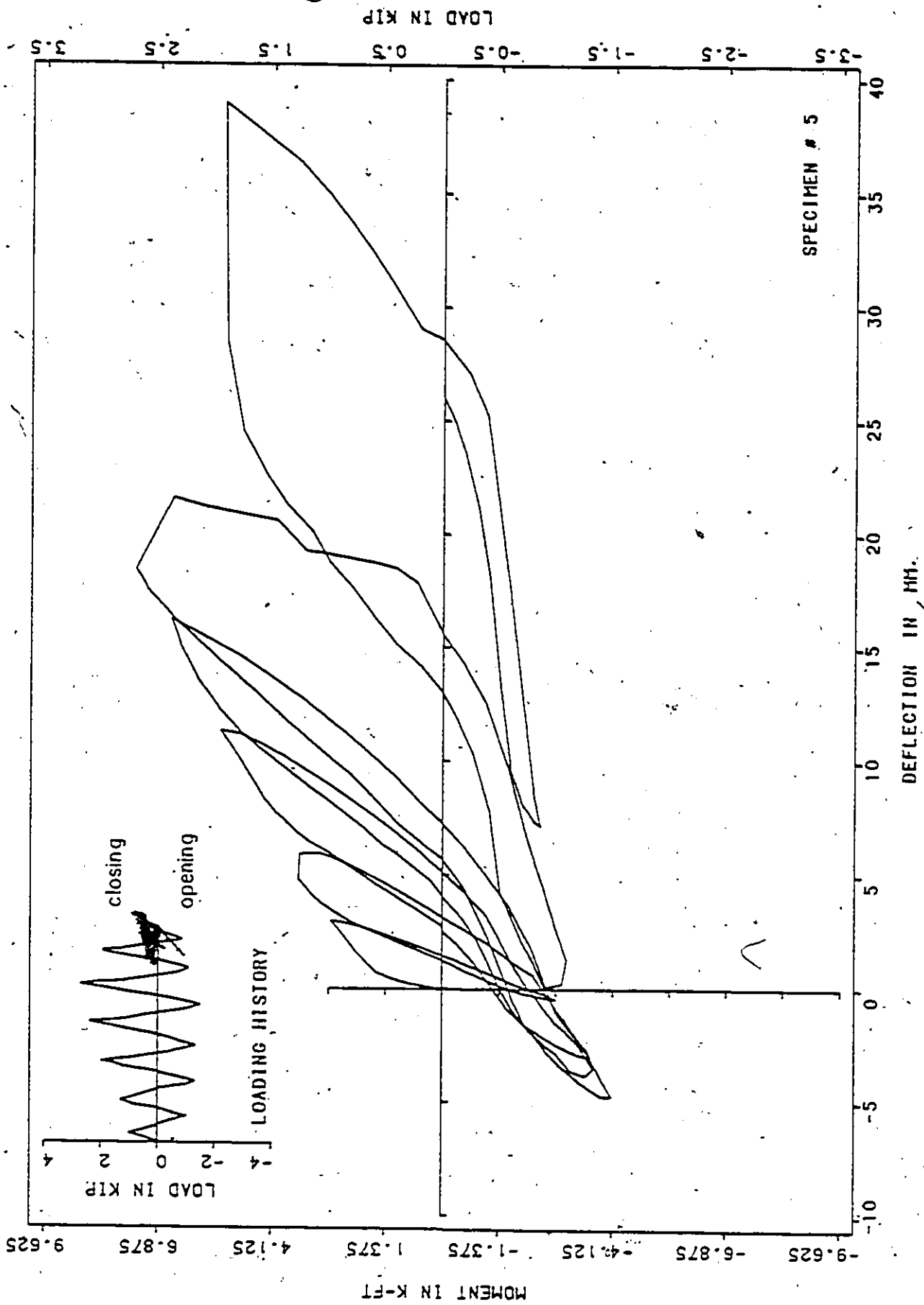


FIG. 52-b MOMENT-DEFLECTION CURVE

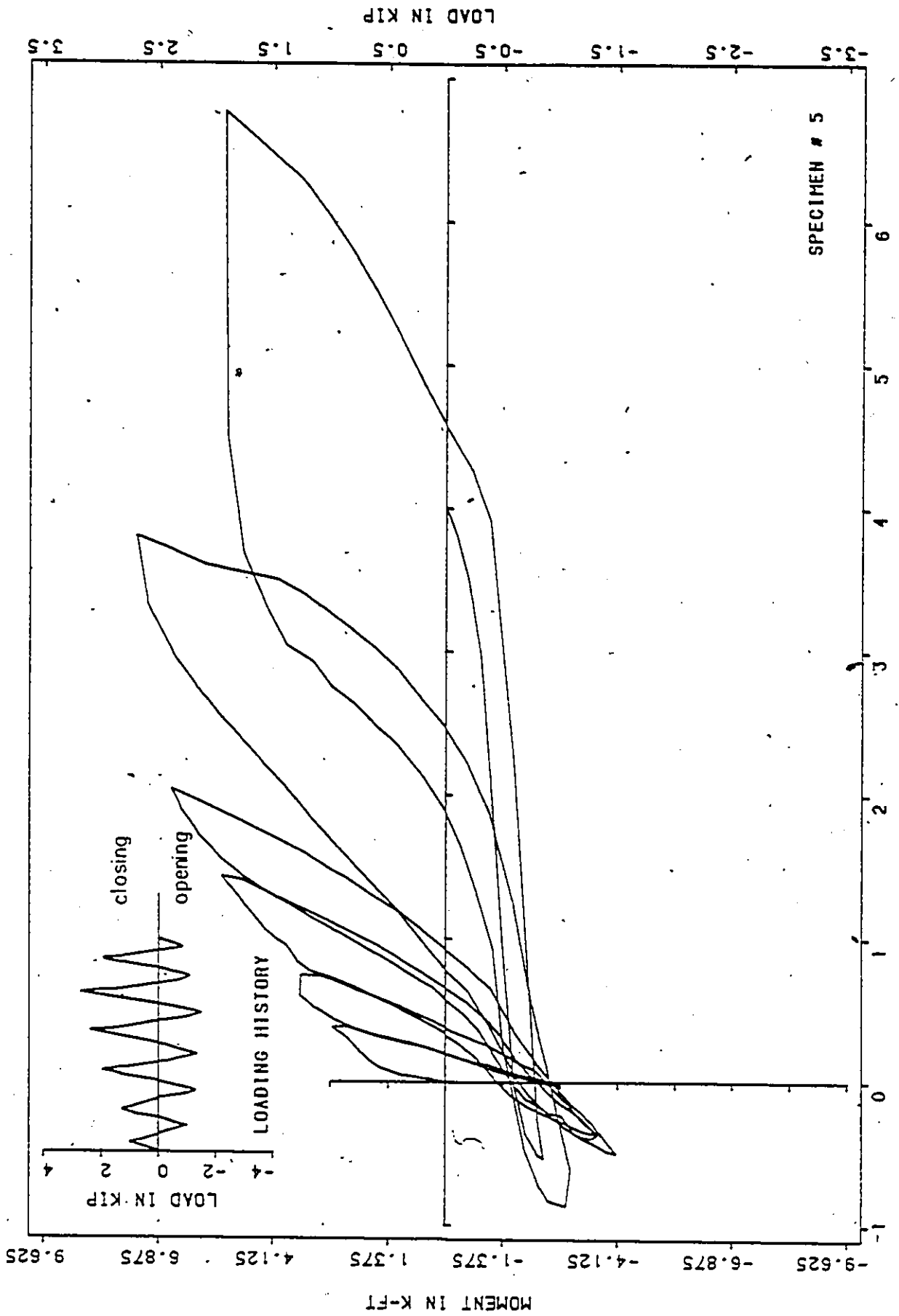


FIG. 52-c MOMENT-ROTATION CURVE

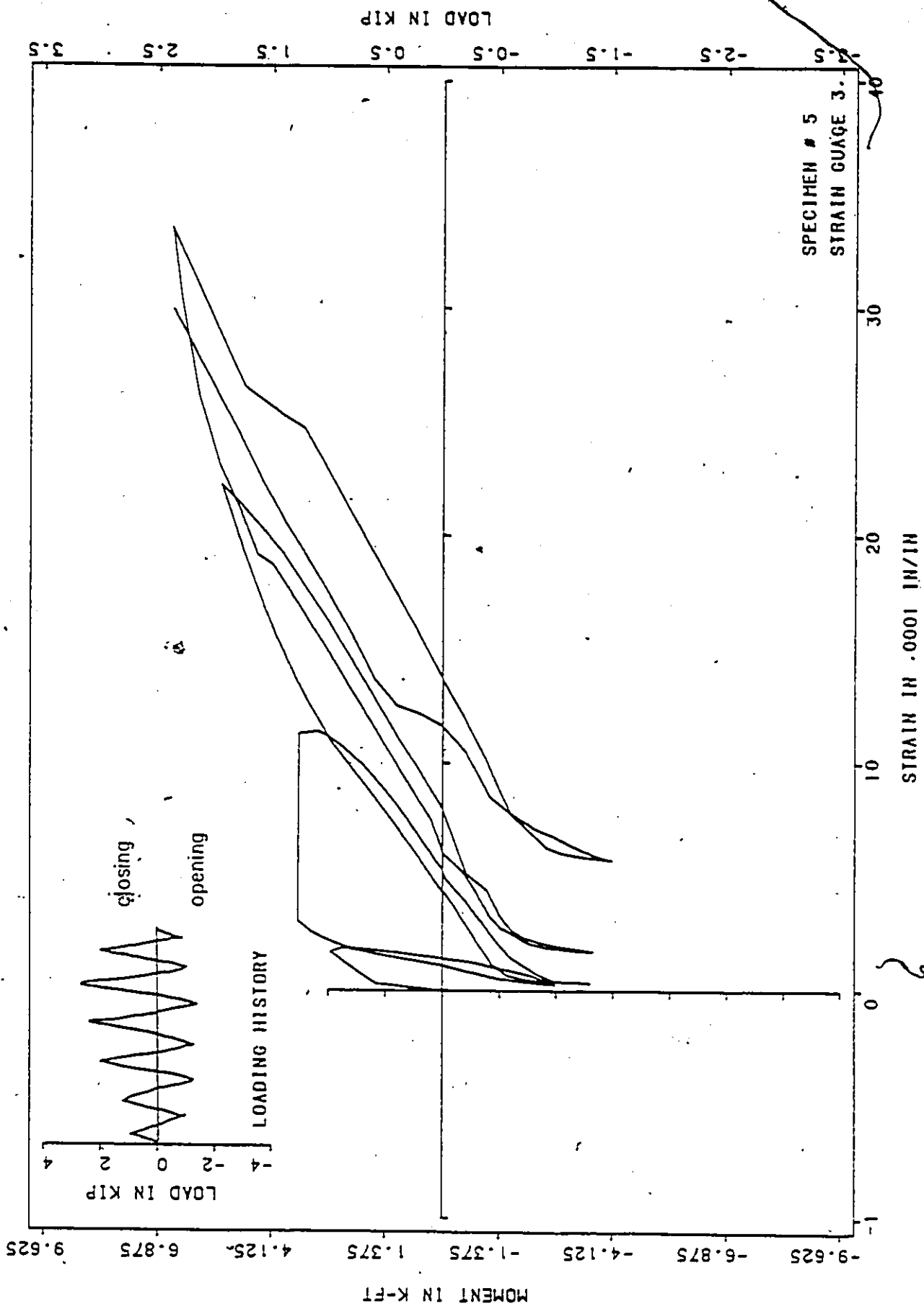


FIG. 52-d MOMENT-STRAIN CURVE

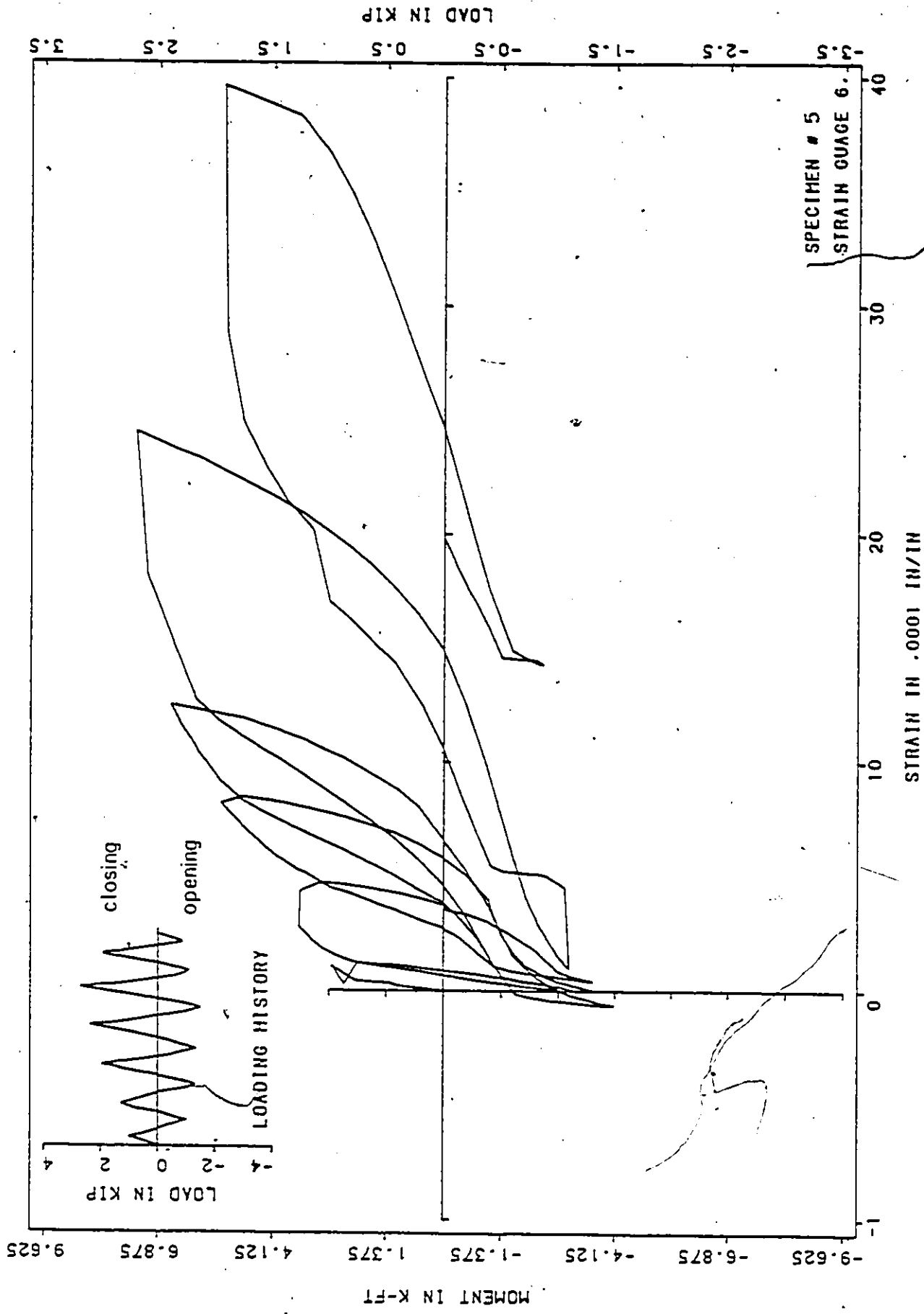


FIG. 52-e MOMENT-STRAIN CURVE



(i)

(ii)

(a) illustration of specimen when test was terminated  
FIG. 53 TEST RESULTS - SPECIMEN 6

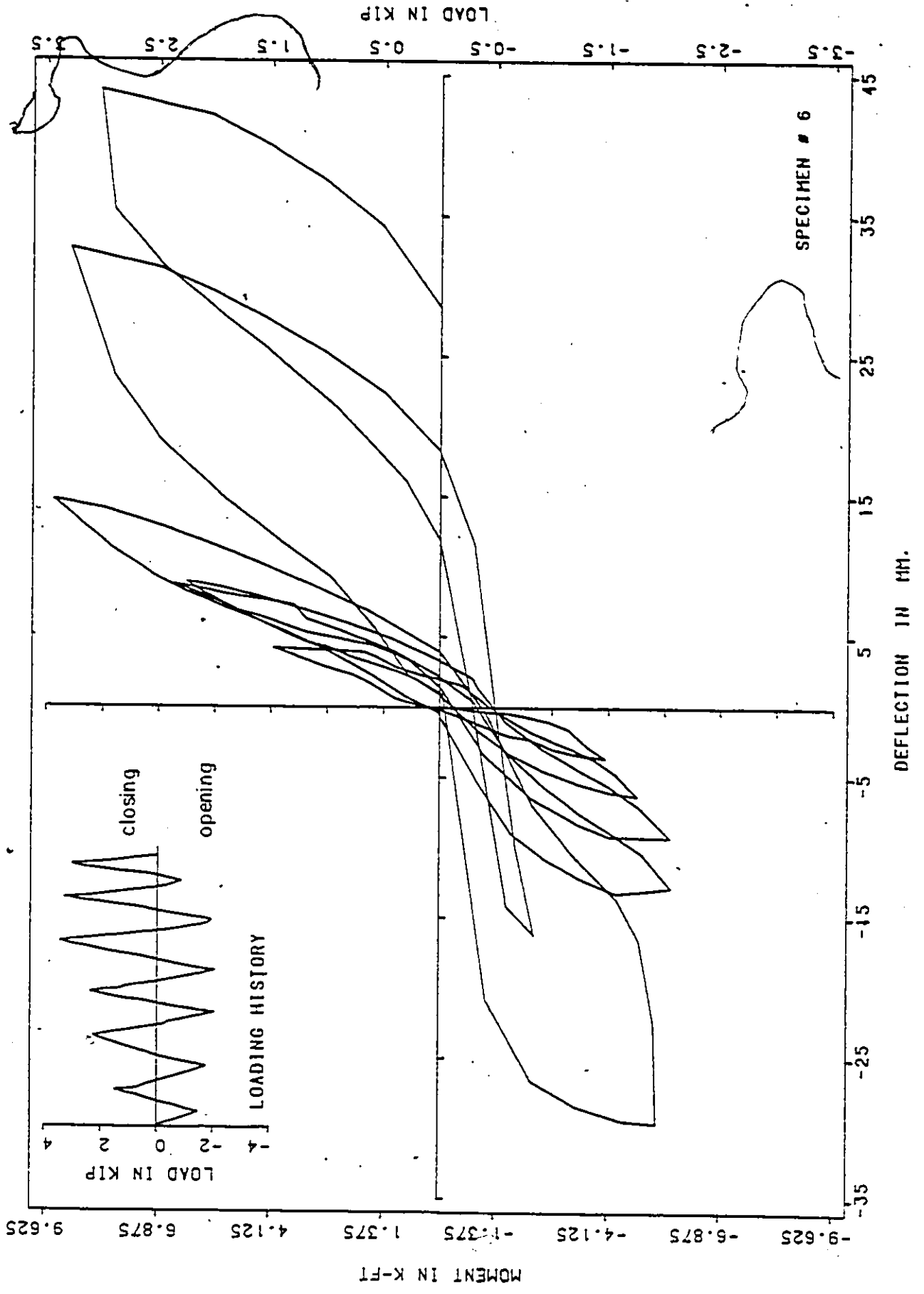


FIG. 53-b MOMENT-DEFLECTION CURVE

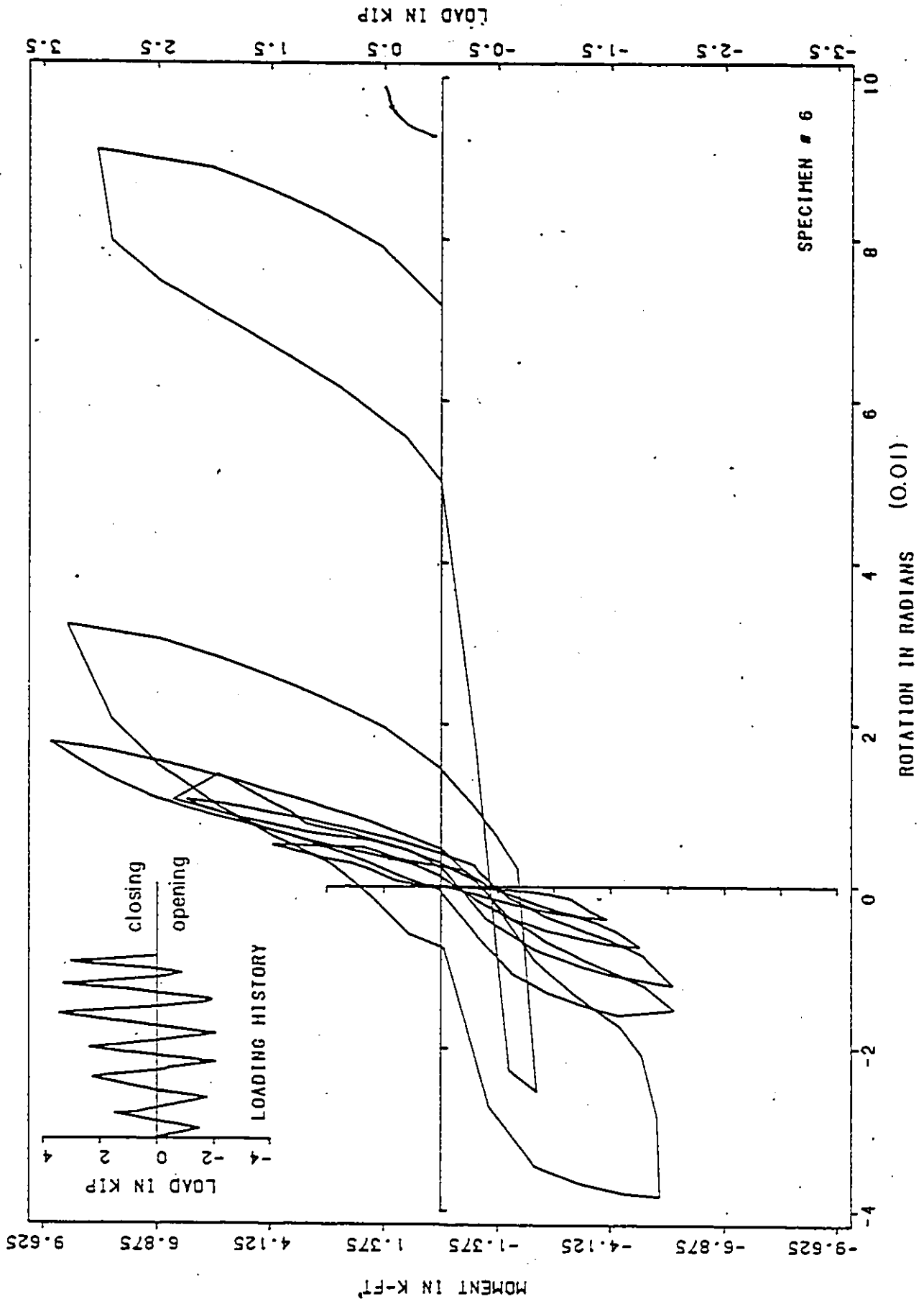


FIG. 53-c MOMENT-ROTATION CURVE

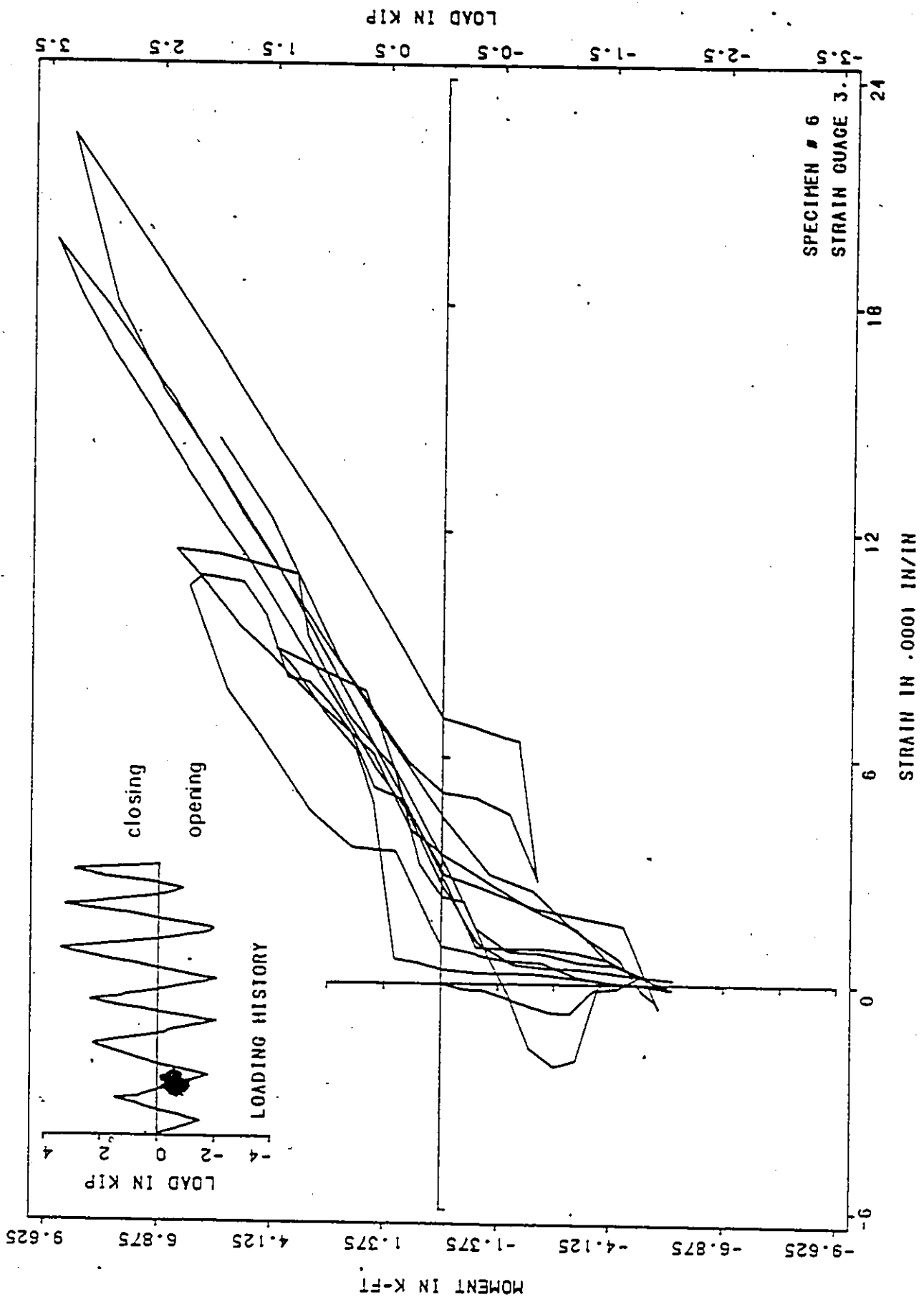


FIG. 53-d MOMENT-STRAIN CURVE

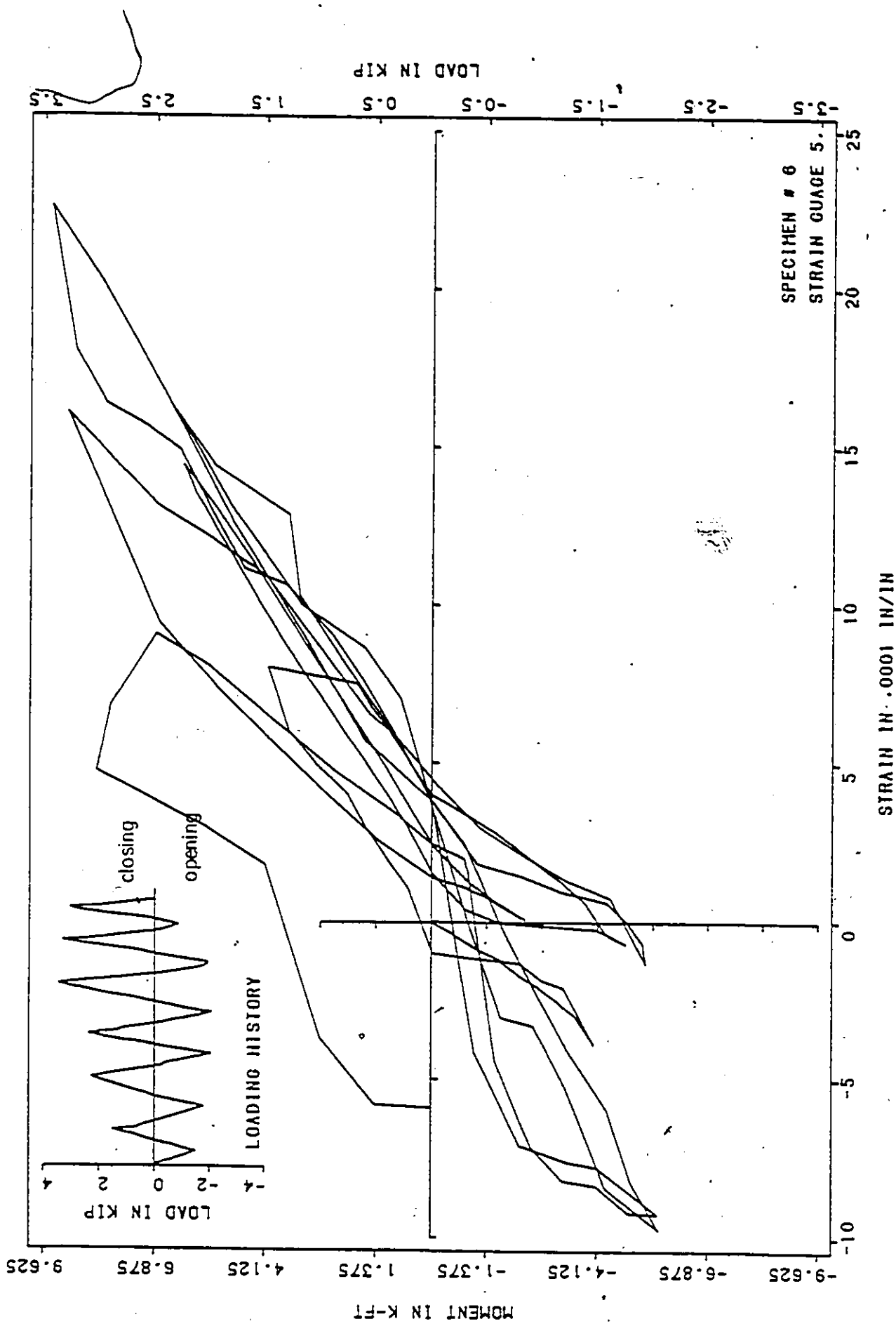


FIG. 53-e MOMENT-STRAIN CURVE

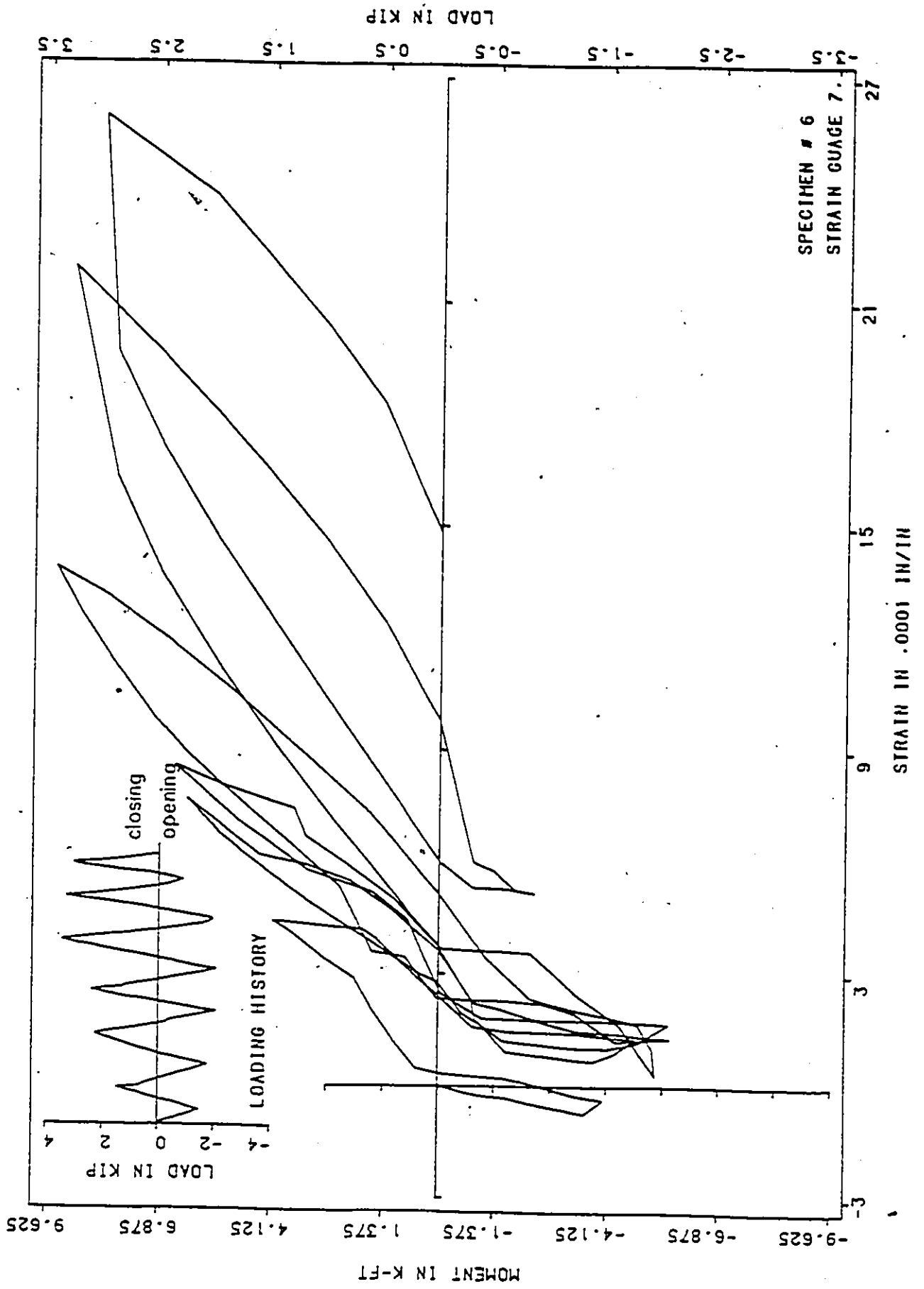


FIG. 53-1 MOMENT-STRAIN CURVE

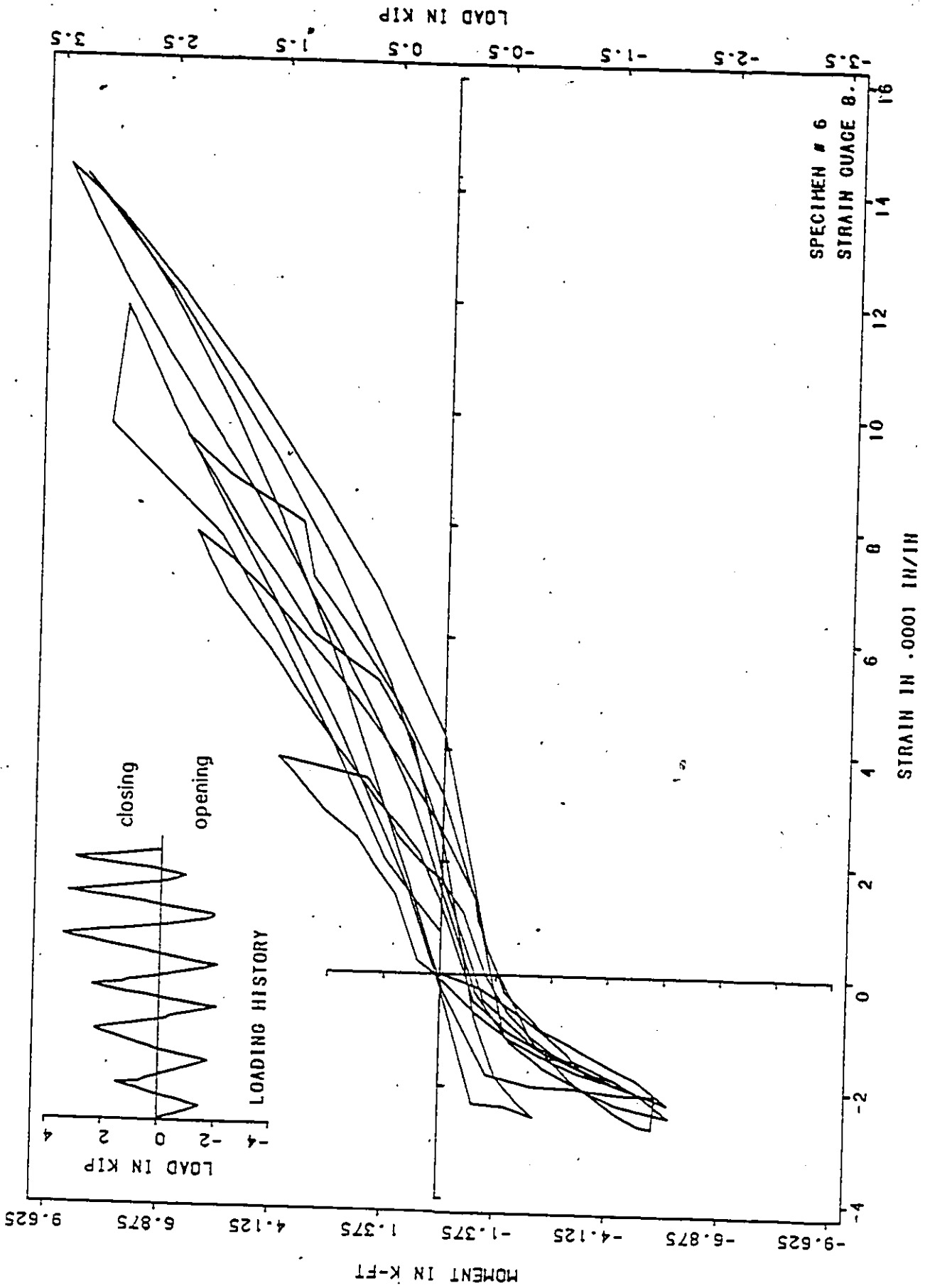


FIG. 53-g MOMENT-STRAIN CURVE

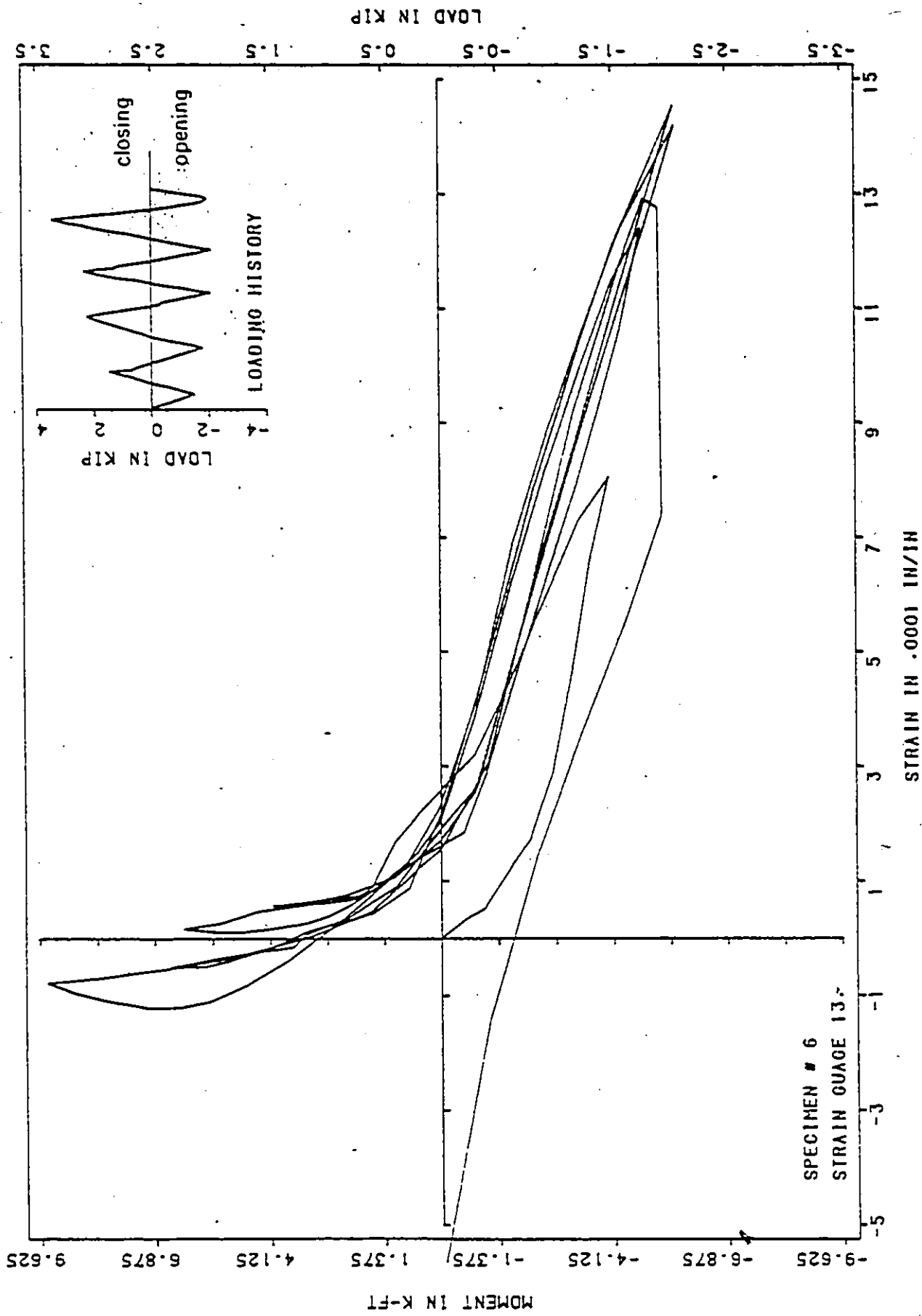


FIG. 53-h MOMENT-STRAIN CURVE

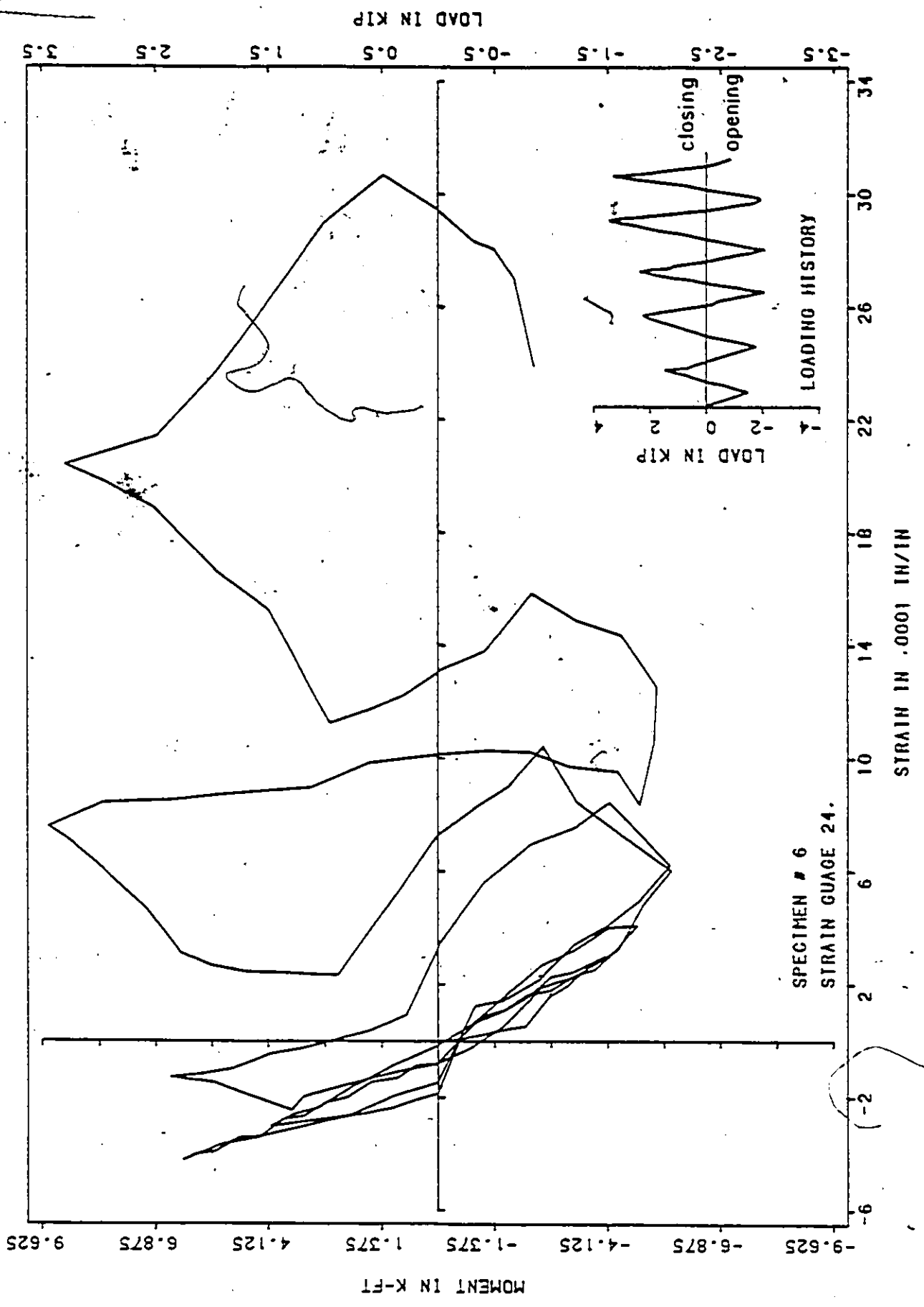
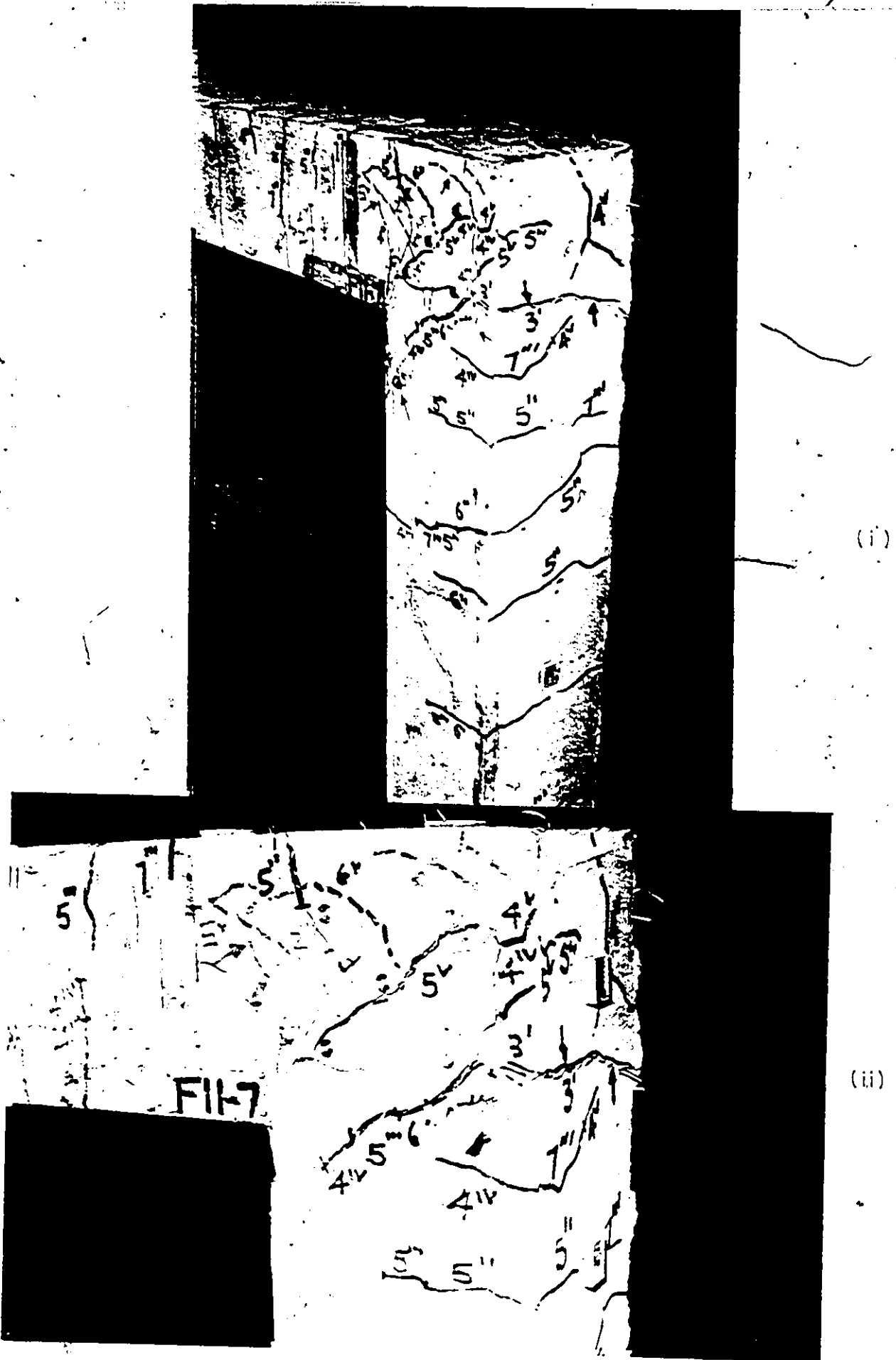


FIG.50-J MOMENT-STRAIN CURVE

COLOURED PICTURES



(a) illustration of specimen when test was terminated  
FIG. 54 TEST RESULTS - SPECIMEN 7

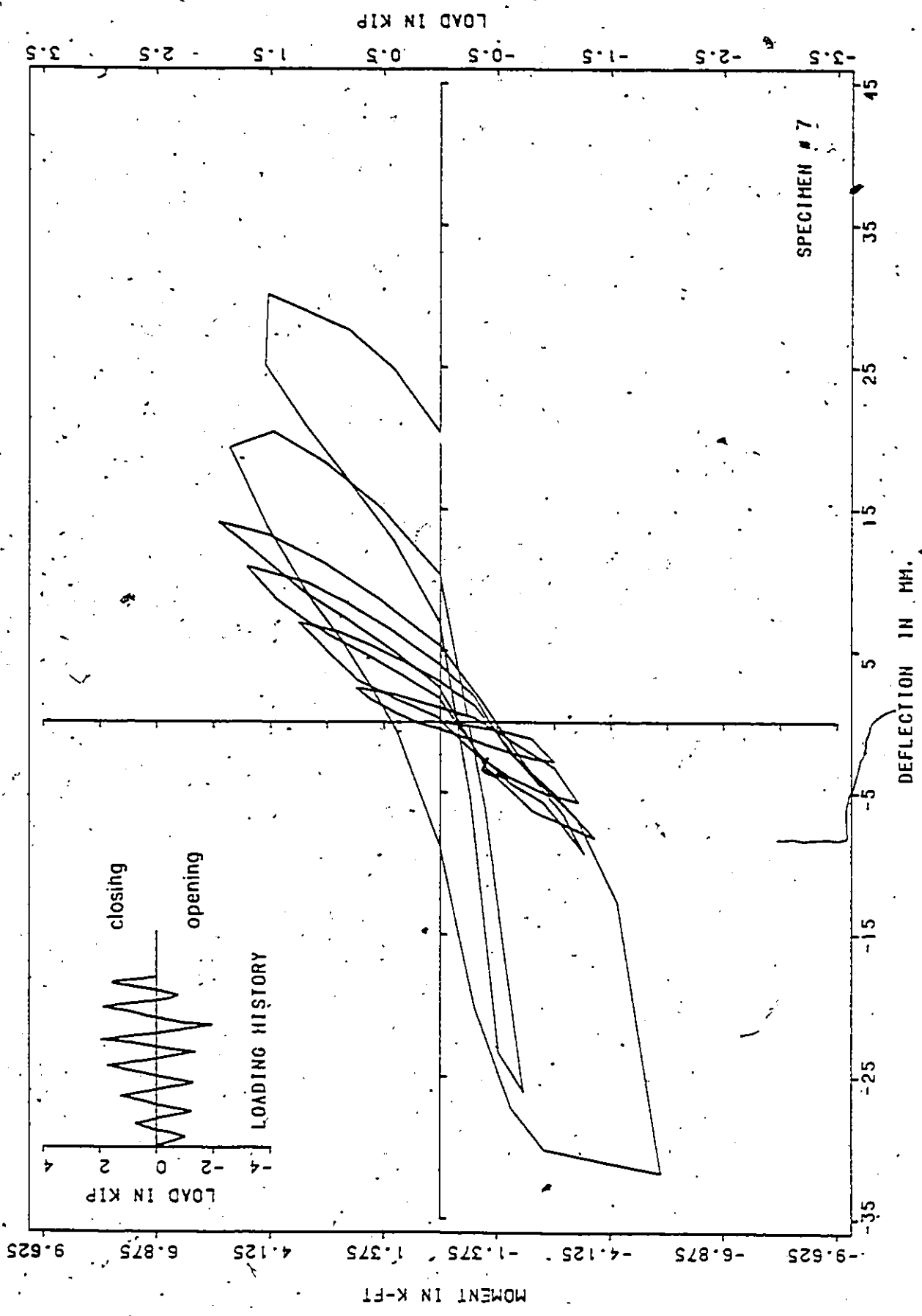
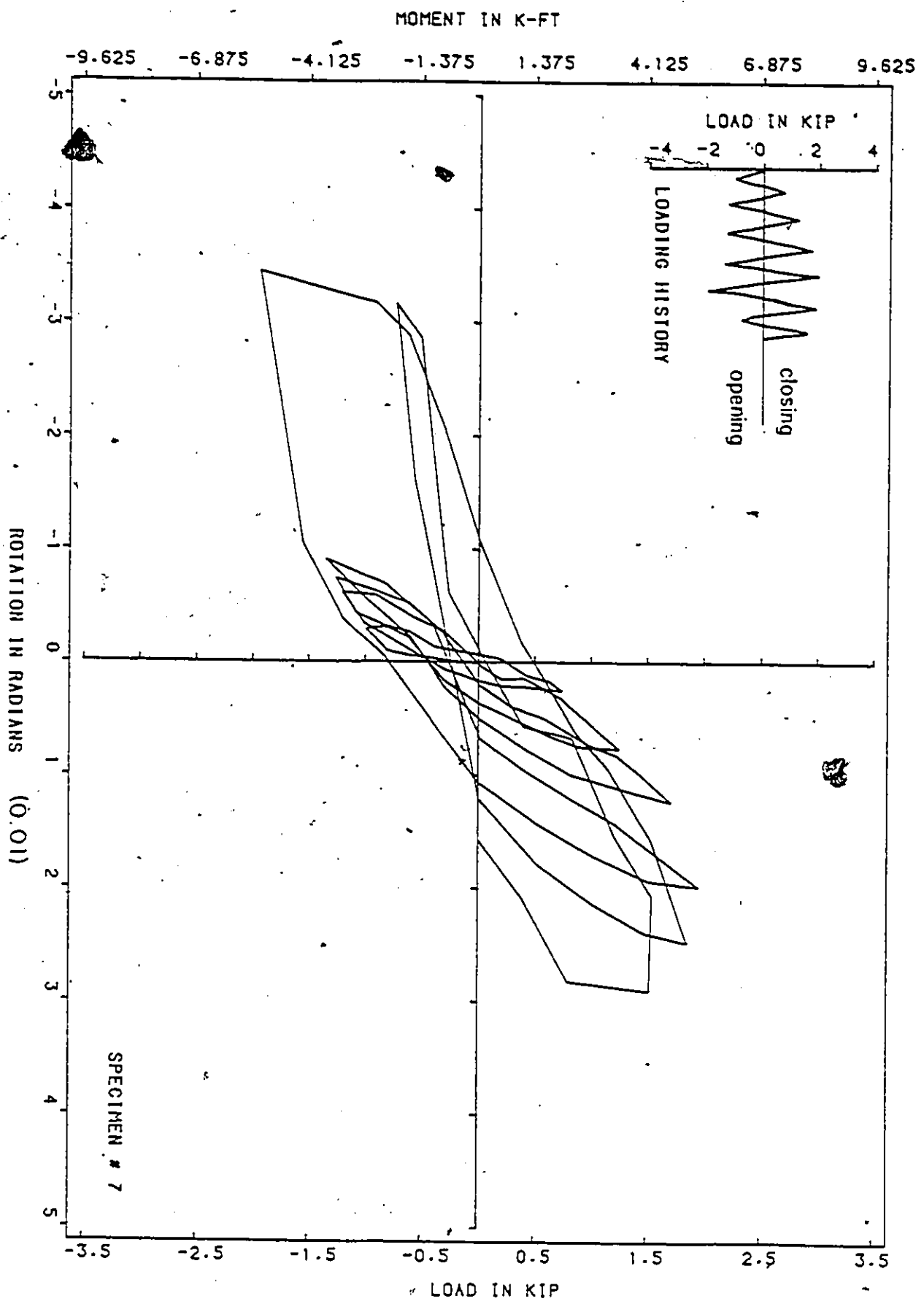


FIG. 54-b MOMENT-DEFLECTION CURVE

FIG. 54-c MOMENT-ROTATION CURVE



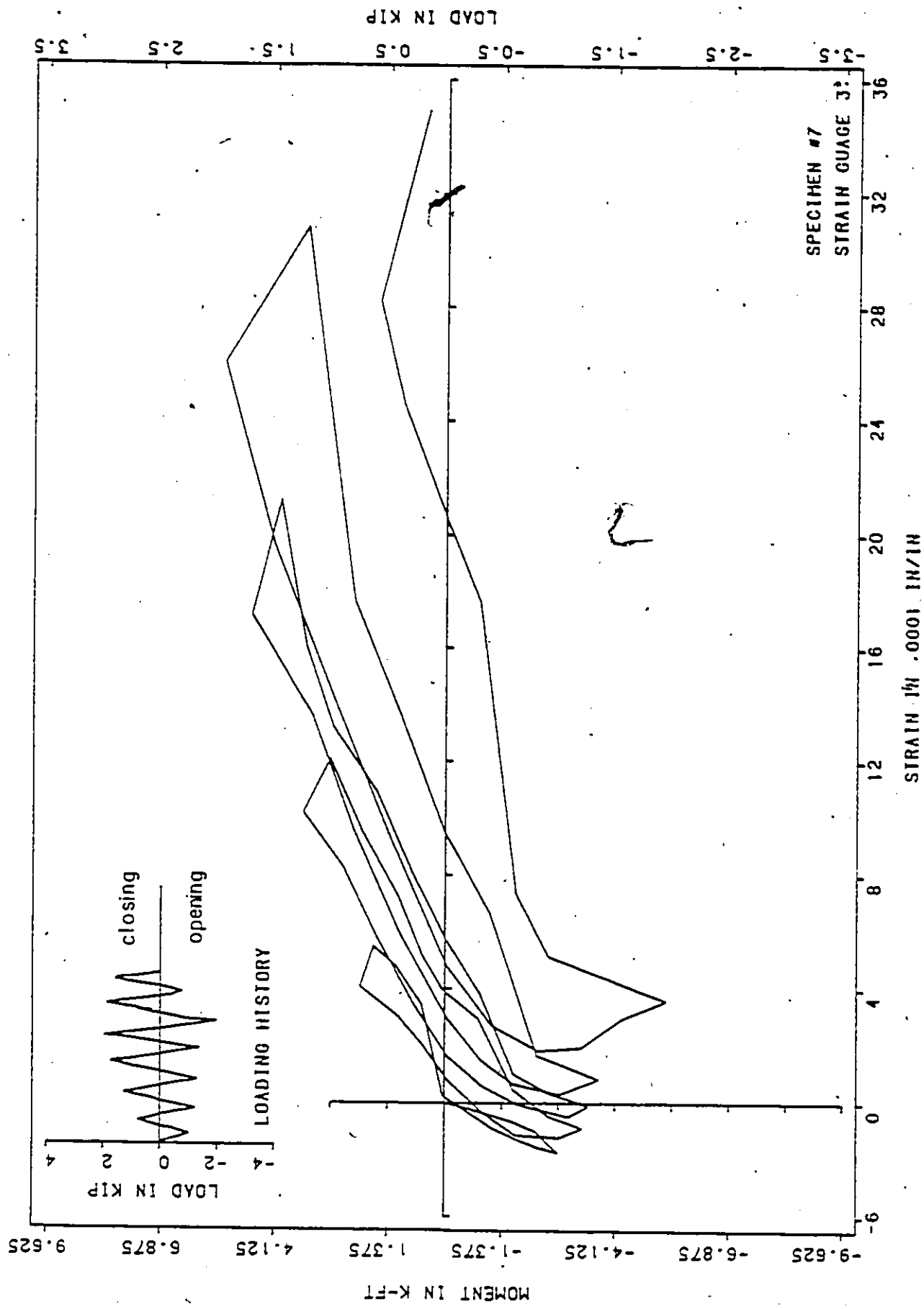


FIG. 54-d MOMENT-STRAIN CURVE

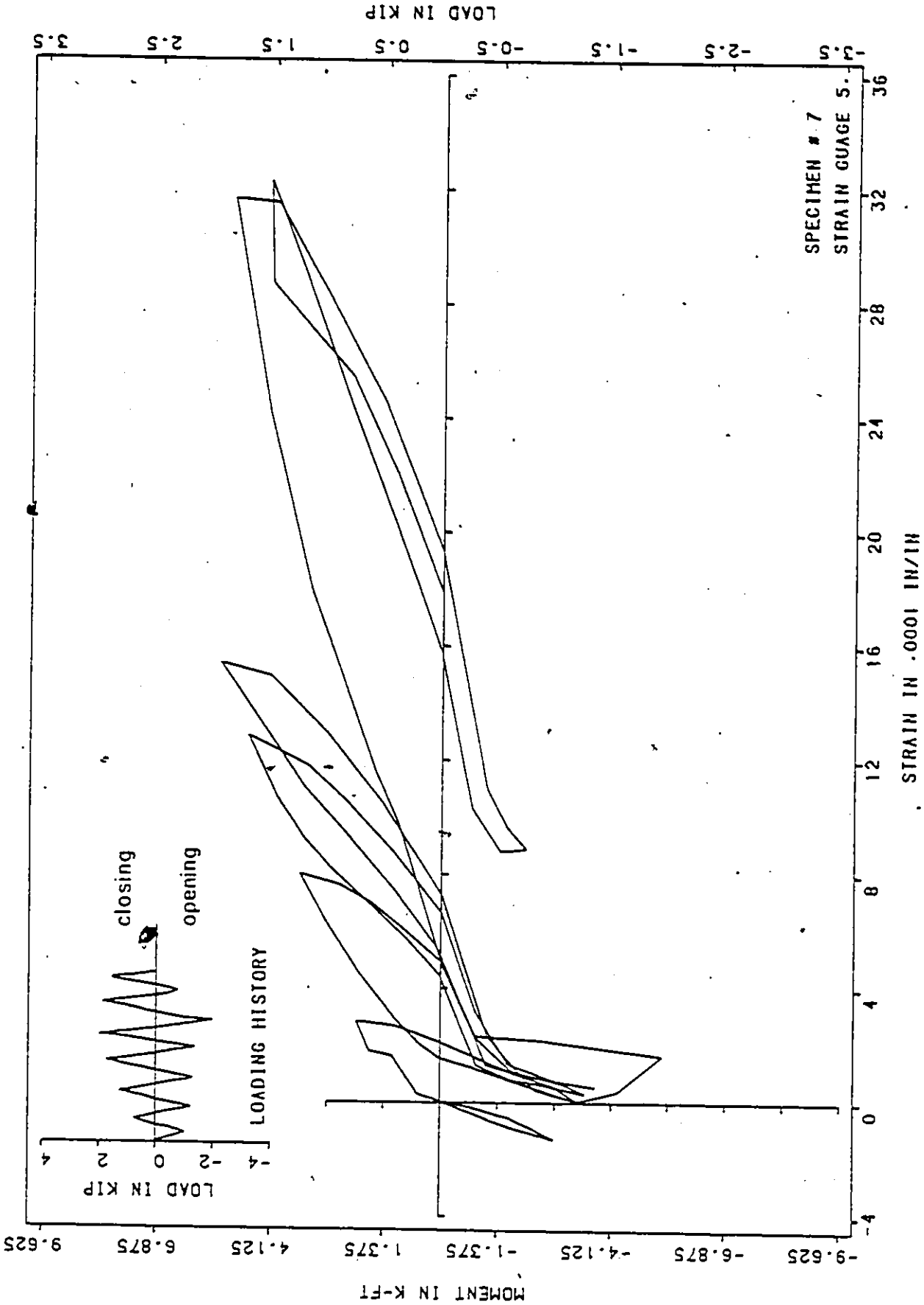


FIG. 54-e MOMENT-STRAIN CURVE

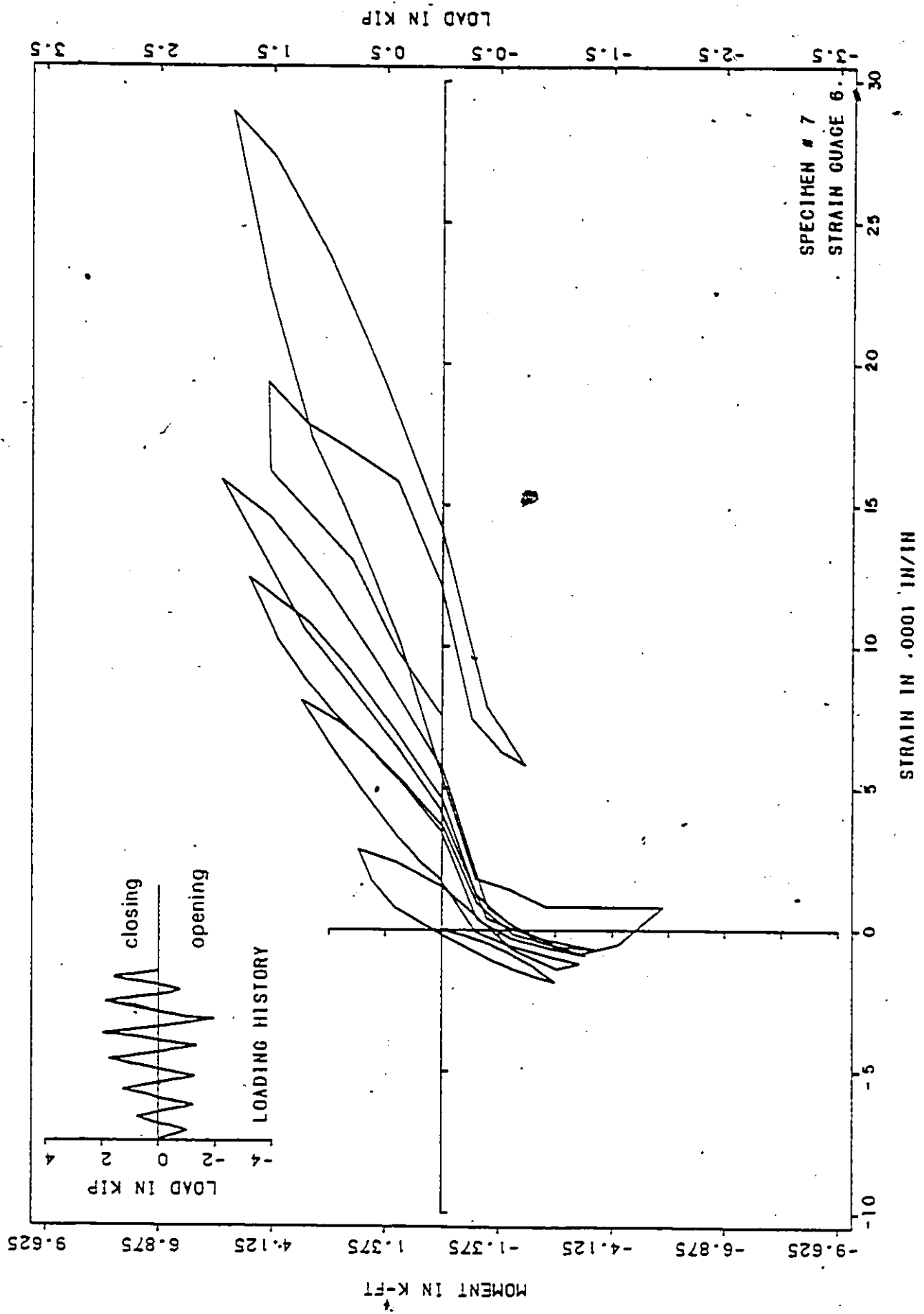


FIG. 54-1 MOMENT-STRAIN CURVE

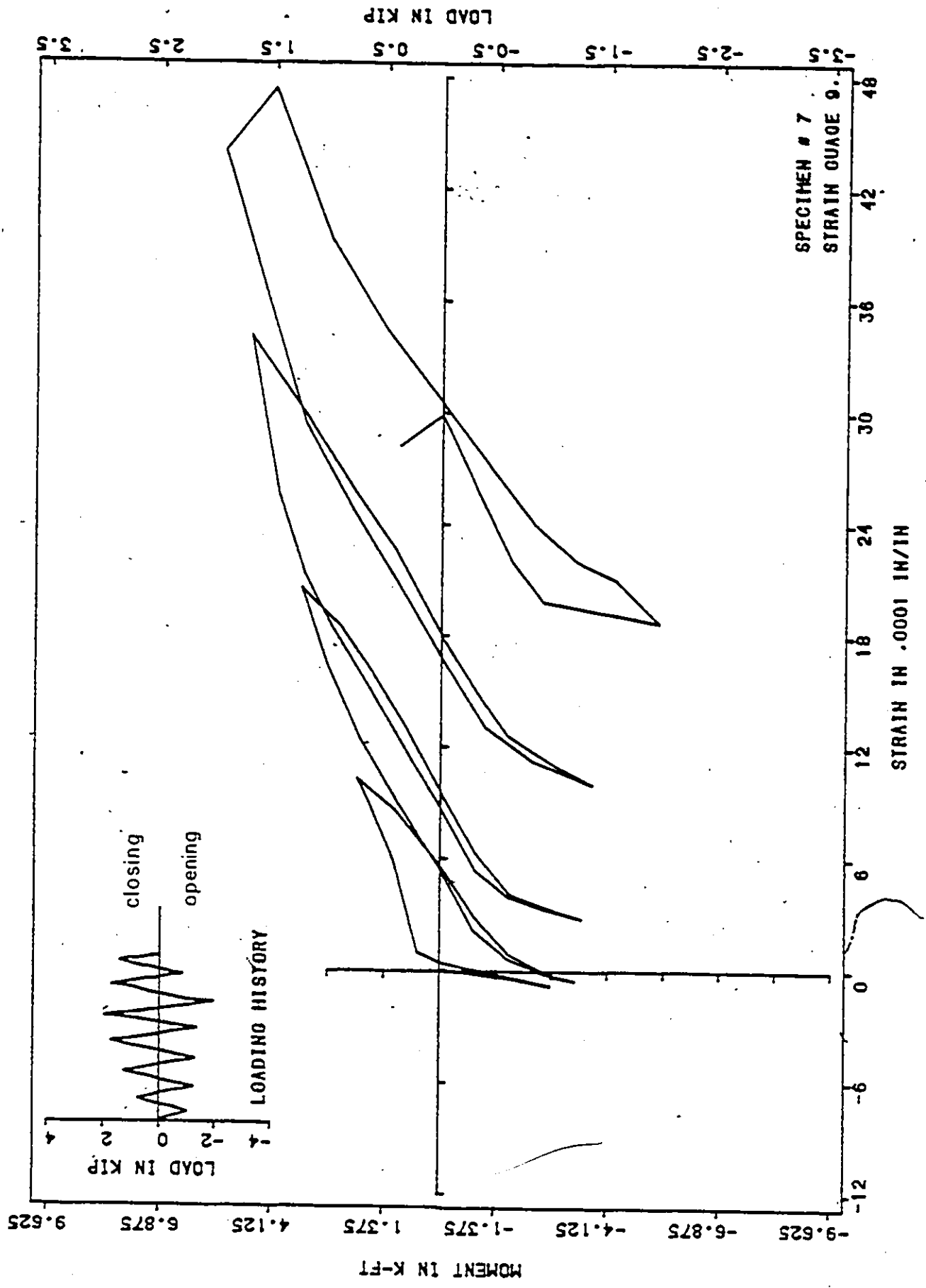


FIG. 54-9 MOMENT-STRAIN CURVE

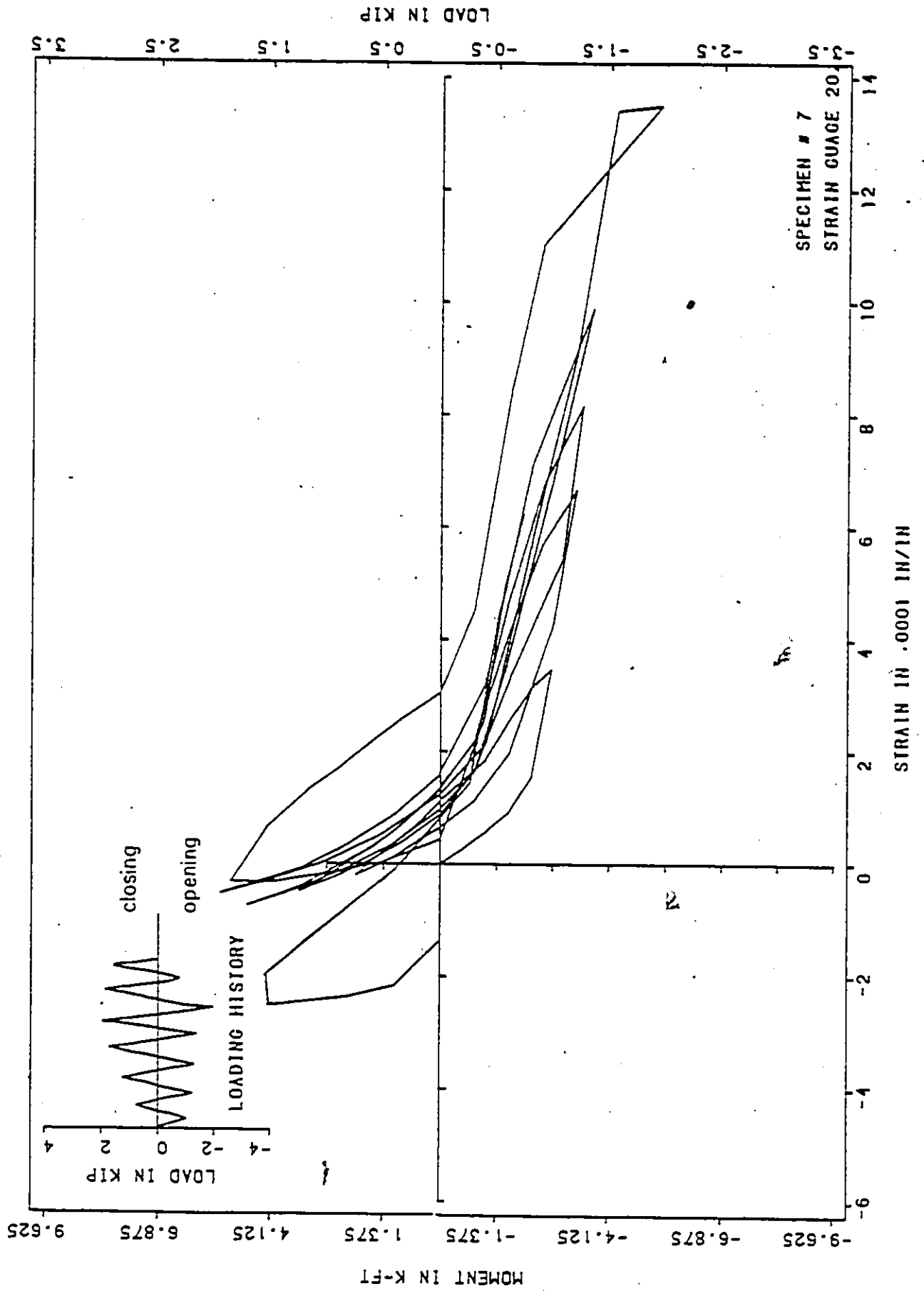


FIG. 54-h MOMENT-STRAIN CURVE

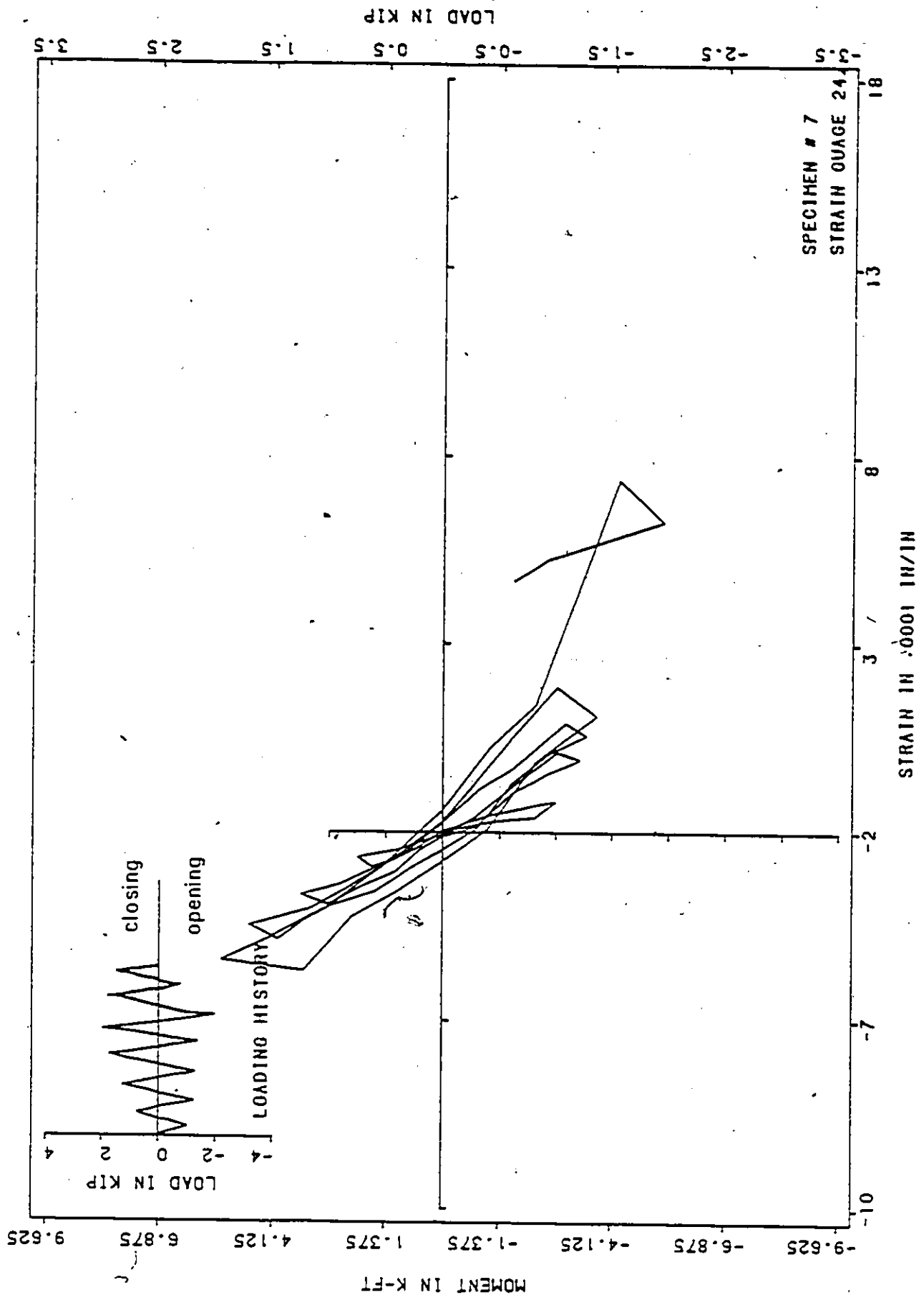


FIG. 54-j MOMENT-STRAIN CURVE

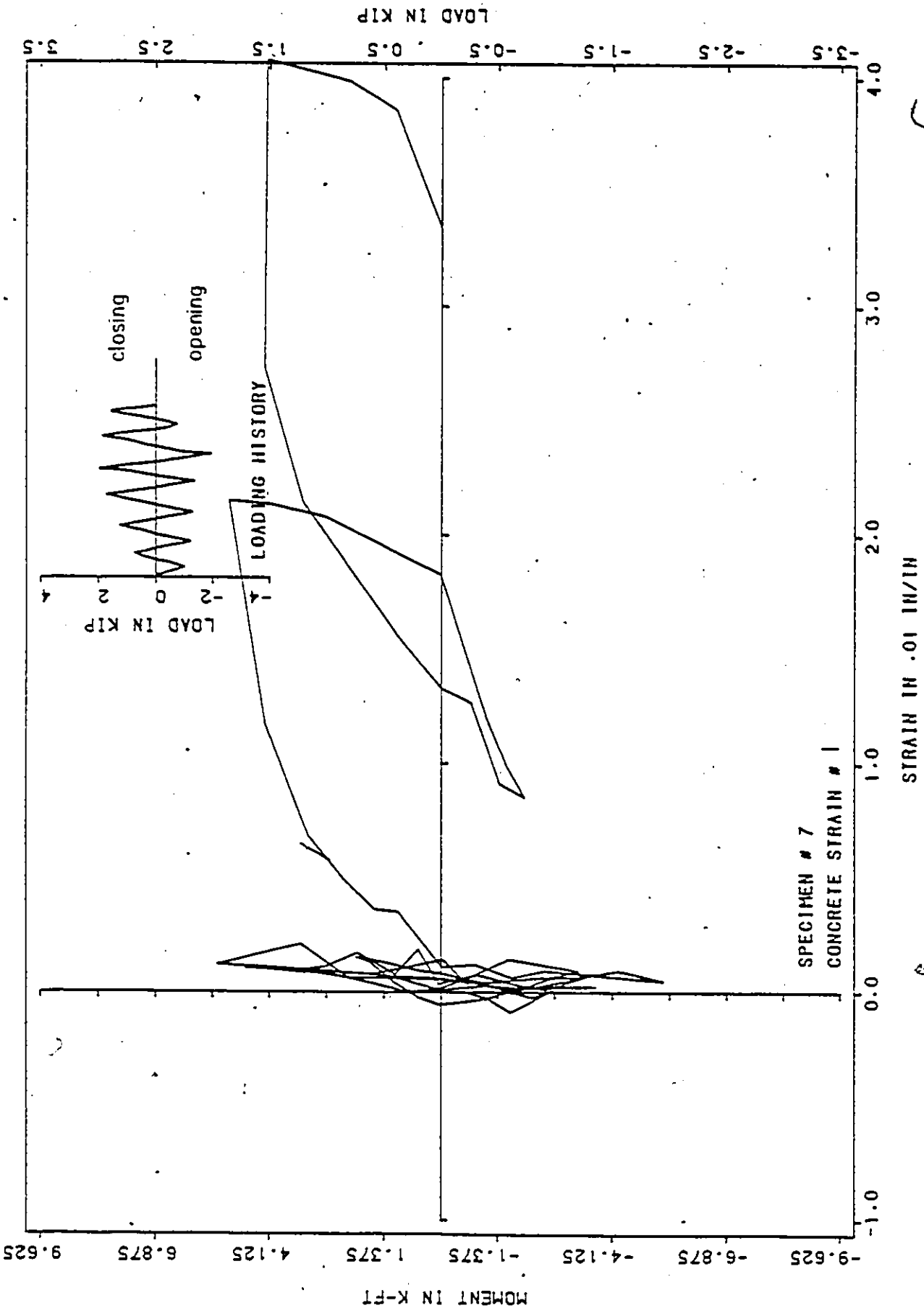


FIG.54-k MOMENT-STRAIN CURVE

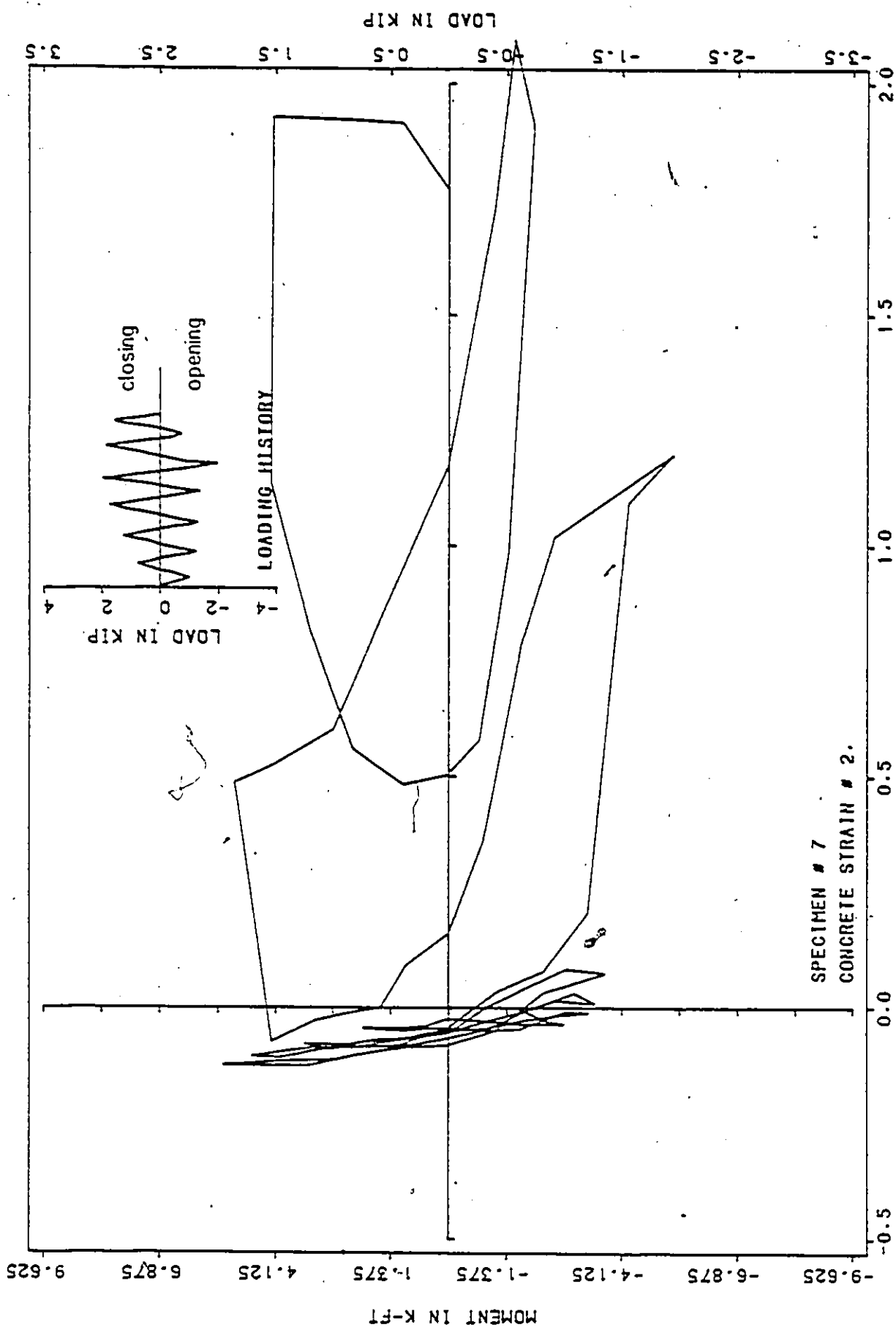
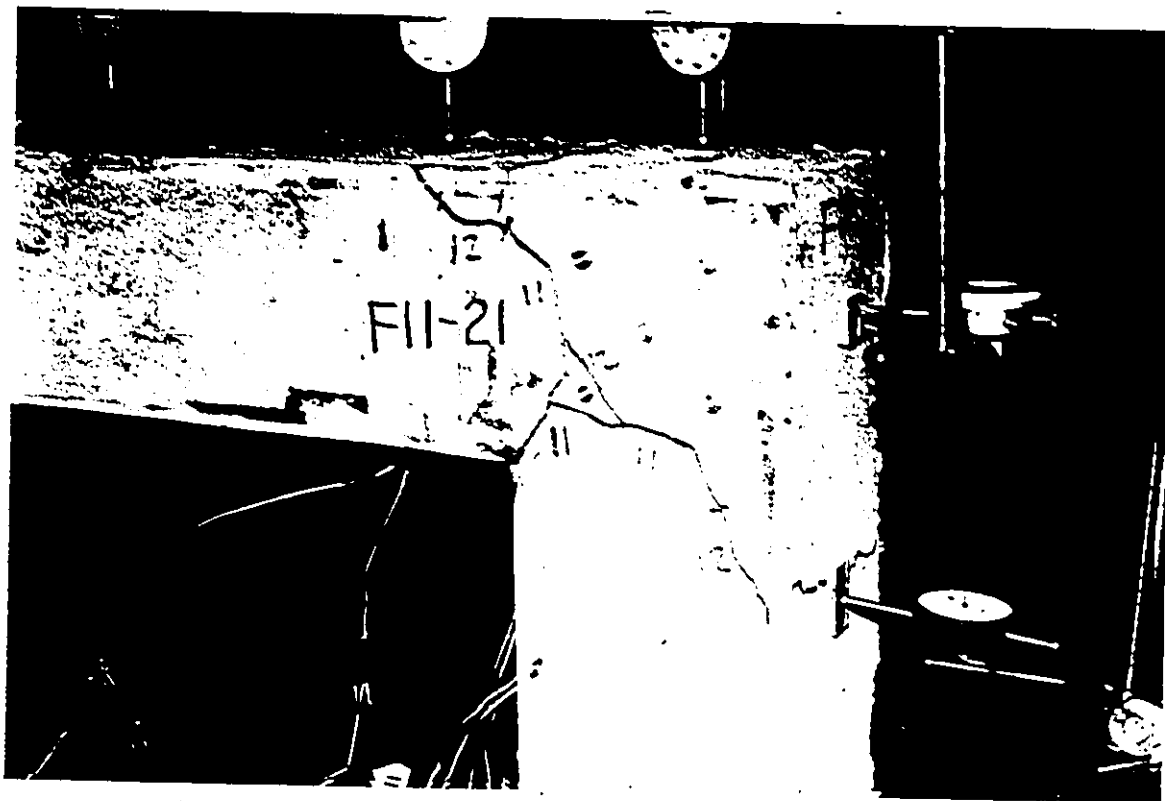


FIG. 54-1 MOMENT-STRAIN CURVE



(a) illustration of specimen when test was terminated

FIG. 55 TEST RESULTS - SPECIMEN, 8

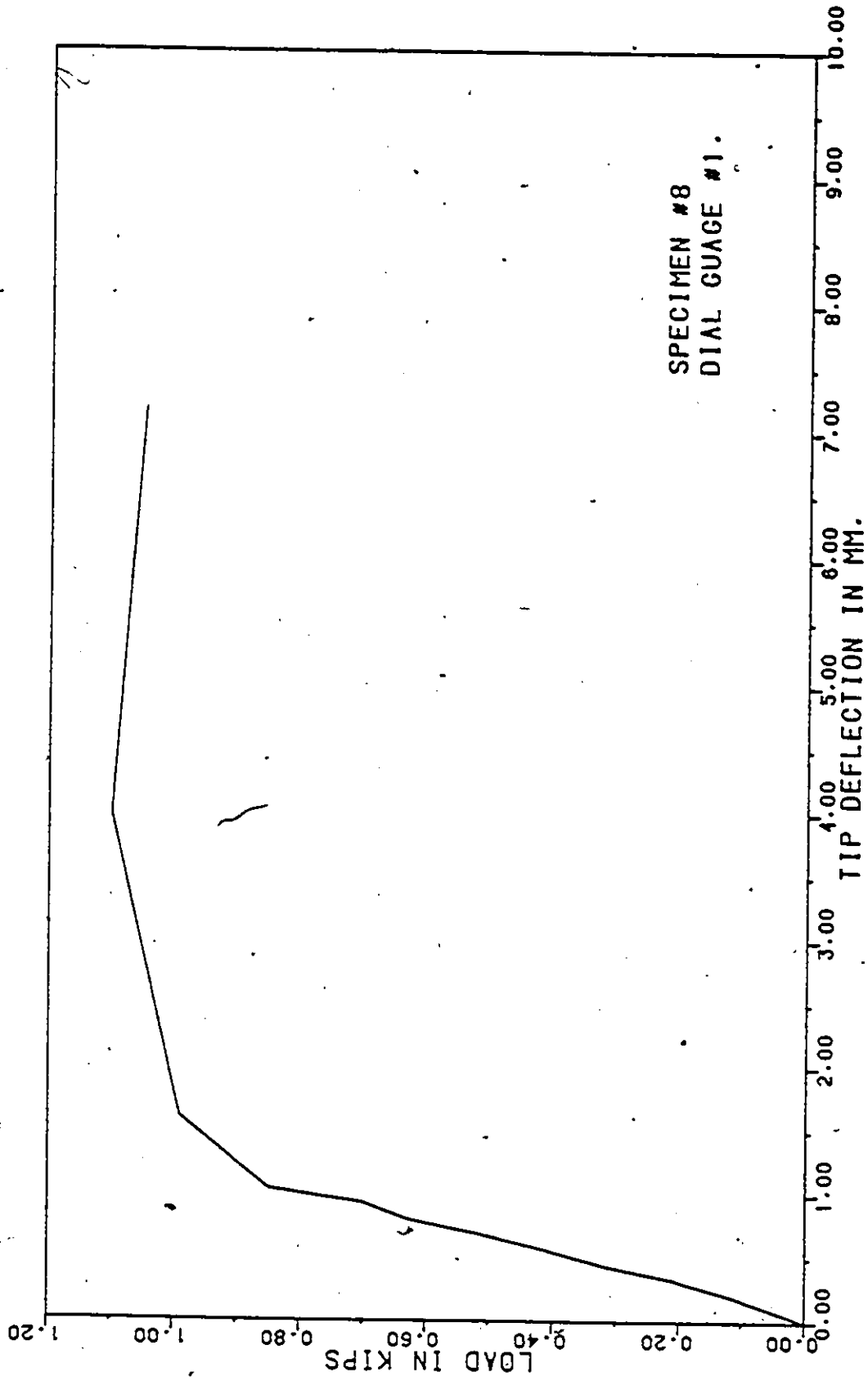


FIG. 55-b LOAD-DEFLECTION CURVE

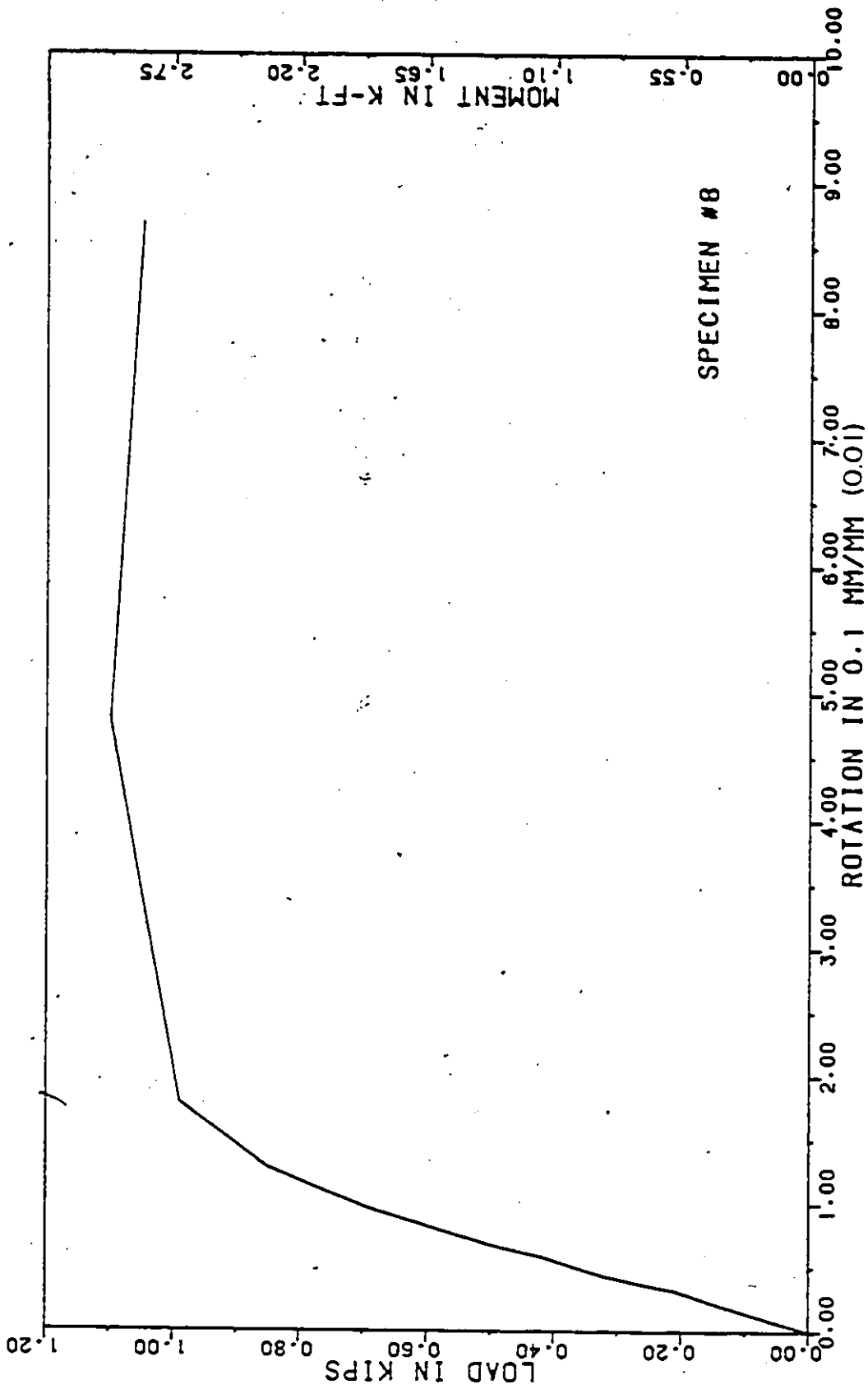


FIG.55-c MOMENT-ROTATION CURVE

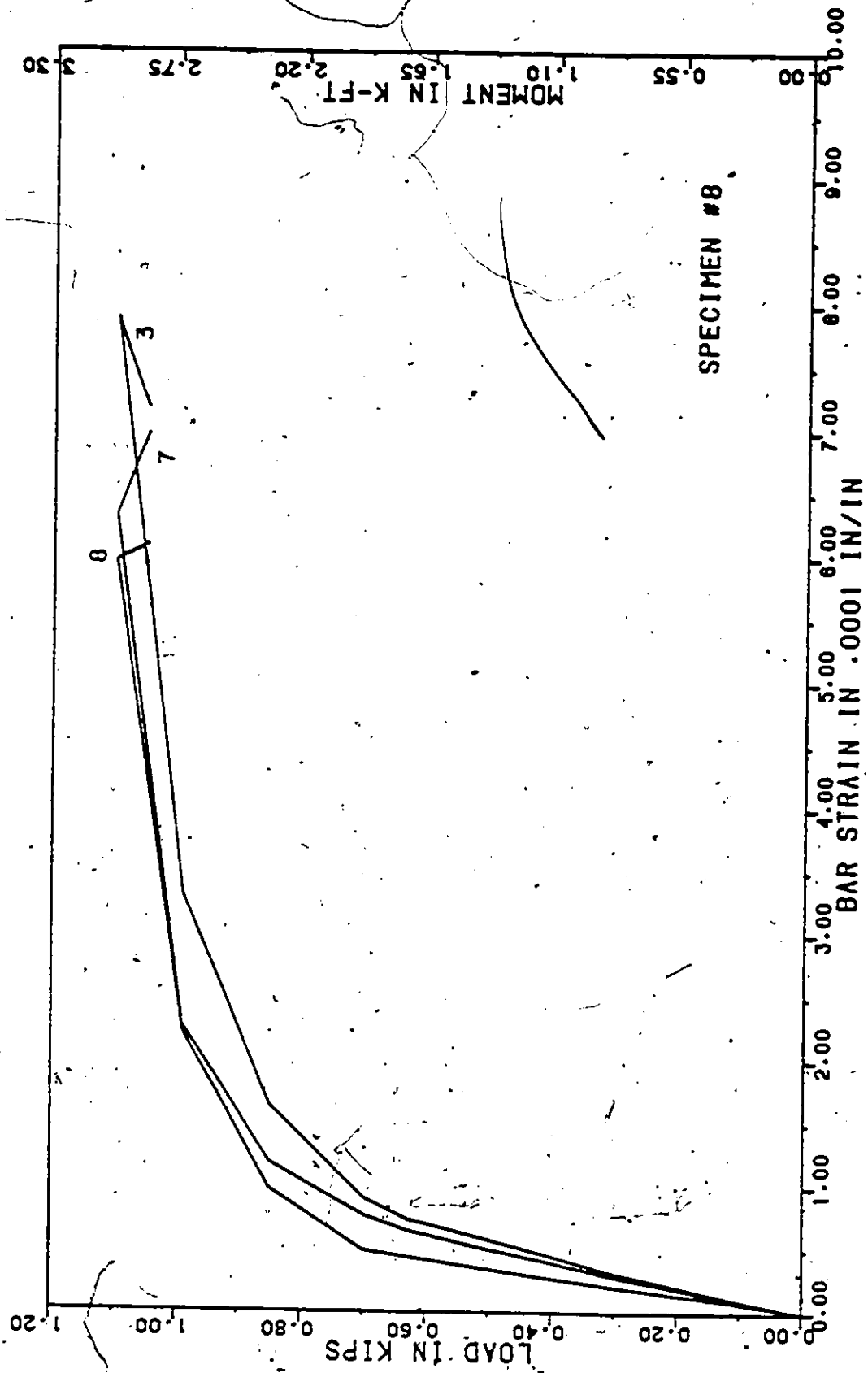
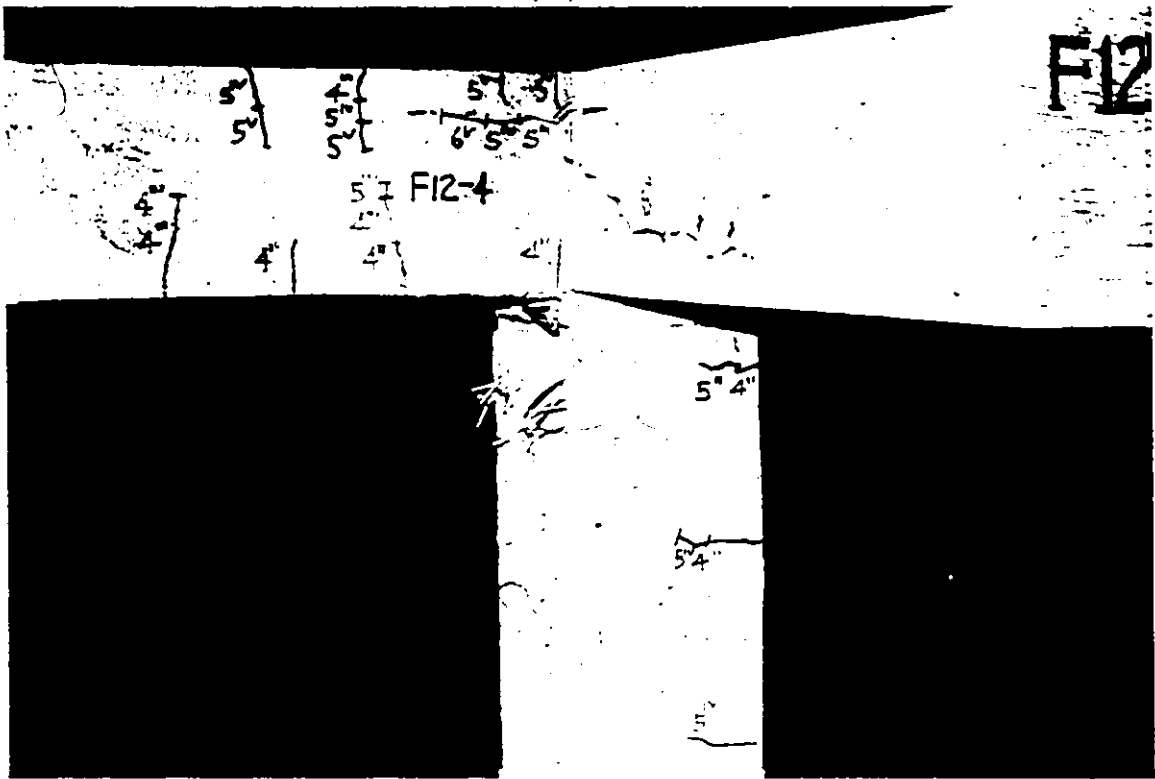


FIG. 55-d REINFORCEMENT STRAINS



(i)



(ii)

(a) illustration of specimen when test was terminated

FIG. 56 TEST RESULTS - SPECIMEN 9

COLOURED PICTURES

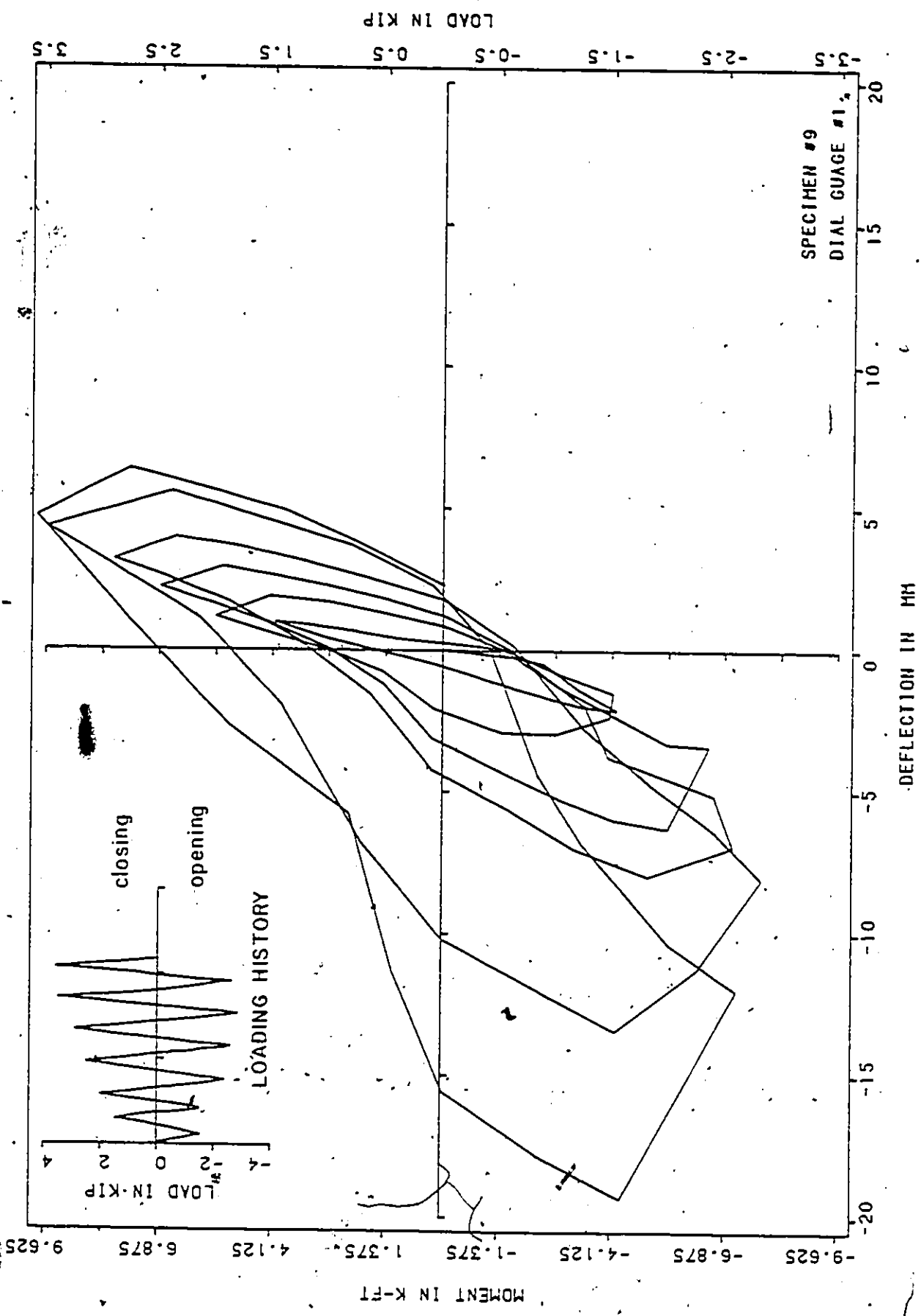


FIG. 56-b LOAD-DEFLECTION CURVE

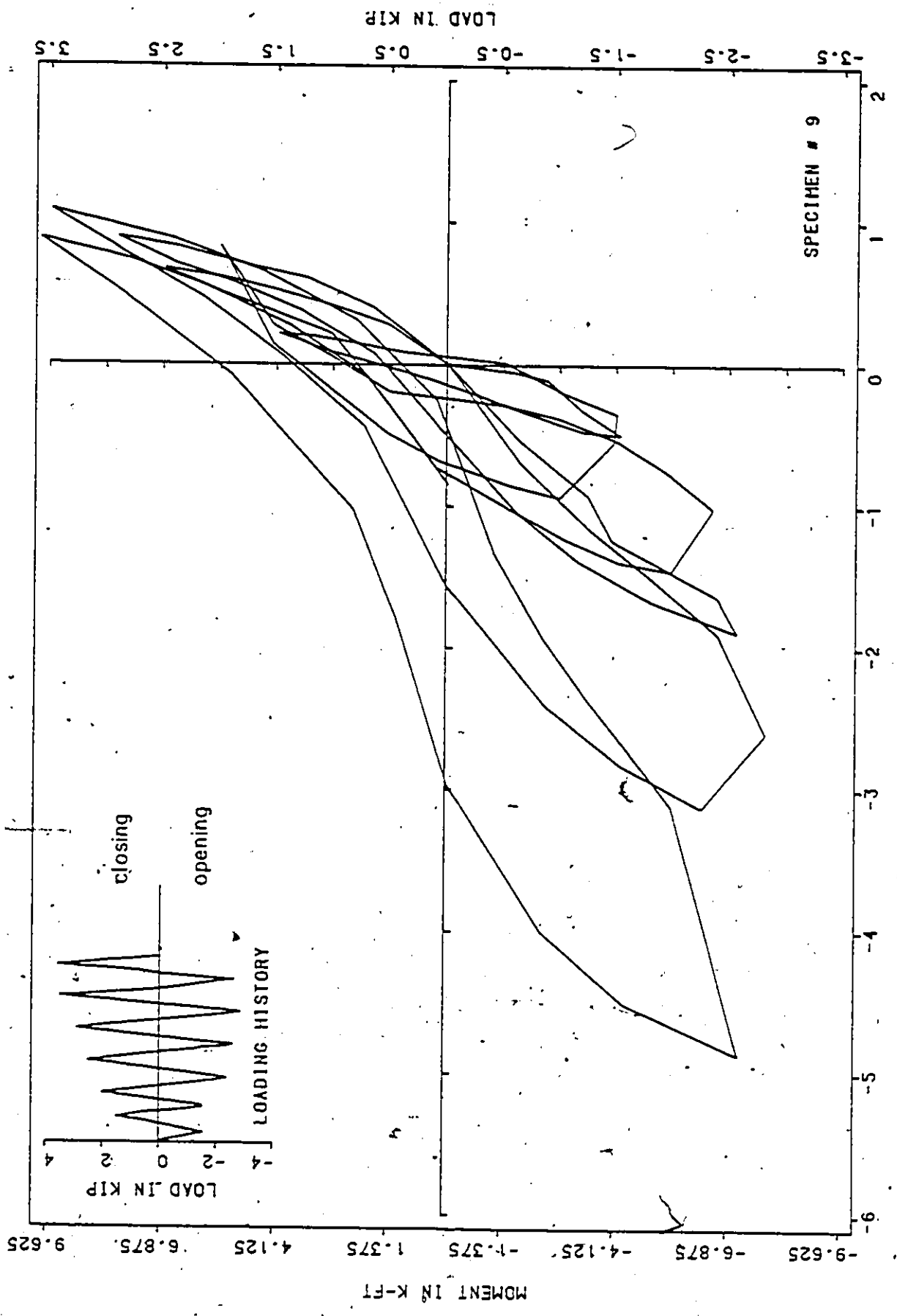


FIG. 56-c MOMENT-ROTATION CURVE

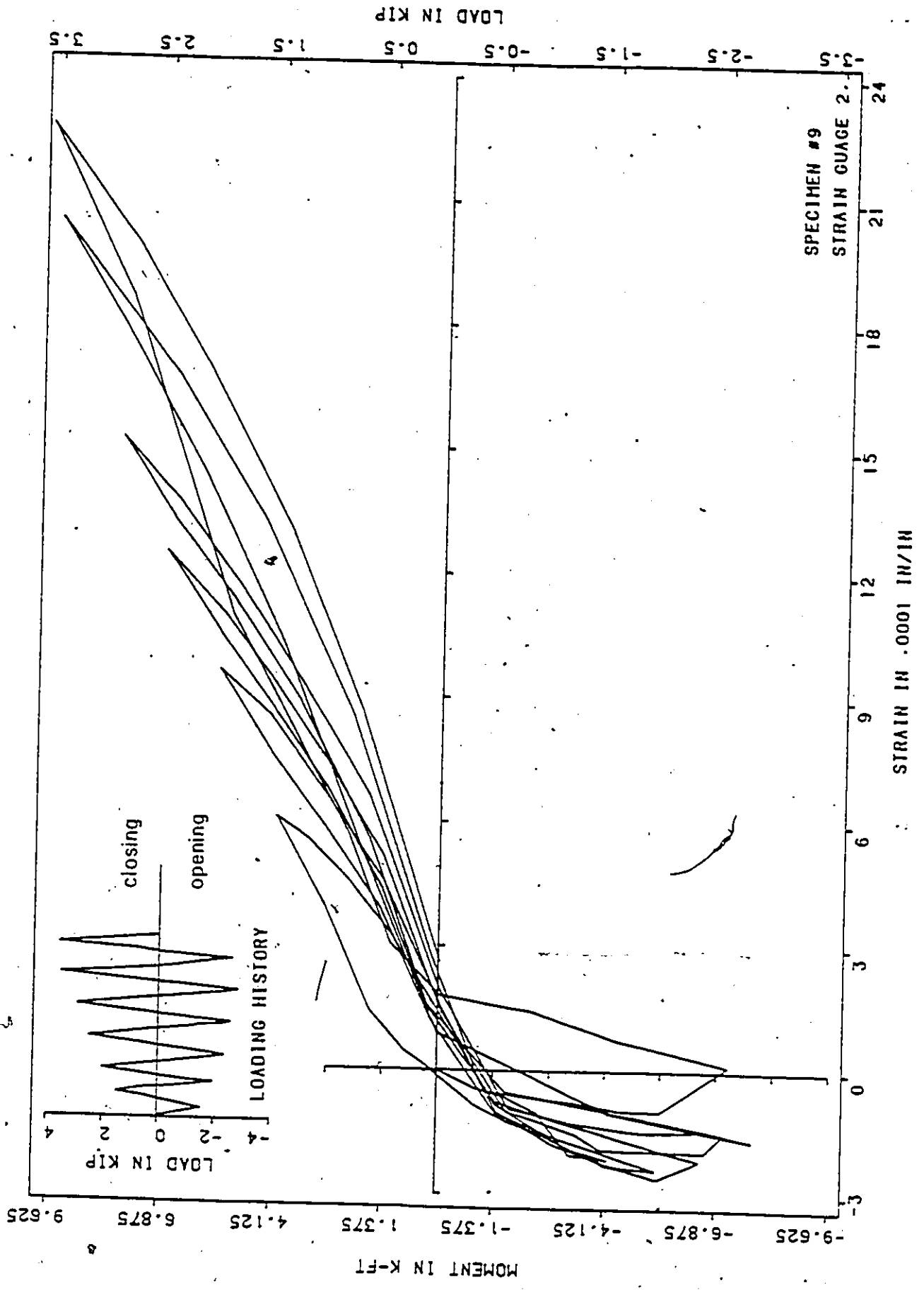


FIG. 56-d MOMENT-STRAIN CURVE

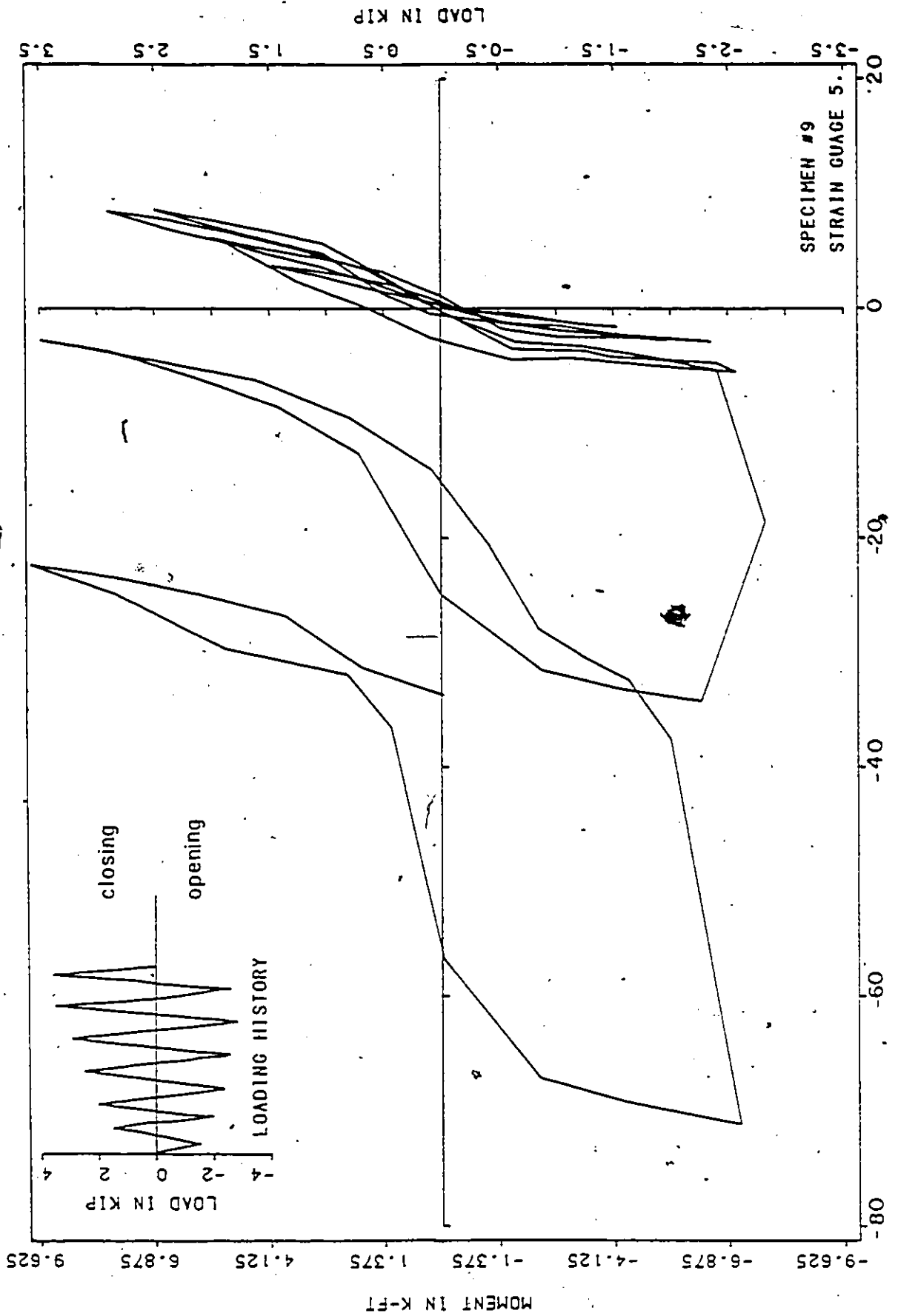


FIG. 56-e MOMENT-STRAIN CURVE

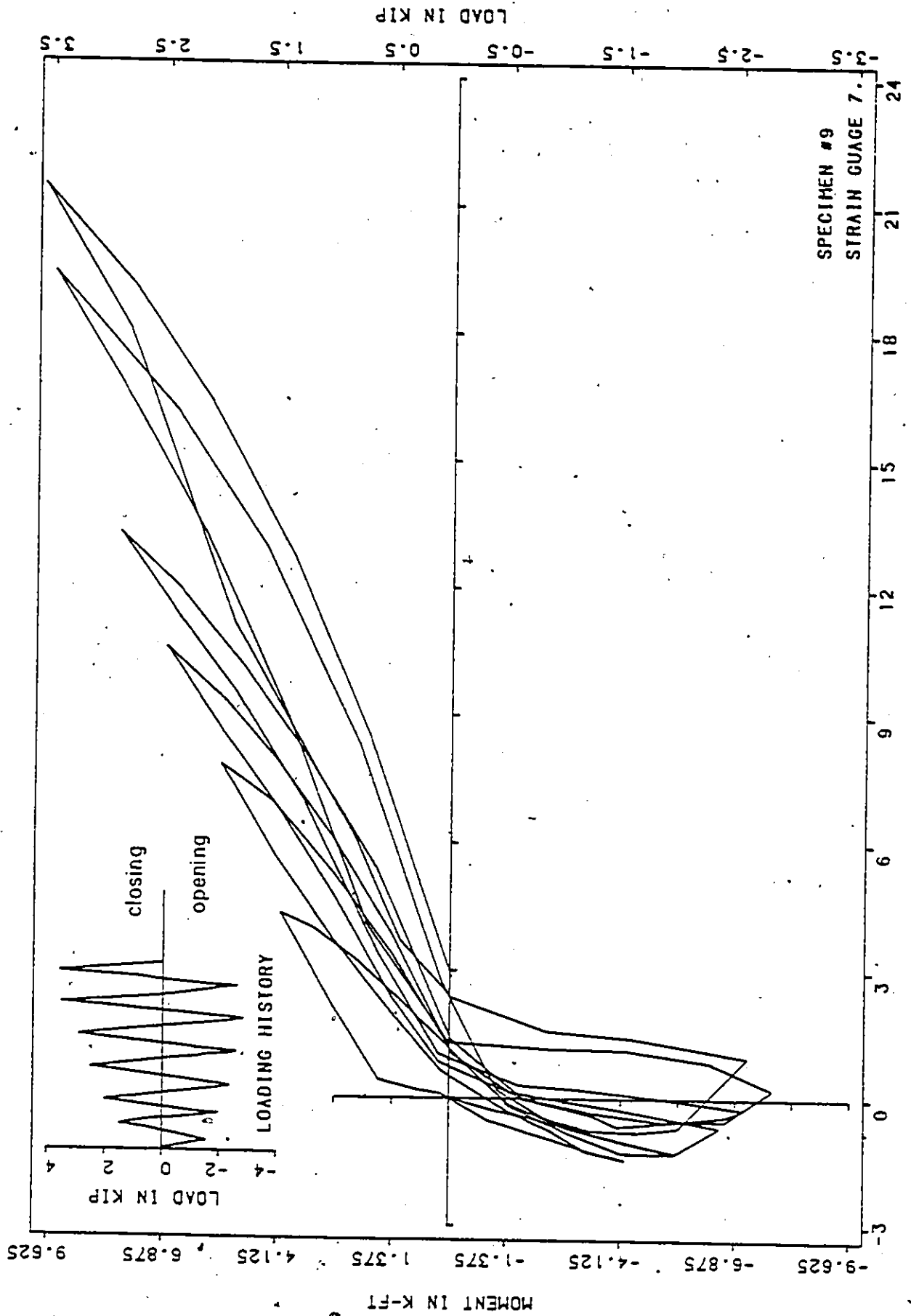


FIG. 56-1 MOMENT-STRAIN CURVE

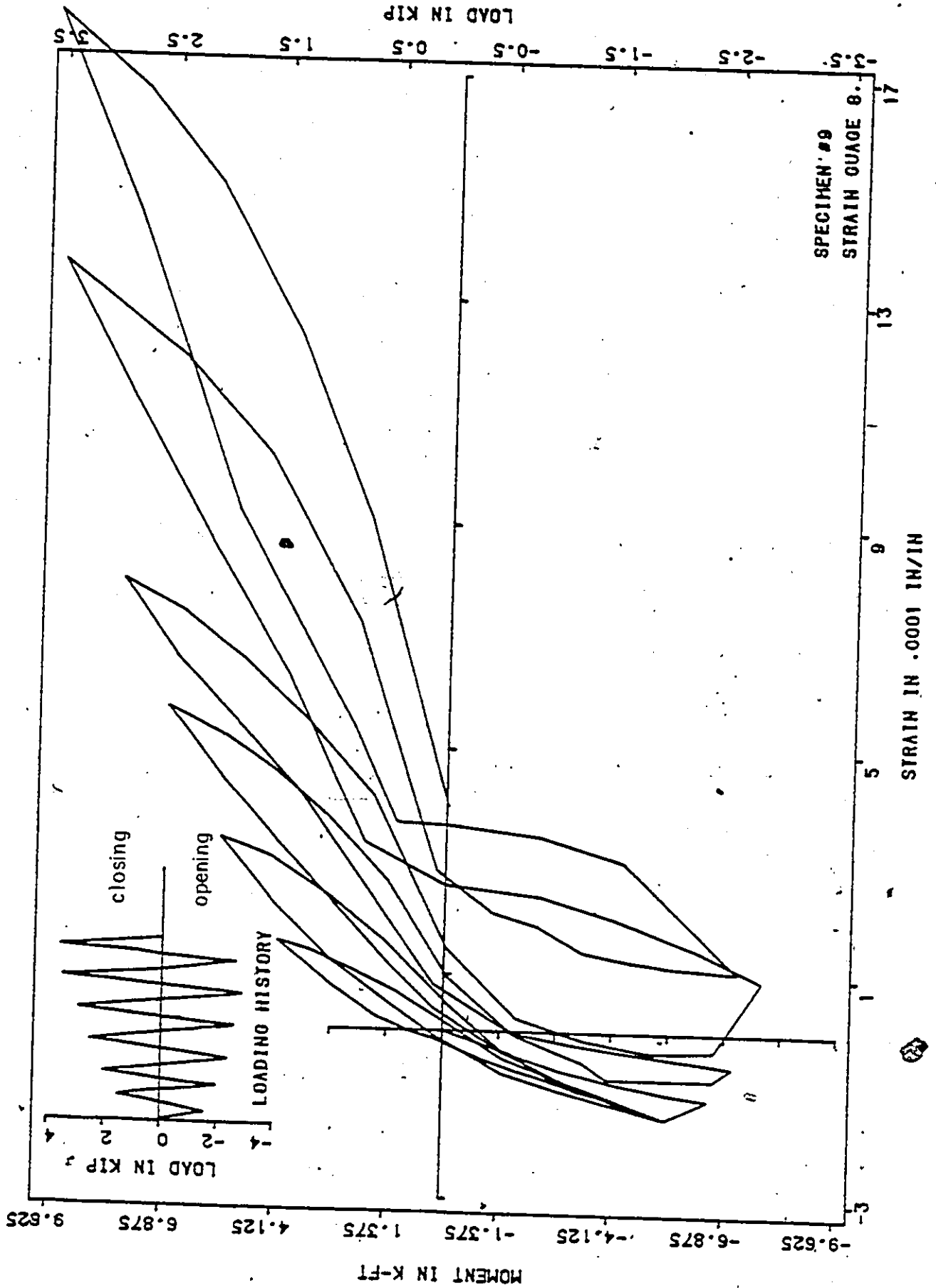


FIG. 56-9 MOMENT-STRAIN CURVE

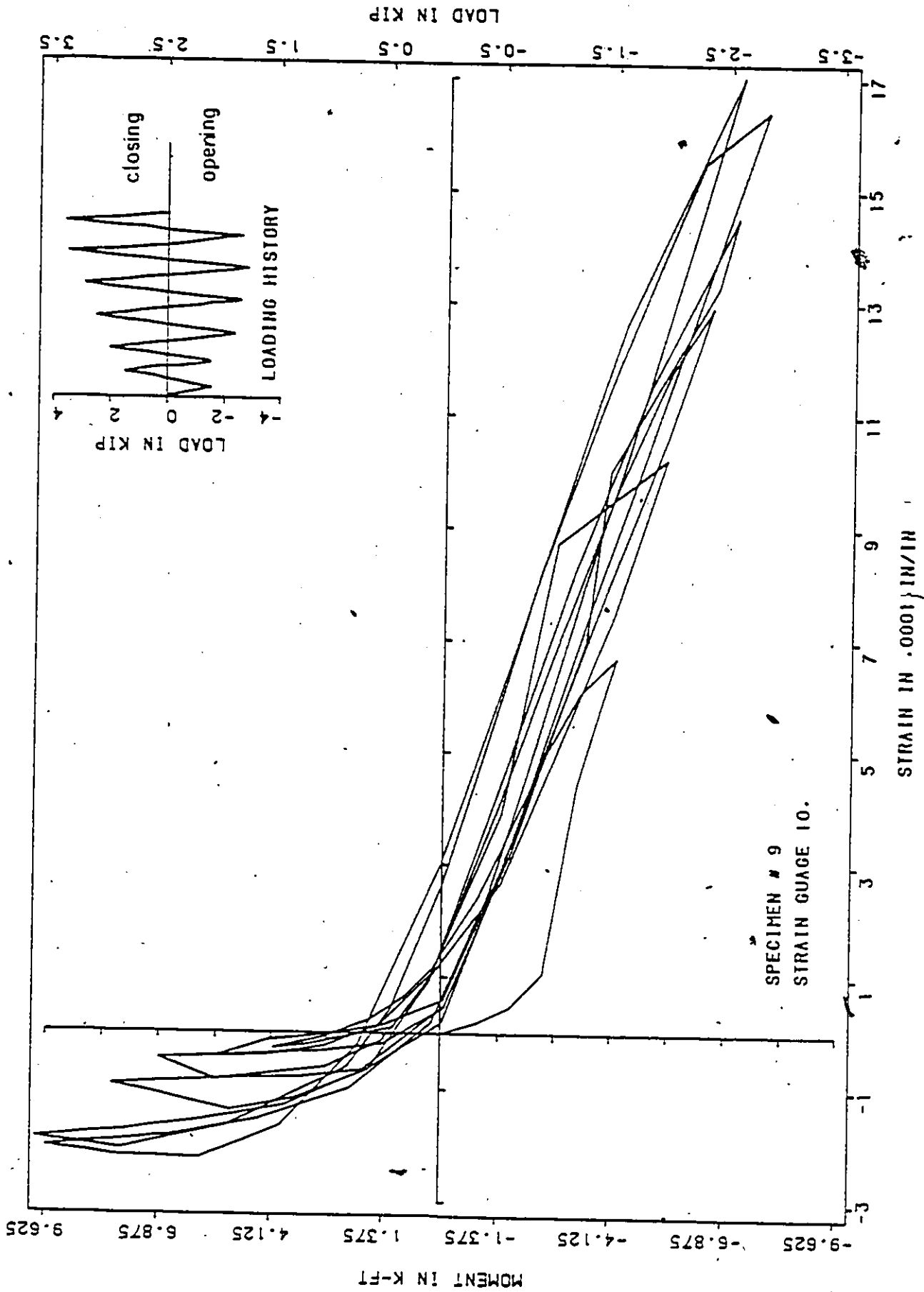


FIG. 56-h MOMENT-STRAIN CURVE